ORGANOTITANIUM SPECIES AS CATALYSTS FOR SYNTHESIS - AN ELECTROCHEMICAL STUDY.

by

INGRID M M FUSSING

A Thesis Submitted for the Degree of

DOCTOR OF PHILOSOPHY

July 1993

Department of Chemistry

University of Southampton

To my Mum

UNIVERSITY OF SOUTHAMPTON

ABSTRACT

FACULTY OF SCIENCE

CHEMISTRY

Doctor of Philosophy

ORGANOTITANIUM SPECIES AS CATALYSTS FOR SYNTHESIS - AN ELECTROCHEMICAL STUDY.

by INGRID M M FUSSING

A series of $CpTiCl_2[OR]$ complexes (Cp = η-cyclopentadienyl, R = alkyl, aryl) were synthesised and characterised by ^1H and ^{13}C nmr and mass spectrometry. Their electrochemical behaviour in THF was investigated by cyclic voltammetry and controlled potential electrolysis. The voltammetric response of the $CpTiCl_2[OR]$ solutions is dependent on whether the R group is alkyl or aryl and also on the degree of residual water present in the solution. An experimental procedure to minimize the amount of water in the electrolytic solution was developed. This involved the use of Schlenk techniques and cells connected to a vacuum line. $CpTiCl_2[OR]$ complexes where R = aryl (Ar) display a reversible one electron reduction. Any water present causes some of the starting complex to be consumed in a chemical reaction; the product has been postulated to be the complex $CpTiCl_2[OH]$ which also displays a reversible one electron reduction but at less negative potentials than $CpTiCl_2[OR]$. The complexes where R = alkyl display a similar one electron reduction, albeit at slightly more negative potentials than the aryl analogues, and a similar reaction with water prior to the application of any potential to the cell. In this case however, the reduction is rarely completely reversible since the anion produced is unstable in the presence of small amounts of water. A chemical reaction with water produces the anion $[CpTiCl_2[OH]]^-$ and hence a mechanism involving a 'scheme of squares' has been proposed to account for the behaviour observed. Attempts at synthesising novel monocyclopentadienyl titanium complexes containing bidentate diol ligands proved difficult and no well characterised product was obtained.

The reduction of titanocene dichloride, Cp_2TiCl_2 in the presence of trimethylphosphine in THF has been investigated also by cyclic voltammetry and controlled potential electrolysis. The reduction produces the Ti(III) and Ti(II) complexes $Cp_2TiCl(PMe_3)$ and $Cp_2Ti(PMe_3)_2$ respectively. These two complexes have been prepared both chemically and electrochemically and the voltammetry of their THF solutions, both on their own and in the presence of free chloride ions, recorded in an analysis of the mechanism postulated to account for the electrochemical behaviour of Cp_2TiCl_2 in the presence of phosphine ligands. It is concluded that the most stable titanium species at each of the oxidation states are Cp_2TiCl_2 (Ti(IV)), $Cp_2TiCl(PMe_3)$ (Ti(III)) and $Cp_2Ti(PMe_3)_2$ (Ti(II)). The voltammetry of a titanacyclooctene is reported although attempts to generate this species by electrochemical methods were not optimised.

CONTENTS

ACKNOWLEDGEMENTS

First and foremost I must thank Derek Pletcher for his patient supervision and guidance. Being part of his group has always involved a large degree of amusement and enjoyment, even in the stress-filled moments during thesis writing, which has helped make the inevitable frustrations of research endurable. I must also thank Richard Whitby for many helpful discussions and suggestions throughout my Ph.D.

I am forever grateful to my Mum for providing both immense emotional and material support, for encouraging me all the way through my formal education and for never doubting my abilities and achievements. My sisters, Vibeke and Kirsten deserve a special acknowledgement too, for always keeping me in touch with reality.

I would like to thank my fellow researchers, past and present, for all the laughs they have provided throughout my years in Southampton and, to those who have had to tolerate me through the stresses and strains of the past few months, I apologize and fully appreciate their understanding.

However significant chemistry is, it isn't everything and to all those friends with whom I've shared a pint, lost a game of squash to, had a political argument or a good gossip with, I should like to extend my sincere thanks; it all helps to maintain sanity.

Finally, I would like to thank all those who have provided technical support during my time as a postgraduate student, not least the glassblowers, Mike and Clive who have refrained from shouting at me when I most deserved it and to Carole Chatley for filling me in the on essential information necessary to survive in the Electrochemistry Group!

Ingrid Fussing

July 1993

ABBREVIATIONS AND SYMBOLS

a	radius (of a microdisc electrode, cm)
c	concentration of species in bulk solution (mol cm^{-3})
D	diffusion coefficient (cm^2 s^{-1})
E	potential vs a reference electrode (V)
Ep	peak potential (V)
$E_{p/2}$	half_peak potential (V)
$E_{½}$	half-wave potential (V) (similarly for $E_{¼}$ and $E_{¾}$)
ΔEp	difference in peak potentials (V)
ESR	electron spin resonance spectroscopy (also denoted EPR)
F	Faraday constant (9.65 x 10^4 C mol^{-1})
i	current (A or mA)
I	current density (A cm^{-1} or mM cm^{-2})
Ip	peak current density (A cm^{-2} or mA cm^{-2})
k	rate constant (generally s^{-1})
K	equilibrium constant
mM	concentration (moles x 10^{-6} cm^{-3})
n	number of electrons
q	total charge (C)
SCE	saturated calomel electrode
α	transfer coefficient
ν	scan rate (mV s^{-1})

Ar	aryl
Bz	benzene
Bu	butyl (prefixed n-normal, t-tertiary)
Cp	cyclopentadienyl (η-C_5H_5)
Cp^*	pentamethylcyclopentadienyl (η-$C_5(CH_3)_5$)
DMF	dimethylformamide
EI	electron impact (mass spectroscopy)
Et	ethyl
Me	methyl
nmr	nuclear magnetic resonance spectroscopy (δ - chemical shift (ppm), J - coupling constant (Hz), s - singlet, d - doublet, t - triplet, q - quartet)
Pr	propyl (prefixed i-iso)
R	alkyl or aryl
THF	tetrahydrofuran

CHAPTER 1

INTRODUCTION

Titanium is found in relative abundance in the earth's crust (0.6 %) mainly in the ores ilmenite, $FeTiO_3$ and rutile, TiO_2. Extraction of the metal involves making $TiCl_4$ by treating the ores with carbon and chlorine at very high temperatures. Titanium metal has a hexagonal close-packed lattice, is a good conductor of heat and electricity, is quite a light metal and because of its oxide film it is fairly corrosion resistant. For these reasons it is commonly used in turbine engines, aircraft and marine equipment. Titanium is the first member of the d-block transition elements and has four valence electrons, $3d^2\ 4s^2$. Ti(IV) is the most stable and common oxidation state, the lower oxidation states, (III), (II), (0) and (-I), tend to be readily oxidised to Ti(IV) by air, water and other reagents. Ti(III) in aqueous strong acid is stable but still a powerful reducing agent. Ti(IV) compounds tend to be covalent in character due to the high energy required to remove four electrons to create the Ti^{4+} ion. The inorganic compounds of titanium are many and varied but are not of concern here; what is of interest however, are the organotitanium compounds, their synthesis, uses and redox behaviour.

The interest in organotitanium species probably stems initially from the discovery of their use as catalysts in the Ziegler-Natta polymerisations of olefins. This has led to organotitanium species being employed as catalysts in isomerisations, hydrogenations and hydrometallations. They have also found a use in the fixation of nitrogen, in biology and quite extensively in organic synthesis.

The catalytic activity of organotitanium species, particularly cyclopentadienyl

derivatives, depends, as with all transition metal catalysts, on their ability to hold varying oxidation states. Low-oxidation state titanium species are often vital intermediates in organotitanium catalysed reactions and are generated by reaction of the parent Ti(IV) moiety with strong reducing agents. As a result the study of their redox behaviour has become necessary in order to determine the exact nature of the active species in a titanium-complex facilitated reaction. A valuable approach to this study is the analysis of such redox behaviour by electrochemical methods. Electrochemistry offers a clean, cheap and efficient way forward in such investigations.

By far the most highly researched and reported organotitanium compounds are those containing cyclopentadienyl ligands. The six electron donating cyclopentadienyl anion offers some stability to an electron deficient titanium centre as well as facilitating the solubility of the titanium-containing complex in organic solvents. The most common of these is dicyclopentadienyl titanium dichloride, (η-C_5H_5)$TiCl_2$ (hereafter Cp_2TiCl_2), I. This is a red crystalline compound (m.p. 230°C) and is the starting material for much of the organotitanium chemistry reported. Cp_2TiCl_2 is made from the reaction of sodium cyclopentadiene, NaCp, with titanium tetrachloride, $TiCl_4$ and has a quasi-tetrahedral structure.

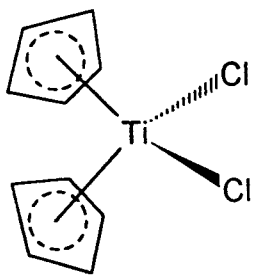

I

1.1. ORGANOTITANIUM CATALYSTS.

1.1.1. Ziegler-Natta Catalysts.

In 1955 Ziegler first reported the use of a $TiCl_4$-Et_3Al system as a catalyst in the polymerisation of ethylene [1]. Since this discovery, there has been considerable interest in organotitanium species and their suitability as catalysts in certain polymerisation reactions. Many different systems have been cited as being effective in this area, these are mostly based on transition metal halides or alkoxides, alkyl or aryl derivatives with a main group metal alkyl or alkyl halide [2]. There has been much discussion on the mechanism of the catalytic process; it is generally thought that the role of the main metal group alkyl or alkyl halide is to alkylate, and sometimes reduce, the transition metal and possibly to complex with it. The alkylated metal centre is then the site for polymerisation initiation. Cossee proposed a mechanism for the polymerisation of ethylene at an alkylated titanium centre where propagation occurs through the insertion of ethylene into a titanium-alkyl bond [3] (scheme 1). Cossee reported that the presence of unfilled d-orbitals in transition elements are responsible for their catalytic activity and that the polymerisation occurred at titanium atoms which possessed a vacant orbital site. The function of the main group metal activator is to replace a chlorine ligand of an octahedrally coordinated titanium atom by an alkyl group. The alkene monomer is then π-complexed to the titanium at the vacant site, this has the effect of weakening the titanium-alkyl bond, thus the alkyl group is transferred to the bound alkene via a 4-membered cyclic intermediate in which the alkene now forms a σ-bond to the titanium. The final titanium species is similar to the first activated species but the alkyl ligand and the vacant active site have exchanged positions. Cossee and Arlman suggest that these now re-exchange positions before further insertion [4].

Cyclopentadienyl titanium species do feature in the long list of compounds effective as Ziegler-Natta catalysts. In 1959 Breslow and Newburg reported the

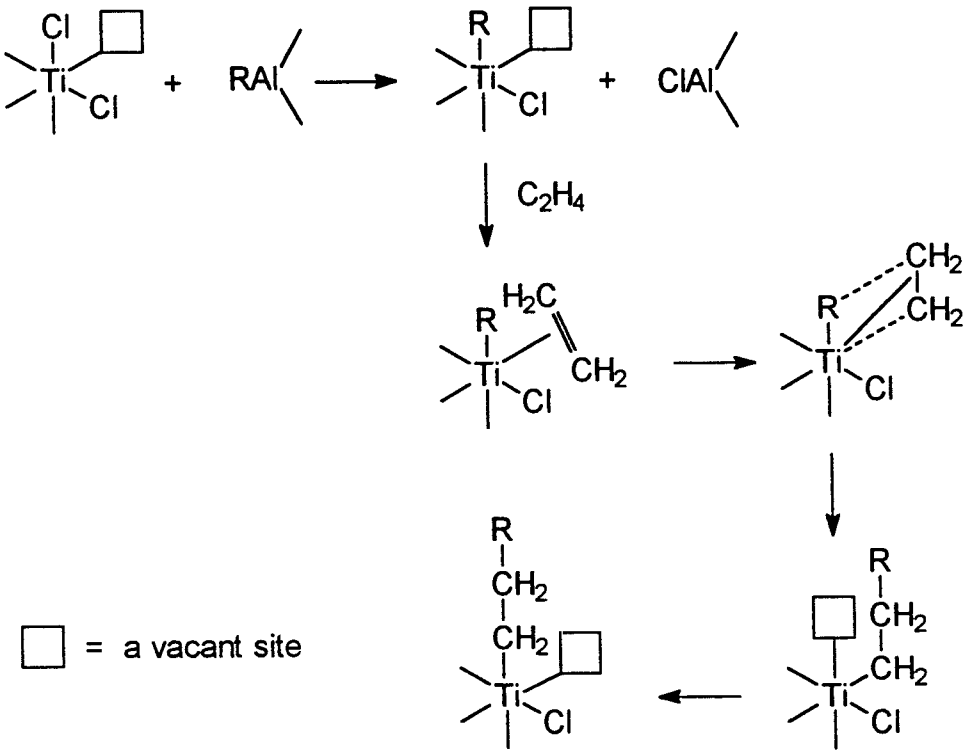

Scheme 1

use of Cp_2TiCl_2 and Et_2AlCl in the polymerisation of ethylene [5] (scheme 2). Since then, many other cyclopentadienyl titanium/alkyl aluminium systems have been cited [6a-f for the more important ones]. One advantage of cyclopentadienyl titanium systems is their solubility in organic solvents and although they have yet to be incorporated into an industrial process, much mechanistic work has been carried out with them. The solubility of cyclopentadienyl titanium species creates a homogenous catalysis system, hence enhancing efficiency since all the catalyst is available. There is no catalyst inactivation by polymer coating as is possible when the catalyst is a solid surface and, in addition, the catalyst is readily removed from the polymer. Mechanistic studies have also been greatly enhanced by the availability of such soluble catalyst systems. With cyclopentadienyl titanium catalysts, it is largely accepted that propagation occurs at the alkylated titanium centre as described in scheme 1, although it is still unclear which oxidation state of titanium is the active form; both Ti(III) and Ti(IV) have been proposed [4,5,7].

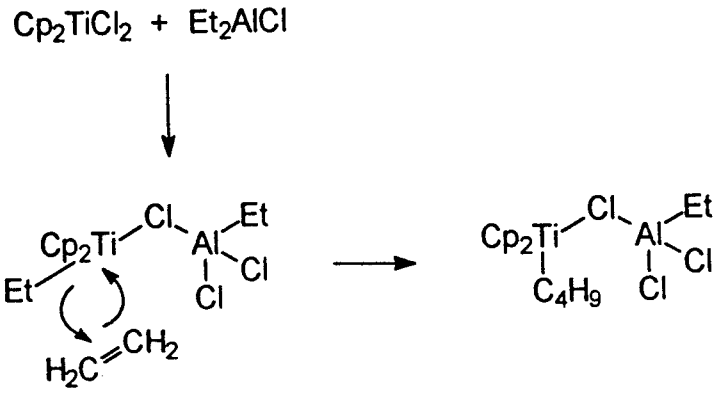

Scheme 2

1.1.2. Olefin Isomerisations and Hydrogenations.

In contrast to the drive for soluble cyclopentadienyl systems to give homogenous catalysts for Ziegler-Natta polymerisations, those investigating the use of such titanium species as catalysts for olefin isomerisation and hydrogenation have investigated the use of polymer-bound catalytic moieties. Grubbs and Brubaker have reported the binding of Cp_2TiCl_2 to a polymer and the use of this system to catalyse the reduction of olefins [8a]. They argued that a basic requirement for a transition element to be able to catalyse a reaction, is an available open co-ordination site on the transition element at an intermediate stage in the reaction. The opening up of a co-ordination site on the metal often results in some degree of polymerisation of the complex thereby blocking the open coordination site by way of a bridge forming. As is the case of the titanocene moiety, 'Cp_2Ti', which has been reported to rapidly dimerize once formed [9] (scheme 3).

Brubaker et al sought to prevent this dimerisation by attaching the titanocene precursor, Cp_2TiCl_2, to a polystyrene-divinylbenzene copolymer resin [8b]. On reduction of the titanium by butyllithium, a hydrogenation catalyst was produced with an efficiency greater than that for the corresponding unattached

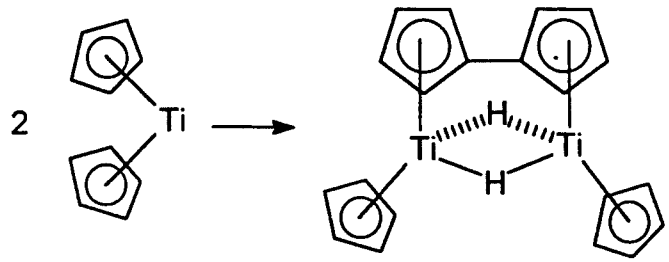

Scheme 3

species. Bergbreiter and Parsons also capitalised on this idea and reduced polystyrene-bound Cp_2TiCl_2 with alkylmagnesium halides producing a catalyst for olefin isomerisation [10] (equation 1). A polystyrene-supported titanocene dichloride has also been reported to be an excellent heterogenous catalyst for the hydroalumination of olefins [11].

$$RCH_2CH{=}{=}CH_2 \xrightarrow[R`MgBr]{Ps{-}{-}Cp_2TiCl_2} RCH{=}{=}CHCH_3 \quad \text{(mainly E)}$$

Ps = polystyrene

Equation 1

1.1.3. Titanium in Nitrogen Fixation Systems.

Another process by which titanocene derivatives have found some catalytic usefulness is in the fixation of molecular nitrogen. A review on nitrogen fixation by Vol'pin and Shur describes some of the titanium-containing systems that are effective in this area [12]. One example is given by Van der Weij and co-workers who report the reduction of the dinitrogen ligand in a $(Cp_2TiR)_2N_2$-sodium naphthalene system which, after acidification, gave ammonia and some hydrazine. The $(Cp_2TiR)_2N_2$ species is the product of the action of a Grignard reagent on Cp_2TiCl_2 and the subsequent reaction with N_2 at -90°C

[13]. Another example is one where the products of the electrochemical reduction of Cp_2TiCl_2 at Pt or Hg electrodes in THF or methanol catalyse the reduction of dinitrogen to ammonia [14].

In biology, titanocene dichloride has been found to possess tumor-inhibiting properties [15] and recently reported is an assessment of the anti-tumor activity of some dicyclopentadienyl titanium compounds [16].

1.2. TITANIUM IN ORGANIC SYNTHESIS.

The catalytic applications of organotitanium compounds represent only part of the usefulness of such species to the synthetic chemist. Other notable areas where the employment of titanium compounds has proved beneficial in promoting desirable transformations include their use as Lewis Acids in Friedel Crafts alkylations and in Diels Alder reactions [17] and in the employment by Sharpless of an alkoxy titanium species for his very successful enantioselective epoxidation of allylic alcohols [18]. This section, however concentrates on the examples of low-valent organotitanium species, that is, species containing titanium with a formal oxidation state below +4 and bonded to one or more organic ligands, that facilitate C-C bond forming reactions.

Reduction is an essential step in the formation of these low-valent species and Cp_2TiCl_2 has proved the most convenient starting material. +3 and +2 are the most common lower oxidation states discussed for titanium although some zero-valent organotitanium compounds have been proposed [19]. The mechanisms suggested by those generating low-valent titanium species for use in organic transformations do include discussions on the nature of the active species. However, unless this active species is isolable it is difficult to present an accurate picture of the mechanism and, in many cases, only speculative evidence exists for the oxidation state of the titanium in the active complex.

1.2.1. Low-valent Titanium and the Coupling of Carbonyl Compounds.

The first significant use of low-valent titanium complexes in organic synthesis was in the early 70's when the reductive coupling of carbonyl compounds to afford diols or alkenes was brought about by the reduction of titanium tri- and tetra-chloride systems (equation 2) [20].

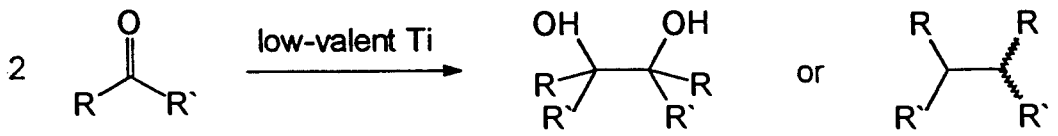

Equation 2

In 1974, in a review on the organic chemistry of low-valent titanium species, McMurry reported on the reduction of $TiCl_3$ by $LiAlH_4$ forming a Ti(II) species that facilitated the reductive coupling of ketones and aldehydes to olefins [21], this reaction has now come to be known as the 'McMurry reaction', later it was reported that the active species is in fact a Ti(0) moiety [25]. As an example of the synthetic use of this reaction McMurry reported the formation of β-carotene, a symmetric polyolefin of commercial use as a food-colouring agent and a precursor of vitamin A, in 85% yield from the action of the $TiCl_3$-$LiAlH_4$ reagent on retinal (equation 3).

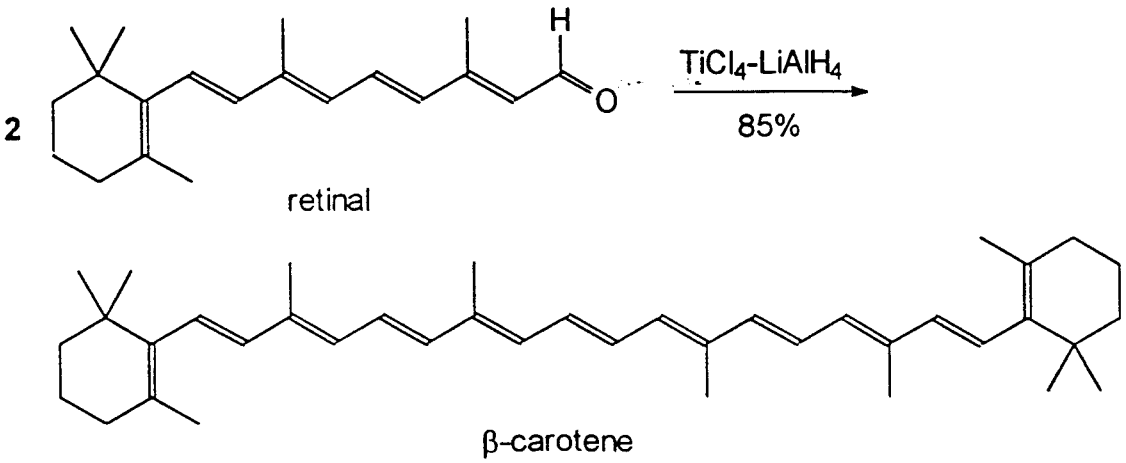

retinal

β-carotene

Equation 3

In this review it was suggested that the reaction was probably limited to the synthesis of symmetrical olefins but, in fact, later on McMurry and co-workers did successfully apply their method to the coupling of two different carbonyl compounds [22]. This they did by employing an excess of the cheaper, more accessible carbonyl compound. For example, in the isopropylidenation of carbonyl groups, an excess of acetone was added to cholestanone in the presence of $TiCl_3$-$LiAlH_4$ to give the mixed coupled product in 54% yield (equation 4).

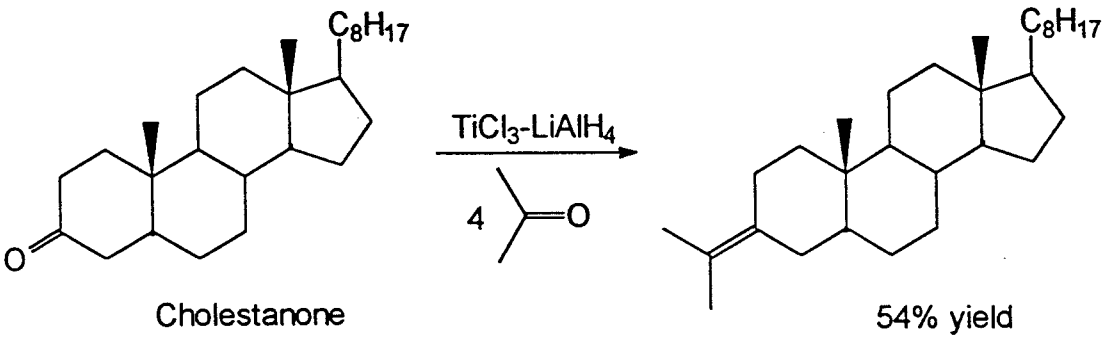

Cholestanone 54% yield

Equation 4

By 1983 this titanium-induced carbonyl coupling had been successfully applied to a large range of substrates including both saturated and unsaturated, aliphatic or aromatic, ketone or aldehyde. Also the reaction occurs both intermolecularly to yield acyclic alkenes and intramolecularly on dicarbonyl compounds to give cycloalkenes [23]. It is also the case that a variety of reducing agents have proved active in the generation of the necessary low-valent titanium species; $TiCl_3$ with potassium, zinc, zinc/copper and lithium have been used. A variation in the titanium species has also been reported; $TiCl_4$ has been used alongside the $TiCl_3$. $Cp_2Ti(CO)_2$ has promoted the reductive dimerisation of aldehydes and ketones to olefins and, a Cp_2TiCl_2-Na system, their reduction to alkanes [20].

The coupling of carbonyl groups by low-valent titanium yielding alkenes proceeds via an intermediate stage in which a diol is formed. It is possible to stop the reaction at the diol stage, as shown by Corey in some examples of

intramolecular carbonyl coupling (equation 5) [24].

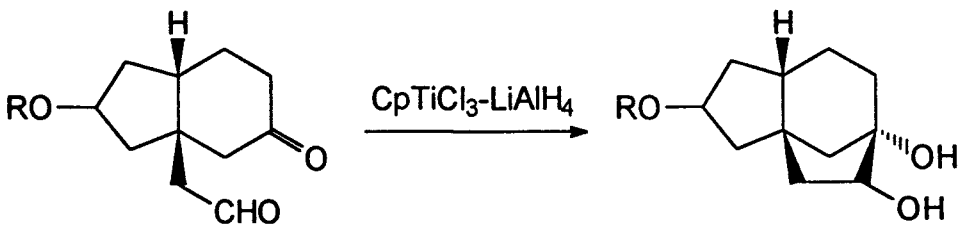

Equation 5

An analysis of the mechanism and stereoselectivity of these coupling reactions can be found in a review by Lenoir [25]. This report also summarises the application of these low-valent titanium systems in reductive elimination reactions. For example the deoxygenation of glycols can be brought about by such systems (equation 6) as can the reductive elimination of bromohydrins to alkenes (equation 7). The Ti(0) is reported to be formed according to the stoichiometric equation 8.

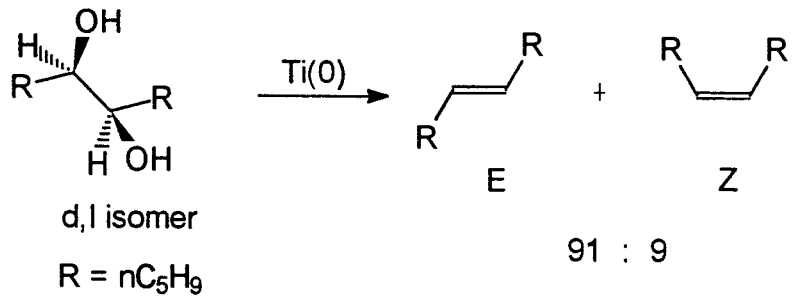

Equation 6

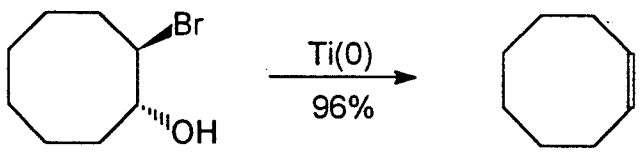

Equation 7

Equation 8

1.2.2. Titanocene Carbene Complexes.

Titanocene carbene reagents are another group of titanium species that have found an application in organic synthesis. The Tebbe reagent [26] prepared from the reaction of trimethylaluminium with dicyclopentadienyl titanium dichloride (equation 9) has been used extensively in Wittig-type methylation of carbonyl compounds (equations 10 & 11) [25, 27]. It is particularly useful for the methylation of hindered or base sensitive ketones.

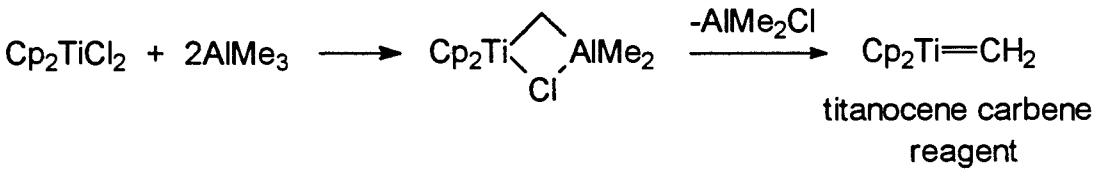

Equation 9

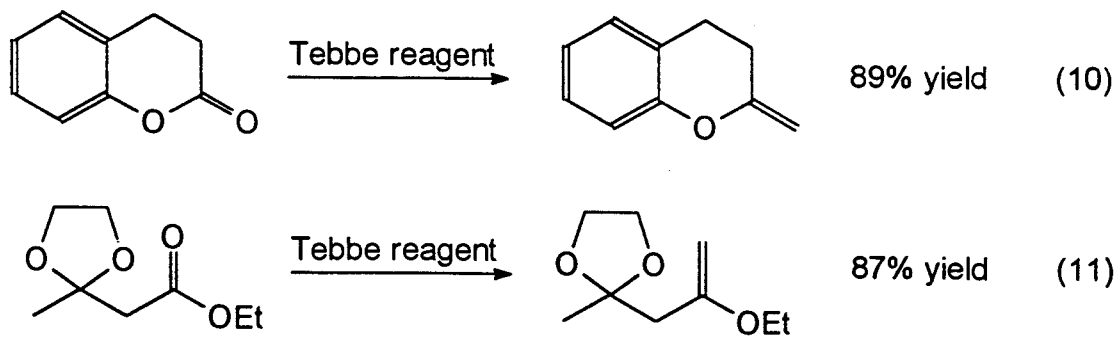

Equations 10 & 11

Perhaps a more convenient and very mild source of the reactive intermediate $Cp_2Ti{=}CH_2$ is the titanocyclobutane shown in equation 12 which was developed by Grubbs et al [28]. The versatility of this reagent is illustrated in

scheme 4 [29].

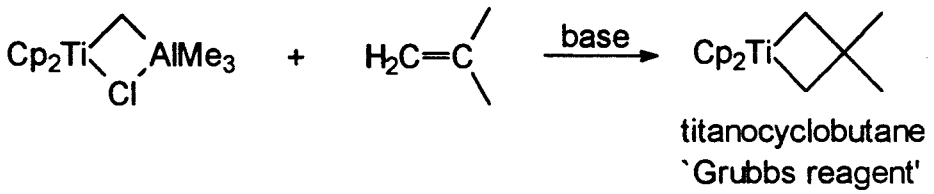

Equation 12

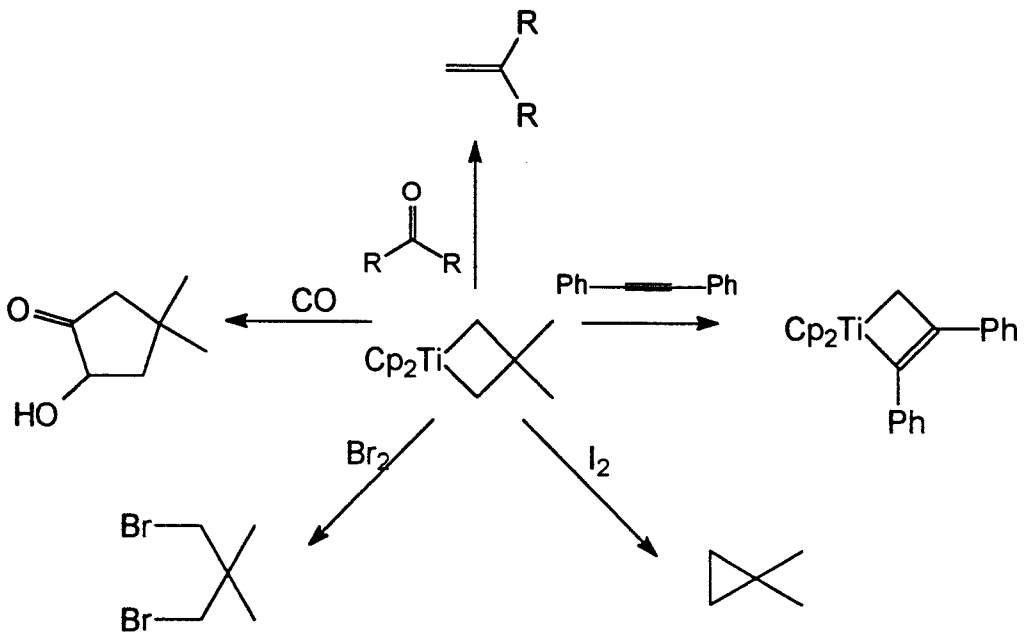

Scheme 4

1.2.3. 'Cp_2Ti' Induced Cyclisations.

One very interesting area of organic synthesis where low-valent titanium species have been applied is in the intramolecular coupling of dienes, enynes and diynes yielding bicyclic products. Parshall and co-workers reported the cyclisation of diynes using a titanocene moiety 'Cp_2Ti' (scheme 5). The reagent used in this case is titanocene dichloride, Cp_2TiCl_2, which is reduced by a

sodium amalgam in the presence of an alkylphosphine thereby forming a relatively stable Ti(II) species which is then mixed with the diyne [30].

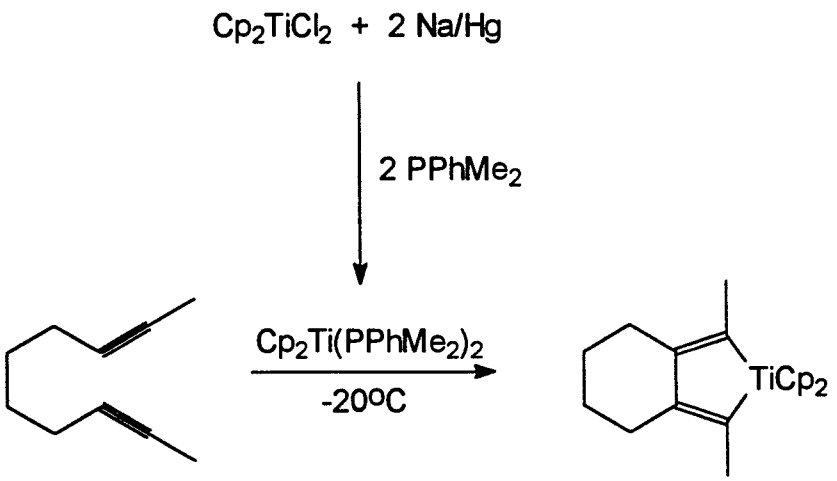

Scheme 5

Alkylphosphine ligands are employed to stabilize the $Cp_2Ti(II)$ moiety, without them there is a danger of hydrogen-abstraction from the cyclopentadienyl ligand and the consequent formation of a dimeric species [9]. The diyne cyclisation shown in scheme 5 was developed from the known reductive dimerisation of diphenylacetylene with a variey of transition metal reagents including cyclopentadienyl titanium reagents (equation 13) [31]. In these metallocycles the titanium is in the +4 oxidation state and its co-ordination sphere contains 16 electrons which is favourable for titanium.

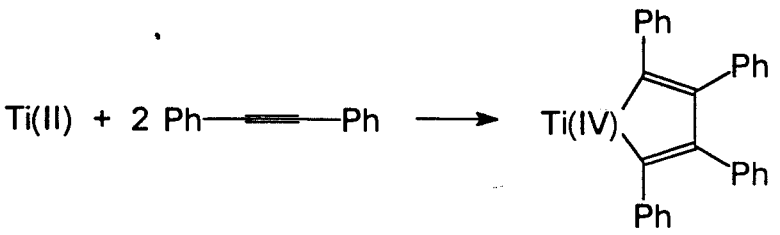

Equation 13

Many of the developments of this intramolecular coupling reaction have involved zirconium species. Negishi et al introduced a zirconocene equivalent into these reactions by means of a zirconacyclopropene formed from the reduction of Cp_2ZrCl_2 by n-butyllithium and consequent β-hydride elimination, then used it in various coupling reactions, examples of which are shown in equations 14 and 15 [32].

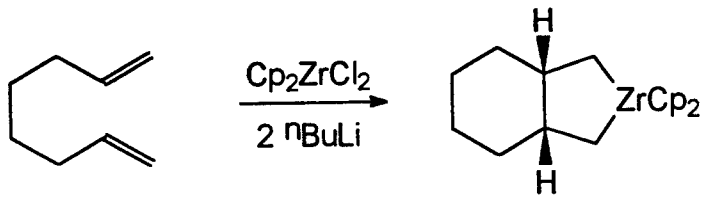

(14)

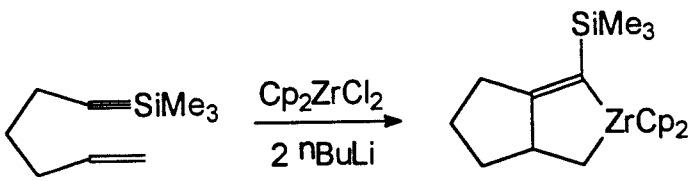

(15)

Equations 14 & 15

Hewlett and Whitby extended the use of the low-valent titanium complex, $Cp_2Ti(PMe_3)_2$ to the intramolecular coupling reaction between carbonyl groups and alkenes or alkynes (equations 16, 17 and 18) [33].

Further manipulation of all these metallocycles is necessary if the reactions are to be viable C-C bond forming reactions in organic synthesis. Hydrolysis of the titanocycle in scheme 5 gives an exocyclic diene with exclusively the E,E-structure which is reactive with many conventional dienophiles in Diels-Alder reactions (equation 19) [30]. The heteroatom-metallocycles shown in equations 16, 17 and 18 can be transformed into bifunctional cyclic compounds by halogenation followed by hydrolysis (equation 20) [33, 34].

Reactions of the zirconacycles have involved hydrolysis as well as halogenation and insertion of carbon monoxide forming a bicyclic ketone (scheme 6) [32].

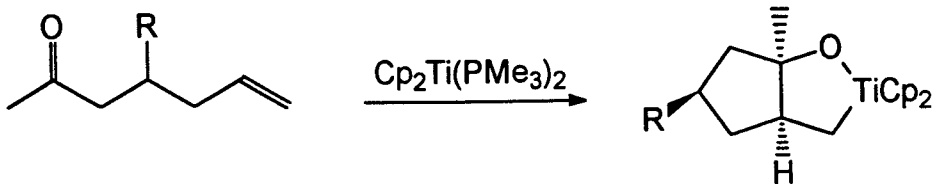

(16)

R = H 76% yield
R = Ph 83% yield

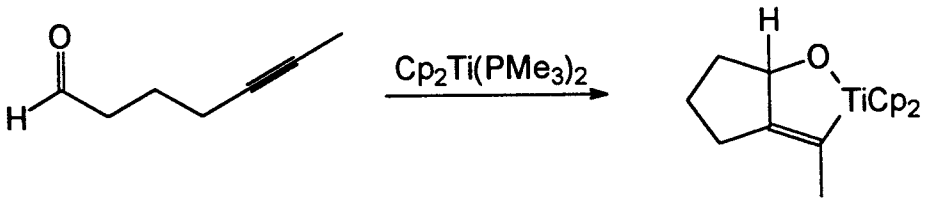

(17)

79% yield

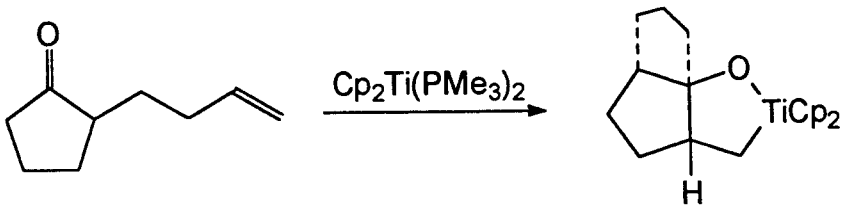

(18)

53% yield

Equations 16, 17 & 18

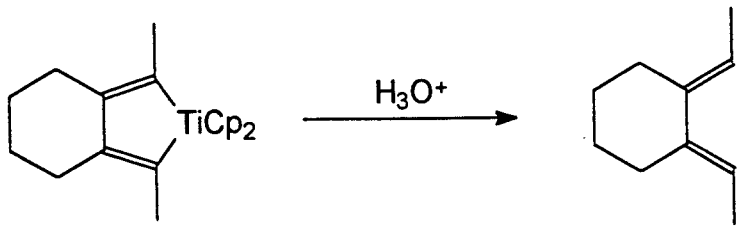

(19)

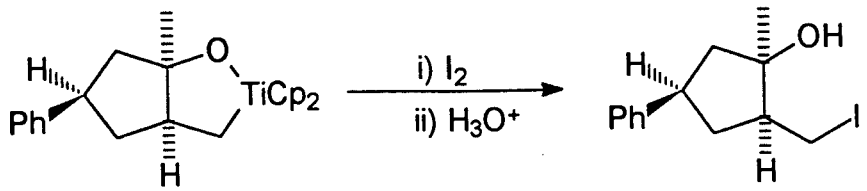

(20)

Equations 19 & 20

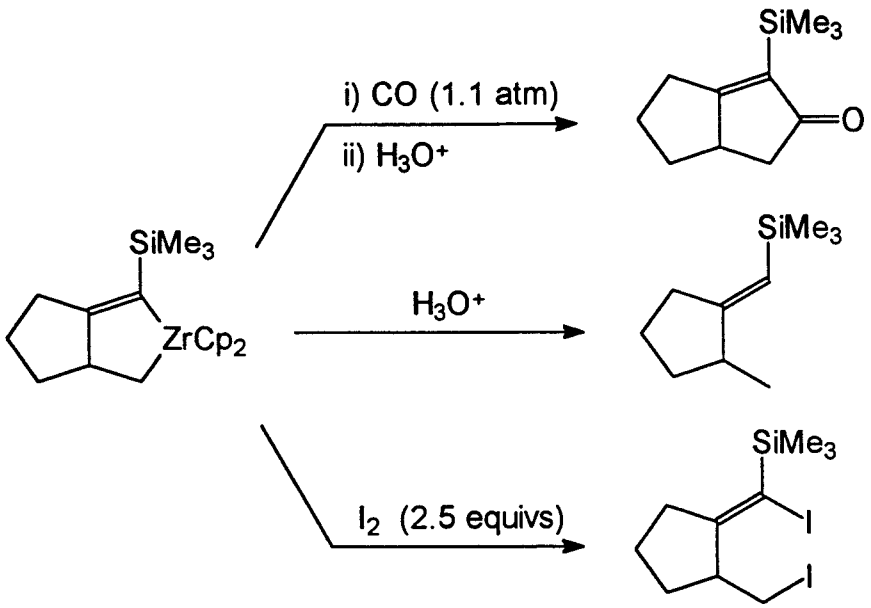

Scheme 6

A recent publication by Doxsee and co-workers reports on the role of titanium metallocycles as intermediates in the synthesis of acyclic and heterocyclic compounds [35]. It concentrates on the reactions of titanocyclobutenes with nitriles, ketones and aldehydes yielding pyridine derivatives (II) and conjugated dienes (III), (scheme 7).

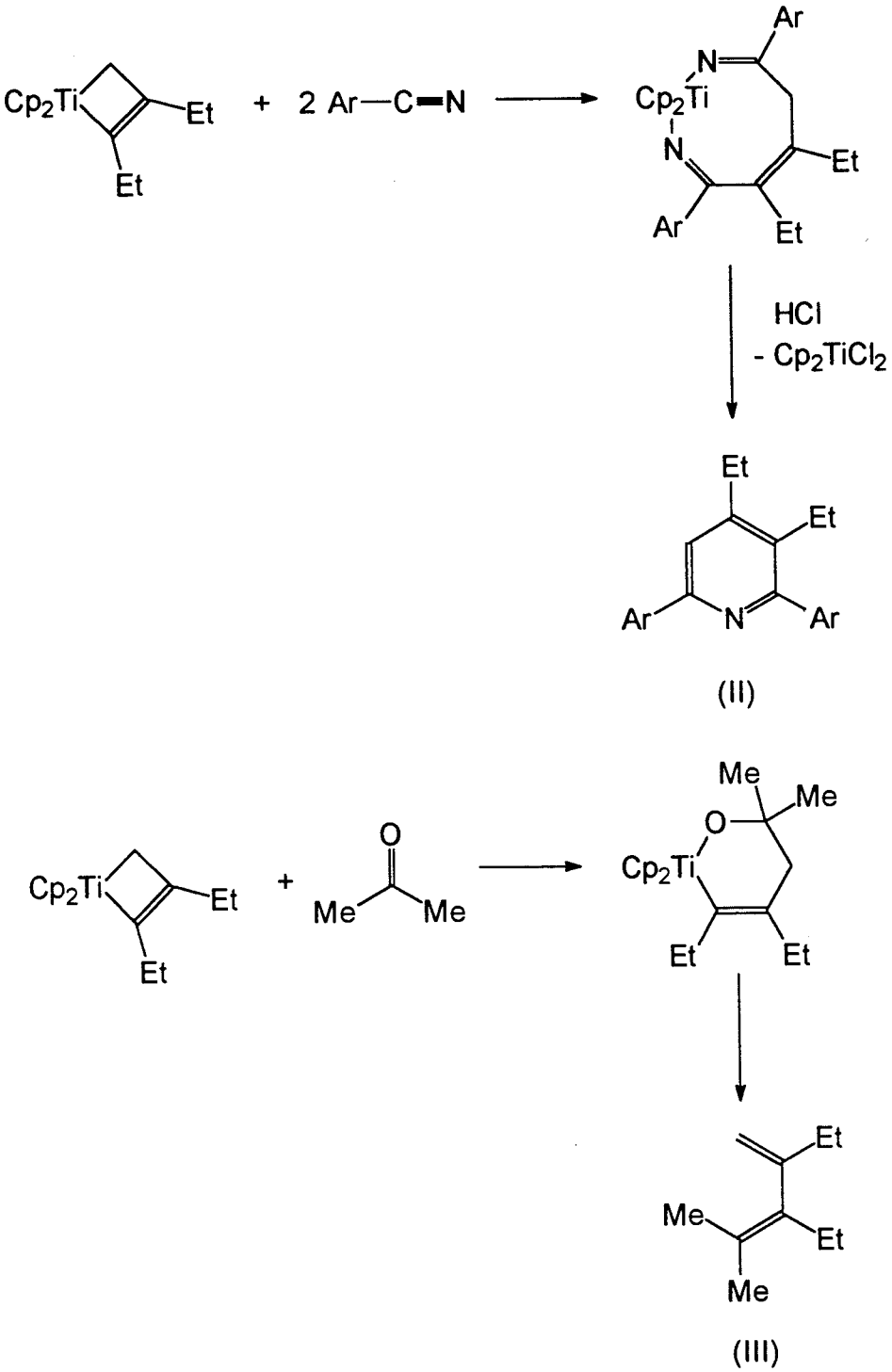
Cp2Ti
Et
Et
+ 2 Ar—C≡N
Ar
N
Cp2Ti
N
Et
Ar
Et
HCl
- Cp2TiCl2
Et
Et
Ar
N
Ar
(II)
Cp2Ti
Et
Et
+
O
Me
Me
Me
Me
O
Cp2Ti
Et
Et
Et
Me
Et
Me
(III)

Scheme 7

1.2.4. Monocyclopentadienyl Titanium Complexes.

The 'Cp_2Ti' unit, while useful in many transformations as illustrated above, does have its limitations. It is quite a sterically hindered moiety and this, along with its relative stability, may explain the limited examples of useful reactions of the metallocycles in equations 16-20. Since the presence of two identical ligands renders the titanium centre achiral any possibility of asymmetric induction is also limited. Monocyclopentadienyl titanium complexes may well provide the versatility required to effect the asymmetric transformations which are of such enormous value to the synthetic chemist.

There exists a fair number of examples of the synthesis of monocyclopentadienyl titanium species in the literature; monocyclopentadienyl titanium trichloride, $CpTiCl_3$, is perhaps the most familiar. $CpTiCl_3$ can be prepared in good yield by a redistribution reaction between Cp_2TiCl_2 and $TiCl_4$ [36]. A more recent method involving trimethylsilylcyclopentadiene, $CpSiMe_3$, and $TiCl_4$ reporting a yield of 92% has been cited by Cardoso et al [37]. $CpTiCl_3$ has frequently been used as the starting point for other mono-Cp titanium complexes. Pandey and Sengupta have reviewed the synthesis of various mono-Cp titanium alkoxides, phenoxides, carboxylates and alkyls along with sulphur- and nitrogen-bonded analogues using $CpTiCl_3$ as the starting material [38]. Höhlein and Schobert investigated the reaction of Cp_2TiCl_2 with alcohols and found that under certain conditions the displacement of a cyclopentadienyl ligand occurred and a mono-Cp alkoxy compound formed [39]. The highest yields of $CpTiCl_2(OR)$ obtained were from the reaction of Cp_2TiCl_2 with secondary alcohols in the presence of stoichiometric amounts of triethylamine (equation 21). Similar behaviour was also reported by Bharara when he treated Cp_2TiCl_2 with ethanol and triethylamine forming $CpTiCl_2(OEt)$ if the reaction was carried out at room temperature [40]. Refluxing the reaction mixture led to the formation of titanium tetraethoxide, $Ti(OEt)_4$.

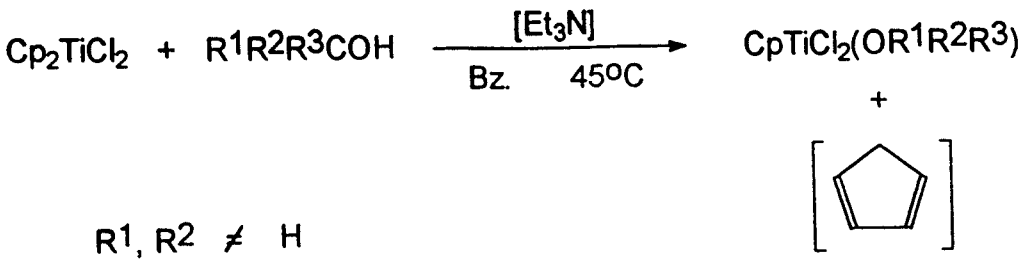

Equation 21

In this paper the authors suggested that by incorporating chiral alkoxy ligands these complexes would become potentially chiral-inducing themselves, thereby facilitating asymmetric transformations. Duthaler et al have confirmed this using their mono-Cp titanium glucose complexes. These workers used $CpTiCl_3$ as the starting point to synthesise their chiral complexes and then went on to use them in the enantioselective allylation of carbonyl compounds [41, 42]. An example is given in scheme 8 where the allylic compound shown was produced with an enantiomeric excess of 90%. These workers were also successful in incorporating a diol into a mono-Cp titanium complex, IV (3C, chapter 3), this they were able to use successfully in a similar allylation reaction [43].

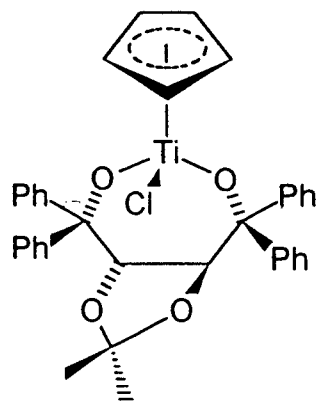

IV (3C)

Other monocyclopentadienyl titanium complexes that have been synthesised include some amido complexes, $CpTiCl_2NHR$ (R = Et, ^{i}Pr, ^{t}Bu, Ph) which were

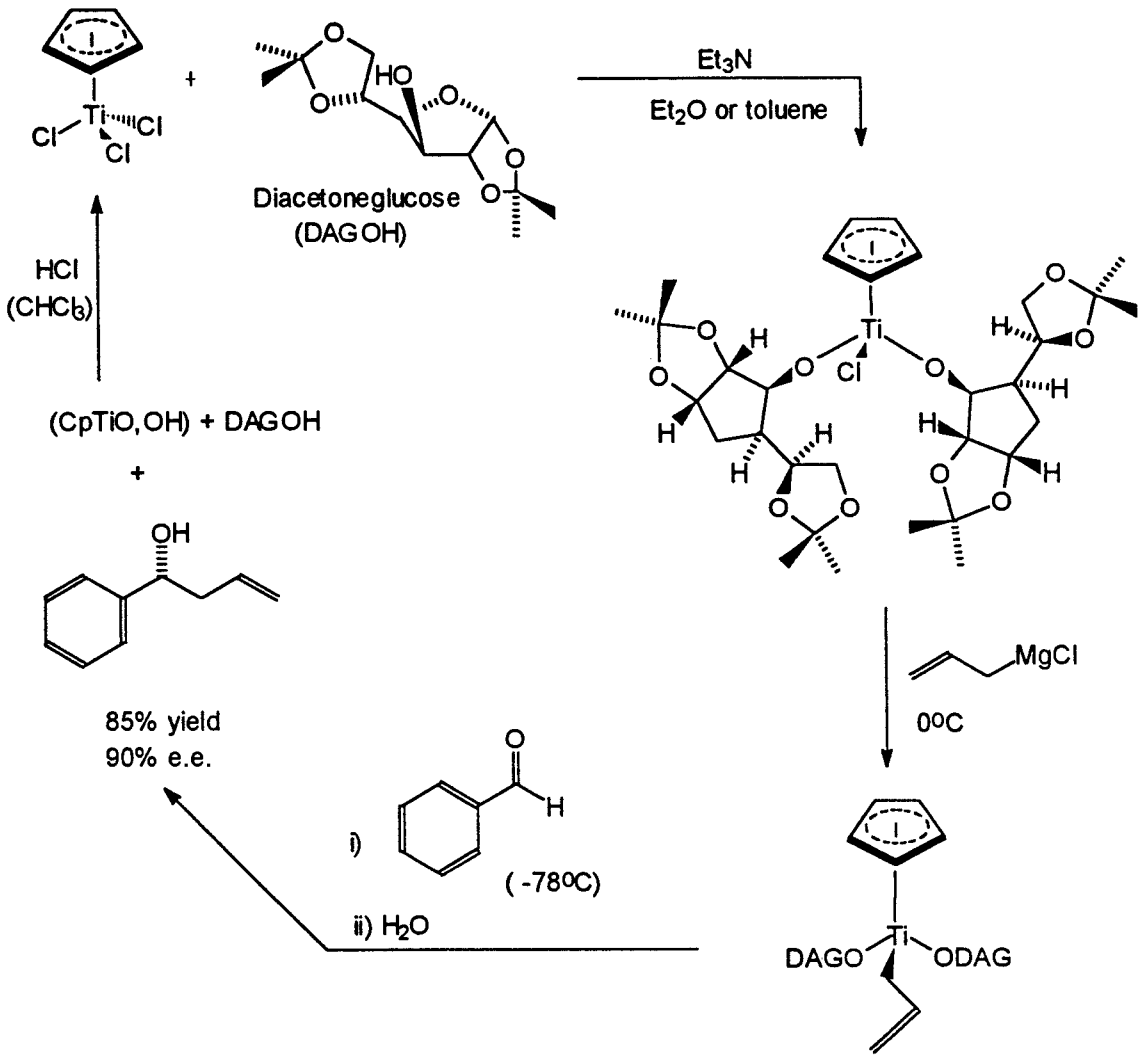

Scheme 8

again made from $CpTiCl_3$ and the corresponding silylamine [44]. Low-valent mono-Cp titanium complexes are also known: Coutts et al used zinc to reduce $CpTiCl_3$ in THF solutions and characterised the product as $CpTiCl_2(THF)$ which on heating lost the coordinated solvent molecule affording the Ti(III) species $CpTiCl_2$ [45]. Later the same workers introduced nitrogen-containing ligands such as pyridine, into solutions of these mono-Cp-Ti(III) complexes forming either non-ionic six-coordinate dimeric species (V) or five-coordinate monomeric species (VI) [46]. Rausch and co-workers also reduced $CpTiCl_3$ in THF solutions, this time however using magnesium as the reducing agent and performing the experiment in the presence of trimethylphosphine, forming $CpTiCl_2(PMe_3)_2$ (VII), the X-ray structure of which proved it to have the 'piano-

stool' geometry shown below [47].

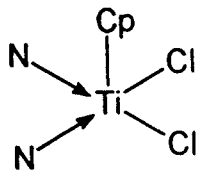

VI

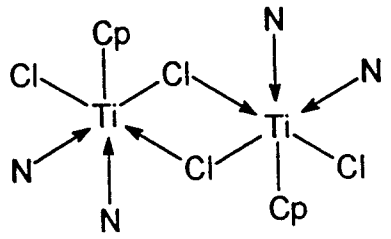

V

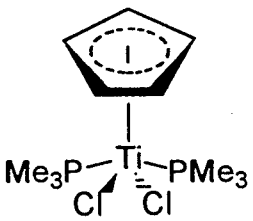

VII

1.2.5. Ti(III)-induced Radical Cyclisations.

Finally it is probably worth mentioning the cyclisation of epoxyolefins via a radical mechanism induced by a cyclopentadienyl Ti(III) species. Nugent and RajanBabu reported the direct synthesis of functionalised cyclopentane derivatives in this way [48] using Cp_2TiCl (scheme 9). Treatment of the nucleophilic organotitanium derivative in scheme 9 with iodine provides a route to a bifunctional cyclopentane derivative.

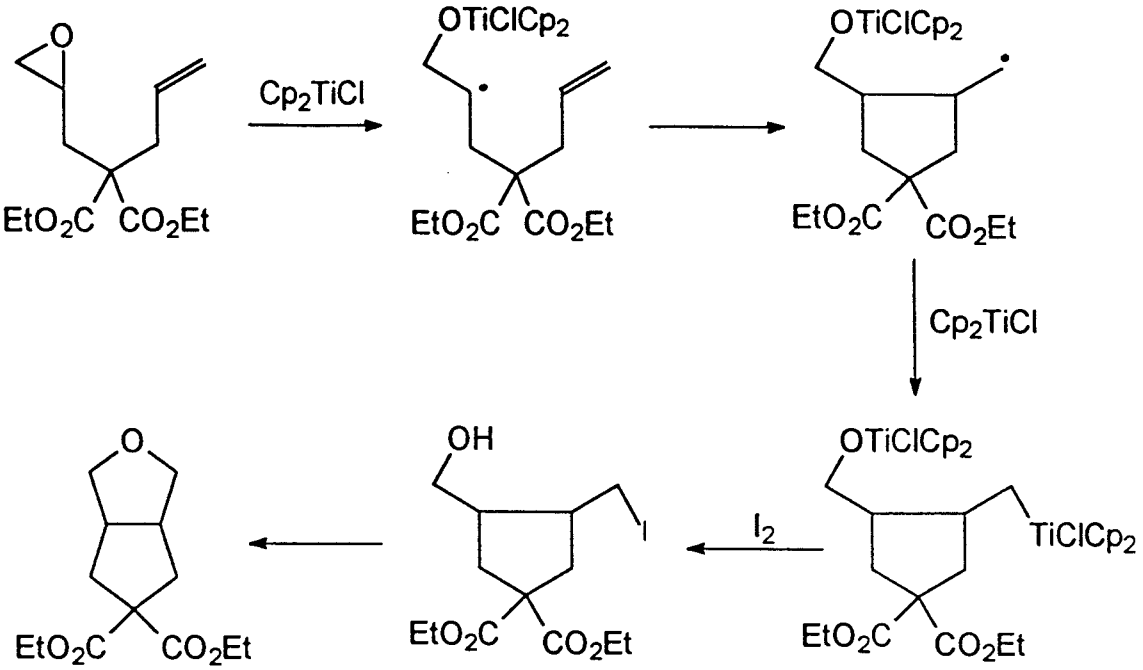

Scheme 9

1.3. THE ELECTROCHEMISTRY OF SOME CYCLOPENTADIENYL TITANIUM DERIVATIVES.

The catalytic activity of systems based on cyclopentadienyl titanium derivatives generally involves the metal in a low oxidation state which is generated by strong reducing agents. An understanding of the mechanisms of these organic reactions is dependant on knowing the oxidation state of the metal in the active species. Electrochemistry offers one approach to defining the redox chemistry of Cp_2TiCl_2 and related compounds. Titanocene dichloride, Cp_2TiCl_2, is by far the most researched organotitanium complex but the mechanism of its electrochemical reduction remains the subject of some controversy.

1.3.1. The Electrochemistry of Titanocene Dichloride, Cp_2TiCl_2.

The mechanism of the electrochemical reduction of Cp_2TiCl_2 has been debated strongly in the literature, the arguments being centred around the first one electron transfer. Two basic mechanisms have been proposed. One group advocates the anion radical as the stable product of the first one electron reduction, scheme 10. The other suggests that this anion rapidly loses a chloride ion (perhaps being replaced by a solvent molecule) but suggests that in many solvents the displacement of Cl^- is fully reversible, scheme 11.

$$Cp_2TiCl_2 + e^- \rightleftharpoons [Cp_2TiCl_2]^-$$

Scheme 10

$$Cp_2TiCl_2 + e^- \rightleftharpoons [Cp_2TiCl_2]^- \qquad (a)$$

$$[Cp_2TiCl_2]^- + L \overset{k}{\rightleftharpoons} Cp_2TiClL + Cl^- \qquad (b)$$

Scheme 11

It should be emphasised that the observation of a reversible system on the cyclic voltammogram, as is extensively reported, does not alone distinguish between the two mechanisms.

When considering the mechanism in scheme 11 where the rapid substitution of Cl^- by a solvent molecule or other suitable ligand occurs with the anion $[Cp_2TiCl_2]^-$ the cyclic voltammogram can only show a wholly reversible electron transfer under restricted conditions. The reverse reaction of eq. b, scheme 11, is second order and can only occur rapidly if Cp_2TiClL and Cl^- are in close proximity to each other and the reaction is fast. The Cp_2TiClL and Cl^- will only remain close together if their diffusion coefficients are equal. While this is unlikely, the magnitude of the difference and its influence on the cyclic

voltammetry is difficult to predict. A large excess of chloride ions in solution, for example from the supporting electrolyte, would render this reaction pseudo first order and a consideration of the rates of diffusion involved would not have to be made.

It is also a consequence of the mechanism in scheme 11 that the cyclic voltammogram should display a shift in both anodic and cathodic peaks to potentials more positive from the standard potential of the $Cp_2TiCl_2/[Cp_2TiCl_2]^-$ couple. The magnitude of this shift will depend on the equilibrium constant, K, for the reaction shown in eq. (b), scheme 11. The stronger the interaction of the solvent with the titanium centre the larger the shift will be.

A detailed electrochemical analysis of the redox behaviour of Cp_2TiCl_2 (and similar analogues) was reported in 1969 by Gubin and Smirnova [49]. They proposed that the reduction of Cp_2TiCl_2 in DMF at a dropping mercury electrode proceeds via two irreversible one electron transfers with cleavage of a Ti-Cl bond producing Cl^- at each stage. A similar mechanism was later proposed by Mugnier et al who studied the reduction of Cp_2TiCl_2 in THF, DMF and pyridine [50]. In THF Cp_2TiCl_2 gave three reduction waves at a platinum disc electrode with half-wave potentials of -0.80, -2.10 and -2.38 V vs SCE. The first wave showed all the characteristics of a reversible one electron transfer. In DMF three reduction waves are again seen at -0.63, -1.80 and -2.37 V vs SCE. The less negative potential in DMF compared to THF supports the occurrence of the reaction shown in eq. (b), scheme 11 since DMF is a more strongly binding ligand than THF. In DMF, the first reduction stage however, is irreversible except when LiCl is employed as the supporting electrolyte. In pyridine a reversible system can be seen at slow sweep rates but becomes irreversible when the sweep rate is increased. This is unusual in voltammetry but could arise if, at fast scan rates, the reverse reaction (of eq. a) is becoming important. This data together with voltammograms and ESR spectra on the products of bulk electrolysis at the potential of the first reduction wave, led Mugnier and co-workers to propose the mechanism shown in scheme 12 for

the first one electron reduction of Cp_2TiCl_2 (L is a solvent molecule or other suitable ligand.).

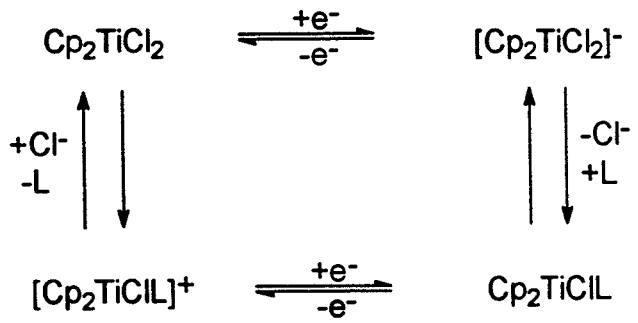

Scheme 12

The anion produced after the first one electron reduction is unstable and rapid substitution of Cl^- by a solvent molecule occurs. The reverse of this, ie the return of Cl^- to the metal can be seen if L is not strongly bound and/or the sweep rate is slow, hence the reversibility in THF (which is weakly bound) and in pyridine (intermediately bound between THF and DMF) at slow sweep rates. The anodic peak for the process $Cp_2TiClL \rightarrow [Cp_2TiClL]^+$ is seen at fast sweep rates (in pyridine) and when L is strongly bound (in DMF). Cp_2TiCl_2 is regenerated, so, on a repetitive sweep, the first reduction peak is seen again.

To support their mechanism Mugnier et.al. looked at the electrochemical oxidation of Cp_2TiClL where L = THF or $PPhMe_2$ in a solution which did not contain chloride ions. They found that Cp_2TiClL is oxidised to $[Cp_2TiClL]^+$ in a one electron step, this cation then rapidly reacts with Cp_2TiClL in solution to form Cp_2TiCl_2 and $[CpTiL_2]^+$. $[Cp_2TiL_2]^+$ can be further oxidised to $[Cp_2TiL_2]^{2+}$, scheme 13. Cp_2TiClL also shows two reduction waves (at -2.12 and -2.42 V vs SCE) which are very similar to the second and third waves of Cp_2TiCl_2.

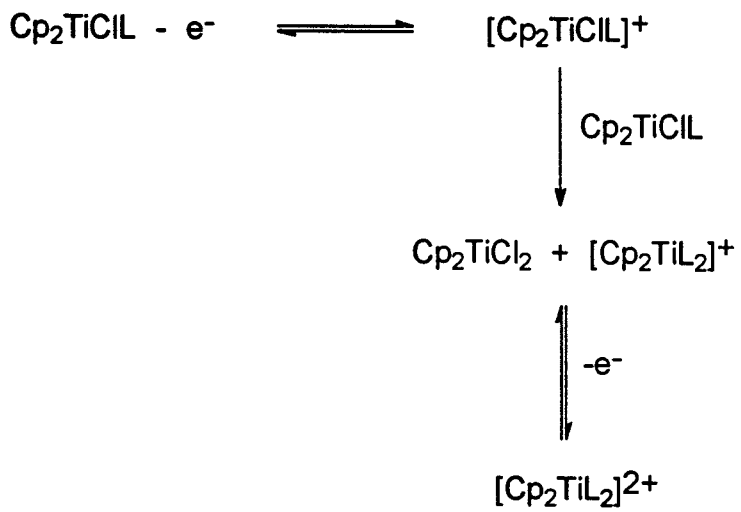

Scheme 13

The mechanism of the reduction of Cp_2TiCl_2 shown in scheme 12 is contested by another group of French workers [51,52]. Their studies suggest that the anion produced after the uptake of one electron is stable. They investigated the electrochemical behaviour of Cp_2TiCl_2 by polagraphy, cyclic voltammetry, coulometry and preparative electrolysis and found that the first electron transfer reaction, out of three, is highly reversible [51]. The other two show slight reversibility at slower scan rates (0.1 Vs^{-1}). The first electron transfer is completely reversible even for a scan rate of 0.001 Vs^{-1} in a thin layer linear potential sweep voltammogram which the authors interpreted as indicating that the one electron reduction of Cp_2TiCl_2 affords the stable radical anion $[Cp_2TiCl_2]^-$. In solutions that have been electrolysed at the potential equivalent to that of the first reduction of Cp_2TiCl_2 no free chloride ion could be detected and their ESR spectra reflect the presence of one unpaired electron, again supporting the idea that $[Cp_2TiCl_2]^-$ is the reduction product. The mechanism of the electrochemical reduction of Cp_2TiCl_2 as proposed by El Murr and co-workers is shown in scheme 14.

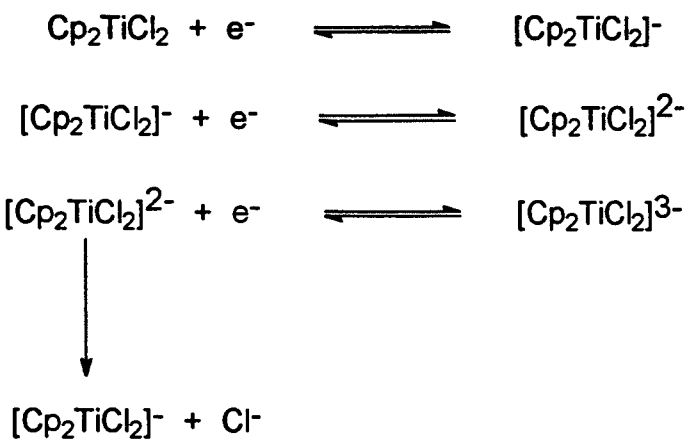

Scheme 14

In a slightly later publication El Murr and Chaloyard present further results of their study of the first one electron reduction of Cp_2TiCl_2 in DMF with Bu_4NPF_6 as the supporting electrolyte [52]. With solutions of low concentration (0.002 M) they obtained voltammograms identical to those published by Mugnier et al [50], but when higher concentrations of Cp_2TiCl_2 (0.01 M) were employed the voltammograms obtained were much different. A reversible system is seen even at very slow scan rates (0.025 Vs^{-1}) which is not reported in [50]. No chloride ion could be detected by El Murr in DMF and there was no change in the voltammogram on addition of Cl^-. When Br^- was added no new peak corresponding to $Cp_2TiClBr$ was observed as would be expected from scheme 13. It was proposed that a concentration of Cp_2TiCl_2 in DMF of 0.002 M is too low to give accurate results considering DMF always contains significant amounts of impurities. For example, any water in the solvent could affect the behaviour; it is easy to imagine L in scheme 12 being H_2O and the organic solvents themselves not acting as ligands at all.

In a attempt to clear up the controversy over the mechanism of the electrochemical reduction of Cp_2TiCl_2 Samuel and Vedel performed EPR studies on the species obtained upon the reduction of Cp_2TiCl_2 (and the bromide and iodide analogues) in THF by both chemical and electrochemical methods [53]. Chemical reduction of Cp_2TiCl_2 (using activated aluminium)

produces the dimer $[Cp_2TiCl]_2$, but in donor organic solvents, this exists as the solvated monomer; Cp_2TiClL (L = a solvent molecule). EPR spectra of this and of the electrochemically reduced species were practically the same and any differences were attributed to residual water in the THF that was used in the chemical reduction. It was claimed that residual water is not present in THF that has been electrolysed. The conclusion was that the first one electron reduction of Cp_2TiCl_2 produced the anion $[Cp_2TiCl_2]^-$ and this rapidly and reversibly loses Cl^- (scheme 12). Cp_2TiBr_2 and Cp_2TiI_2 exhibited the same behaviour. Some other Russian workers also support this mechanism [54, 55].

There is still great difficulty in determining the true mechanism of the reduction of titanocene dichloride, much of the data presented is very similar, it is the interpretations made from them that differ. It is perhaps significant that no Cl^- could be detected by El Murr after a controlled potential electrolysis of Cp_2TiCl_2 at the potential of the first one electron reduction. There has been no in-depth investigation into this system under super-dry conditions. The presence of water, even in very small amounts, is likely to hamper an accurate analysis since H_2O will be a better competitor as a ligand for the Ti(III) species than any of the other ligands considered. In the very low concentration experiments the effect of residual amounts of water will be much more pronounced which is perhaps why Mugnier an co-workers saw no reversibility in the first one electron transfer of 2 mM DMF solutions of Cp_2TiCl_2 [50]. Samuel and Vedel did consider the presence of water in their systems but only used it to explain small differences in the EPR spectra of chemically and electrochemically reduced Cp_2TiCl_2 [53].

A study of the electrochemical reduction of Cp_2ZrCl_2 carried out by El Murr et al reported the reversible generation of $[Cp_2ZrCl_2]^-$ but suggested that the subsequent behaviour of this species was dependant on traces of moisture. These traces of water were not considered in the titanium experiments [51]. Strelets reported that the $[Cp_2ZrCl_2]^-$ anion loses Cl^- at a slower rate than $[Cp_2TiCl_2]^-$ but otherwise follows the same reduction mechanism [54].

The replacement of chloride in Cp_2TiCl_2 by thiocyanate creating $Cp_2Ti(NCS)_2$, and the subsequent electrochemical reduction was reported to give evidence for the stability of the $[Cp_2Ti(NCS)_2]^-$ ion [56]. In THF, $Cp_2Ti(NCS)_2$ exhibits three reduction waves at $E_{½}$ = -0.53, -1.74 and -2.27 V vs SCE. Because NCS^- is more electronegative than Cl^-, $Cp_2Ti(NCS)_2$ reduces at less negative potentials than Cp_2TiCl_2. The first of these waves is wholly reversible, the next two irreversible. In dichloromethane only the first two waves are seen due to the cathodic limit of the solvent. EPR spectra and voltammetry on the products of the first reduction suggest that the anion $[Cp_2Ti(NCS)_2]^-$ is produced, so a process analogous to that shown in scheme 14 is proposed. In DMF the formation of a dimer follows the first electron transfer.

The reduction of Cp_2TiCl_2 under carbon monoxide is also cited as evidence for the stability of the $[Cp_2TiCl_2]^-$ ion [57]. El Murr and Chaloyard studied the generation of $[Cp_2TiCl_2]^-$ ions under CO pressure. As reported previously [51, 52] the cyclic voltammetry of a THF solution of Cp_2TiCl_2 containing Bu_4NPF_6 as the supporting electrolyte at a glassy carbon electrode showed three cathodic peaks at -0.86 V, -2.12 V and -2.44 V vs SCE. The first electron transfer is highly reversible while the other two are only slightly reversible. Under CO pressure a marked change in the cyclic voltammogram occurs; the reversibility of the first electron transfer decreases, the other two disappear and are replaced by two new cathodic peaks at -1.7 V and -2.8 V vs SCE. This indicates that a reaction with CO follows the addition of the first electron to Cp_2TiCl_2. Since CO has been reported not to react with the monomer Cp_2TiCl [58] El Murr and Chaloyard suggested that the CO reacts with the anion $[Cp_2TiCl_2]^-$. They performed controlled potential electrolysis on Cp_2TiCl_2 under CO pressure at the potential of the first electron transfer and found that the CO pressure decreased during the experiment and an IR spectrum of the product showed a CO adsorption band. Electrolysis at potentials after the second electron transfer led to the formation of $Cp_2Ti(CO)_2$. The scheme reported to account for this behaviour is shown in scheme 15. $Cp_2Ti(CO)_2$ is produced in almost quantitative yield in bulk electrolysis experiments since as

$[Cp_2Ti(CO)Cl_2]^-$ is reduced under CO pressure the equilibrium in (b) is shifted over to the right. These workers reported similar behaviour with Cp_2TiBr_2, again isolating $Cp_2Ti(CO)_2$.

$$Cp_2TiCl_2 + e^- \rightleftharpoons [Cp_2TiCl_2]^- \quad (a)$$

$$[Cp_2TiCl_2]^- + CO \rightleftharpoons [Cp_2Ti(CO)Cl_2]^- \quad (b)$$

$$[Cp_2Ti(CO)Cl_2]^- + e^- + CO \rightleftharpoons Cp_2Ti(CO)_2 + 2Cl^- \quad (c)$$

Scheme 15

The most recent work carried out on the redox behaviour of titanocene dichloride was reported by Anderson and Sawtelle in 1992 [59]. They reported on the electrochemical oxidation of Cp_2TiCl_2 in acetonitrile and proposed that this oxidation led to electron abstraction from the Ti–Cl bond, releasing $Cl^·$ upon the coordination of an acetonitrile molecule. Hence the product of the one electron oxidation was the $[Cp_2TiCl(CH_3CN)]^+$ cation. Similar behaviour was observed in CH_2Cl_2 solutions. A wave corresponding to this same oxidation was also observed by Gubin and Smirnova many years before in a polarographic investigation of Cp_2TiCl_2 but a detailed examination of it was not carried out [66].

1.3.2. Electrogeneration of Low-valent Titanium in the Presence of Alkylphosphine Ligands.

The stabilisation of low valent titanium species by alkylphosphine ligands a well known phenomenon in organic chemistry and is often put to use in synthetic applications, some electrochemical studies in this area have also been carried out. In their paper on the electrochemical behaviour of titanocene dihalides under CO pressure El Murr and Chaloyard mentioned the interaction of dimethylphenylphosphine, $PPhMe_2$ with THF solutions of electrolytically

generated $[Cp_2TiX_2]^-$ [57]. ESR analysis of these solutions showed an interaction between the titanium and the phosphine but the authors could not elaborate on the exact species produced. It was reported that the phosphine adduct evidently produced, was electrochemically oxidisable with the final product being titanocene dihalide, Cp_2TiX_2. The rival French group, Mugnier and co-workers, who advocate that a rapid, reversible loss of X^- follows the first one electron reduction of Cp_2TiX_2, reported on the oxidation of titanocene monochloride, Cp_2TiCl, in the presence of $PPhMe_2$. These researchers chemically prepared the Ti(III) species, $Cp_2TiCl(PPhMe_2)$ and went on to look at its redox behaviour using electrochemical techniques [60].

On a rotating disc electrode, $Cp_2TiCl(PPhMe_2)$ in THF gave one reduction wave $E_{½}$ = -2.12 V vs SCE and one oxidation wave, $E_{½}$ = -0.23 V vs SCE. The reduction wave seen at -2.12 V is the same as that observed for the reduction of Cp_2TiCl_2 in the presence of $PPhMe_2$. The oxidation at -0.23 V is also a one electron process. Exhaustive controlled potential electrolysis (oxidation) at E = -0.1 V consumes one Faraday and Cp_2TiCl_2 is isolated in about 50% yield. These results are explained in the equations 22, 23 and 24 below:

The oxidation wave at -0.23 V corresponds to :

$$Cp_2TiCl(PPhMe_2) - e^- \rightleftharpoons [Cp_2TiCl(PPhMe_2)]^+ \qquad (22)$$

The cation produced then reacts with the neutral starting species:

$$[Cp_2TiCl(PPhMe_2)]^+ + Cp_2TiCl(PPhMe_2) \downarrow Cp_2TiCl_2 + [Cp_2Ti(PPhMe_2)_2]^+ \qquad (23)$$

The oxidation in 22 involves only 0.5 electrons since half of the starting species is consumed in a reaction with the cation in which Cp_2TiCl_2 and $[Cp_2Ti(PPhMe_2)_2]^+$ are formed, equation 23. The fact that this oxidation wave

is seen as a one electron transfer in both the rotating disc experiment and the bulk electrolysis is because further oxidation of $[Cp_2Ti(PPhMe_2)_2]^+$ occurs at the same potential, equation 24.

$$[Cp_2Ti(PPhMe_2)_2]^+ \xrightarrow{-e^-} [Cp_2Ti(PPhMe_2)_2]^{2+} \qquad (24)$$

This also only involves 0.5 electrons since only half a mole of $[Cp_2Ti(PPhMe_2)_2]^+$ results from the oxidation of one mole of $Cp_2TiCl(PPhMe_2)$ (eq22). $[Cp_2Ti(PPhMe_2)_2]^{2+}$ is unstable and is consumed in a rapid chemical reaction.

Dimethylphenyl phosphine was also employed in a study of the electrochemical reduction of various substituted cyclopentadienyl titanocene derivatives [61]. From scheme 16 shown below, two anodic peaks could be observed if certain conditions are satisfied:

$$(C_5H_4X)_2TiCl_2 \underset{-e^-}{\overset{+e^-}{\rightleftharpoons}} [(C_5H_4X)_2TiCl_2]^- \underset{+Cl^-,\ -L}{\overset{-Cl^-,\ +L}{\rightleftharpoons}} (C_5H_4X)_2TiClL \qquad (a)$$

$$(C_5H_4X)_2TiClL \underset{}{\overset{-e^-}{\rightleftharpoons}} [(C_5H_4X)_2TiClL]^+ \underset{}{\overset{-L,\ +Cl^-}{\rightleftharpoons}} (C_5H_4X)_2TiCl_2 \qquad (b)$$

Scheme 16

If the recombination of Cl^- with $(C_5H_4X)_2TiClL$ and subsequent loss of L is slow then the oxidation of $(C_5H_4X)_2TiClL$ (eq. (b), scheme 16) should be visible on a cyclic voltammogram. This will be the case if L is strongly bound or if the cyclopentadienyl ligands have electron donating groups on them. Conversely electron withdrawing substituents should increase the rate of recombination.

These researchers reduced titanocene dichloride in the presence of various ligands [50] and found that L is less and less strongly bound in the sequence cyclohexyl isocyanide > DMF > 2,6-dimethylphenyl isocyanide > pyridine > $PPhMe_2$ > THF.

The electron donating character of the methyl groups in $Cp^*_2TiCl_2$ (Cp^* = pentamethylcyclopentadienyl), while shifting the reduction potentials to more negative values compared to those for Cp_2TiCl_2, did slow down the rate of recombination of Cl^- with Cp^*_2TiClL when L = THF. At fast scan rates two anodic peaks (those in equations (a) and (b) above) can be seen on the cyclic voltammogram. When the substituent, X, on the Cp ligand is the electron-withdrawing ester group $-CO_2Me$, the anodic peak corresponding to the oxidation of $(C_5H_4X)_2TiClL$ is not dominant, as the previous argument would suggest. This is because the anion formed from the initial reduction is relatively stable and so the rate of recombination is not such an issue as Cl^- is less willing to leave in the first place. Faster scan rates increase the reversibility of the electron transfer in equation (a), scheme 16, rather than decreasing it as in the case where the anion is less stable and Cl^- is lost rapidly.

The same paper describes the electrochemical reduction of $[\eta^5\text{-}C_5H_4(CH_2)_2PPh_2]_2TiCl_2$, whose reduction potentials are not greatly different from those for Cp_2TiCl_2 since the alkylphosphine substituent has no great electron donating or withdrawing properties. However, it is worth noting that there is no reverse anodic peak coupled to the first one electron reduction for this titanocene derivative. This is reported to be because internal ligandation occurs where the phosphine chelates to the metal after the loss of Cl^- from the anion.

1.3.3. The Electrochemistry of Substituted Cyclopentadienyl Titanium Complexes.

As has already been briefly mentioned alkyl substituents on the cyclopentadiene ring display an inductive effect so making the substituted dicyclopentadienyl titanium dichloride analogues more difficult to reduce at the first stage, although the magnitude of this difference is not great. Further evidence for this comes from Strelets et al who studied the electrochemical

reduction of $(MeC_5H_4)_2TiCl_2$ and $Cp^*_2TiCl_2$ (Cp^* = pentamethylcyclopentadienyl) in THF and found that the half-wave potentials were -0.93 (compared to -0.86 V for Cp_2TiCl_2) and -1.09 V vs SCE [55]. The second reduction became comparatively easier with the introduction of more methyl groups. If the cyclopentadienyl ligands are bridged by an alkyl chain the second electron transfer becomes increasingly difficult the shorter the bridge, for example; ΔE (the difference in half-wave potentials between the first and second reduction waves) for $(CH_2)(C_5H_4)_2TiCl_2$ is 1.29 V whereas it is only 1.16 V for $(CH_2)_3(C_5H_4)_2TiCl_2$. This reflects the difficulty of the Ti(III) → Ti(II) step which is caused by the need to increase the Cp-Ti-Cp angle in going to the titanocene structure ('Cp_2Ti') which is obviously more difficult the shorter the bridge. Schwemlein and co-workers looked at the electrochemistry of tetramethylethylene-bridged dicyclopentadienyl titanium dichloride, $[Me_4C_2(C_5H_4)_2]TiCl_2$, in THF which displayed a one electron reduction at a slightly more negative potential than Cp_2TiCl_2 ($E_{½}$ = -0.92 V vs SCE) which would be due to the inductive effect of the alkyl bridge [62]. Again the second electron transfer proved more difficult, occurring at -2.53 V vs SCE for the bridged complex compared to -2.13 V for Cp_2TiCl_2. For all these bridged titanium complexes a third reduction stage is not seen reflecting the low stability of a bridged titanocene. The bridged complex $[Si(CH_3)_3(C_5H_4)_2]TiCl_2$ is reported to exhibit only one one electron reversible reduction in THF at -0.79 V vs SCE, very close to that of Cp_2TiCl_2 ($E_{½}$ = -0.8 V vs SCE in this work) [63]. the absence of any further reduction is an indication that the $[Si(CH_3)_3(C_5H_4)_2]^{2-}$ ligand stabilizes the Ti(III) oxidation state.

1.3.4. The Electrochemistry of Titanocene Alkyl Derivatives.

Other titanocene derivatives that have been investigated electrochemically are those containing titanium-carbon σ-bonds; Cp_2TiXR and Cp_2TiR_2 (X = halide, R = alkyl or aryl). Again there are some discrepancies over the exact nature of the species produced after electrochemical reduction.

Chivers and Ibrahim conducted electrochemical studies on Cp_2TiClR as part of an investigation into the identity of the active titanium species in nitrogen fixation reactions [64]. Cp_2TiClR (R = CH_3) was reported to lose Cl^- after the addition of one electron at a mercury cathode in DME/Bu_4NClO_4 solution, yielding the Ti(III) species $Cp_2Ti(CH_3)$, which is green. This one electron reduction process at -1.26 V vs SCE was irreversible, as was the second cathodic process observed at -2.32 V vs SCE. When produced in THF the green solution of $Cp_2Ti(CH_3)$ changes to blue. This colour change is seen both under a nitrogen and an argon atmosphere; the authors concluded that this blue complex was not a $[Cp_2TiR.N]_n$ species as was previously cited [65]. A similar behaviour pattern was previously observed for $Cp_2TiCl(C_6F_5)$ and the suggestion was that the blue species is a secondary product resulting from the interaction of the electrochemically generated $Cp_2Ti(III)R$ with the solvent THF, or by isomerization (scheme 17).

$$Cp_2TiCl(CH_3) + e^- \longrightarrow Cp_2Ti(CH_3) + Cl^-$$

$$Cp_2Ti(CH_3) + \text{solvent} \xrightarrow{k} Y$$
green → blue

$$Y + e^- \longrightarrow Z$$

Scheme 17

The voltammetry of $Cp_2TiCl(CH_3)$ does show an oxidation wave on the positive sweep which, on the reverse sweep to cathodic potentials, has associated with it a cathodic wave. These observations are explained by the process shown in equation 25.

$$Cp_2Ti(CH_3) \underset{-e^-}{\overset{+e^-}{\rightleftharpoons}} [Cp_2Ti(CH_3)]^+$$

Equation 25

Gubin and Smirnova include $Cp_2TiCl(CH_3)$ in their electrochemical investigation

into the σ-bonds in some transition metal π-complexes [66]. Their main concern was the rate at which the metal-carbon bond cleaved after reduction and hence the stability of the carbanion initially generated. Polarographic reduction of $Cp_2TiCl(CH_3)$ in a DMF/Bu_4NClO_4 solution gave a wave with $E_{½}$ = -1.17 V vs SCE compared to -0.63 V for Cp_2TiCl_2 showing that the replacement of one chlorine by methyl inhibits reduction. This is again supported when both chloride ligands are replaced by methyl groups; $Cp_2Ti(CH_3)_2$ gave a reduction wave at -1.91 V vs SCE under the same conditions. However when the R groups in Cp_2TiR_2 are both carboranyl groups (VIII) the half-wave potential for the first one-electron reduction moves to positive values ($E_{½}$ = +0.96 V vs SCE). Carboranyl is a strong electron-attracting group and a relatively stable carbanion is formed thereby facilitating cleavage of the Ti-C σ-bond in the one electron reduction of Cp_2TiR_2 (scheme 18).

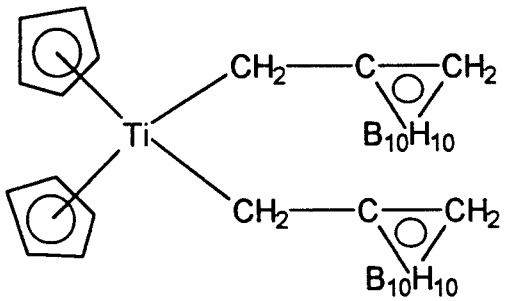

VIII

$$Cp_2TiR_2 + e^- \longrightarrow [Cp_2TiR] + R^-$$

Scheme 18

In a study of alkyl and aryloxy titanocene derivatives El Murr et al propose a reduction scheme involving the cleavage of the Ti-Cp π-bond and the consequent loss of Cp^- after the addition of one electron (scheme 19) [67].

Cyclic voltammograms of these Cp_2TiL_2 species in THF/Bu_4NPF_6 solutions at

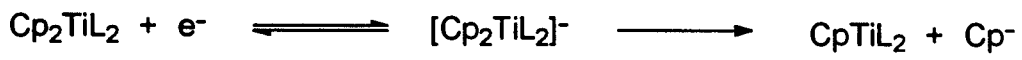

$L = CH_3, CH_2Ph, OAr, OSiR_3$

Scheme 19

platinum or glassy carbon after controlled potential electrolysis at the potential of the first one electron reduction, exhibited no anodic peak corresponding to the process $[Cp_2TiL_2]^- \rightarrow Cp_2TiL_2$, but showed an anodic peak corresponding to the oxidation of the free cyclopentadienyl anion. The conclusion drawn from this was that with complexes of the type in scheme 19, the first one-electron reduction is a reversible process leading to a Ti(III) anion. This then undergoes a chemical rearrangement with loss of a cyclopentadienyl anion giving a neutral monocyclopentadienyl Ti(III) species.

The same investigation into monocyclopentadienyl titanium derivatives, $CpTiL_3$, showed that loss of the alkyl or aryloxy group followed the addition of the first electron (scheme 20).

$L = CH_3, CH_2Ph, OAr, OSiR_3$

Scheme 20

The overall suggestion of this work is that the electrochemical method of reduction of Cp_2TiL_2 and $CpTIL_3$ affords a route to the synthesis of neutral monocyclopentadienyl Ti(III) derivatives and that d^1 dicyclopentadienyl and d^1 monocyclopentadienyl anions are not chemically stable. In the same publication El Murr et al do report that the reduction of Cp_2Ti(biphenyl-2,2'-diyldioxy) (IX) affords a stable anion that is detectable by ESR techniques, but only on the time scale of a voltammetric experiment. When bulk electrolysis is performed only the Cp^- anion is detectable.

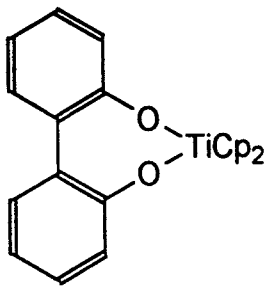

IX

Mugnier and co-workers carried out electrochemical investigations into Cp_2TiR_2 where R this time was a phenylethynyl ligand, -C≡CPh [68]. They expected a more stable anion to form after reduction than that formed when the R group was a biphenyl ligand (IX) because of the presence of the triple bond. This was indeed reported to be the case; $[Cp_2TiR_2]^-$ was comparatively stable, enough so, that the reaction involving loss of Cp^- took longer than one day to reach completion.

1.3.5. The Electrochemistry of Monocyclopentadienyl Titanium Trichloride, $CpTiCl_3$.

Although a fair number of monocyclopentadienyl titanium(IV) complexes have been synthesised [38], there does not exist a wealth of electrochemical data on them. The electrochemical reduction of monocyclopentadienyl titanium alkyl and aryloxy compounds $CpTiR_3$ and $CpTi(OAr)_3$ has already been mentioned [67]. Gubin and Smirnova did run polarographic reductions of DMF/Bu_4NClO_4 solutions of $CpTiCl_3$ and Cp^*TiCl_3 (Cp^* = pentamethyl cyclopentadienyl, $C_5(CH_3)_5$) [49]. Both complexes showed three one electron reduction waves, each one corresponding to the reduction of successive Ti-Cl σ-bonds (scheme 21). In Cp^*TiCl_3 the electron donation from the methyl groups shifts the reduction potentials to more negative values compared to those for $CpTiCl_3$ as was the case with the dicyclopentadienyl complexes.

$$CpTiCl_3 + e^- \longrightarrow CpTiCl_2 + Cl^-$$

$$CpTiCl_2 + e^- \longrightarrow CpTiCl + Cl^-$$

$$CpTiCl + e^- \longrightarrow [CpTi]$$

Scheme 21

1.4. ELECTROCHEMISTRY UNDER 'SUPER-DRY' CONDITIONS.

Whilst most Ti(IV) species are probably stable enough to exist for short periods in a normal atmosphere, at least for the time it takes to prepare the solutions and set up the experiment, the lower oxidation state species are frequently extremely air and moisture sensitive. Since the organic chemistry of titanium compounds invariably involves the reduction of Ti(IV) to a +3 or +2 oxidation state it is necessary to perform these experiments under a carefully controlled atmosphere. For organic manipulations this involves employing conventional Schlenk techniques [69] using a vacuum line to evacuate the reaction vessel and refilling with argon or nitrogen.

Similarly in the electrochemical investigations into the redox behaviour of organotitanium compounds it is essential to employ ultra-dry, inert conditions if reliable conclusions are to be drawn. The low-valent titanium intermediates and products of electrode reactions are highly reactive and are usually generated in concentrations low enough to make small amounts of water and oxygen of critical importance.

Keszthelyi describes how vacuum line techniques can be adapted for electrochemical purposes [70]. Cells need to be designed so that they are completely vacuum tight, there should be a way in which liquids can be injected with minimum risk of air contact and ideally the cell should be made

to withstand temperatures up to 150°C for drying purposes. Heinze, however, suggests that conventional vacuum techniques do not remove all traces of water from the walls of the cell and the supporting electrolyte [71]. Hammerich and Parker, in their investigations of electrogenerated cation radicals advocated the use of superactive neutral alumina to remove trace amounts of water from their systems [72]. They suspended the alumina in their voltammetric solution and saw the reversible oxidation of aromatic cations to dications which, without this extra drying procedure, was an irreversible process. Kiesele adopted the alumina idea in his design for an electrochemical cell for voltammetry, coulometry and synthesis in super-dry media [73].

However, due to the possibility of uncontrolled adsorption, the presence of alumina in the electrolytic solutions makes such systems unsuitable for the preparative scale generation of reactive intermediats [74]. This problem led Kiesele to suggest the filtering of the electrolytic solution through a column of alumina into the working compartment of the cell prior to use.

A cell for use with a vacuum line was designed by Heinze incorporating a system whereby the electrolytic solution can be dried with alumina before being added to the electroactive species in the working compartment [71]. The whole aparatus containing the electroactive could be evacuated before use and refilled with an inert gas. The design was such that if the electroactive species was a liquid it was able to be frozen by placing the cell in liquid nitrogen before evacuation. The electrolytic solution was added through syringe via a rubber septum into a compartment containing the alumina and rotation of this section allowed the dry solution to pass into the working compartment through a glass sinter. Applying a positive pressure of argon to the cell while, at the same time, applying a small vacuum to the Luggin compartment drew some of the solution up to allow the reference electrode to function properly. A magnetic stirrer bead was placed in the working compartment to enable the dissolution of the electroactive species.

Of course there are distinctive disadvantages in employing vacuum techniques to electrochemical investigations, not least the time consuming nature of its use. For example, it may only take a matter of minutes to run a cyclic voltammogram but all day to prepare the apparatus so that the atmosphere and equipment is clean and dry. It is also difficult to control the concentrations of the solutions being used and there is a danger of breakage of specialist glassware which may be expensive and difficult to repair.

An alternative for 'super-dry' electrochemical investigations is the use of a glove or dry-box. Provided a dry-box is fitted with the correct connections, cells can be placed inside and air and moisture sensitive experiments performed quite safely. Compared to vacuum techniques, this enables cheaper apparatus to be used, a better control on concentration and often saves time. However, a dry-box is a very costly item and may prove expensive to install and maintain, working space is limited, temperature studies are not very feasible and it is also necessary to deoxygenate liquids prior to transfer. A detailed consideration of the use of a dry-box in electrochemistry can be found alongside the discussion on vacuum techniques in [70].

1.5. PROJECT OBJECTIVES.

The disagreements over the mechanism of the electrochemical reduction of Cp_2TiCl_2, with both sides of the argument offering compelling evidence in support of their case, indicates that further studies in this area are necessary. Conclusions need to be reached regarding the conditions under which this species is investigated and the intermediates involved. Hence very dry studies were deemed necessary in the extended research into organotitanium derivatives of interest in synthesis.

The general aim was to study, by electrochemical methods, low oxidation state organotitanium compounds. The eventual objective being to optimize

conditions in order to be able to apply such methods to the use of these compounds in organic synthesis, particularly asymmetric synthesis.

CHAPTER 2

EXPERIMENTAL PROCEDURES AND TECHNIQUES

2.1 SYNTHETIC EXPERIMENTATION AND REAGENTS

All experiments were performed in a fume cupboard under an argon atmosphere using standard Schlenk techniques unless otherwise stated, the argon was passed through a column of molecular sieves before entering the reaction vessels and all glassware was dried in an oven at 150°C for at least 12 hours prior to use. Evacuation of apparatus was achieved using an Edwards two-stage oil pump connected via a vacuum line and pressures measured with an Edwards vacustat 2 gauge. Typical evacuation pressures were between 0.05 and 0.20 mbar.

^{1}H and ^{13}C nmr were recorded on a JOEL GX 270 FT nmr spectrometer. Mass spectrometry was performed on a VG Analytical 70-250-SE Normal Geometry Double Focusing mass spectrometer. All electron ionisation (EI) data was recored at 6 kV at 70 eV with a source temperature of 200°C.

Most reagents were supplied by Aldrich, including Cp_2TiCl_2 in 97% purity. 2,6-di-isopropylphenol and 2-iso-propyl alcohol were distilled before use. All solvents were dried and distilled; Et_2O, benzene and THF were distilled from Na/benzophenone, hexane was dried with concentrated H_2SO_4 (neutralizing with Na_2CO_3 afterwards) and $MgSO_4$ before distillation from Na/benzophenone and tetraglyme. Dichloromethane, xylene and triethylamine were distilled from CaH_2. THF was used straight from the still, all other solvents were stored in sealed glass vessels under argon and transferred by syringe.

2.2 SYNTHETIC PROCEDURES[1]

Monocyclopentadienyl Titanium Trichloride, $CpTiCl_3$ [75].

To Cp_2TiCl_2 (12 g, 48 mmol) in xylene (100 ml), $TiCl_4$ (14.7 ml, 130 mmol) was added and the reaction mixture left refluxing. After 3 hours it was allowed to cool down to room temperature when large dirty yellow crystals formed. The solvent was carefully decanted off with a constant stream of argon going through the flask. The crystals were washed with hexane (3 x 30 ml). Benzene (110 ml) with some decolourizing charcoal (3 small spatula heads) added and the mixture was carefully heated and filtered hot through a large glass in-line sinter. A clear yellow solution emerged which was left standing for $CpTiCl_3$ to recrystallize out overnight, giving a first crop of 8.3 g of bright yellow crystals (78 % yield). A second crop was obtained by concentrating down the remaining solution. A total yield of 97% was obtained.

^1H nmr ($CDCl_3$) δ 7.05 (s)
^{13}C nmr ($CDCl_3$) δ 123.6
Melting point: 108-110°C (literature 110°C)

Preparation of (2,6-di-isopropyl)-4-nitrophenol [76].

2,6-di-isopropylphenol (5 ml, 27 mmol) was mixed with iso-octane (2,2,4-trimethylpentane, 10 ml) and 50% aqueous nitric acid (1.6 ml, 0.4 equivalents) was added dropwise while making sure that the temperature did not exceed 30°C. After stirring for about ½ hour the colour of the reaction mixture went from pale yellow to orange and a precipitate formed. Stirring was continued for another 1½ hours, after which time the mixture was cooled and filtered and the residue washed thoroughly with water. This residue was recrystallized from

[1] All preparations that are not referenced relate to novel products.

iso-octane (10 ml), washing the crystals with ice-cold iso-octane then drying them under vacuum afforded the cream coloured product in 18% yield.

^{1}H nmr ($CDCl_3$)	δ 8.0 (2H, s), 5.50 (1H, s), 3.18 (2H, septet, J = 6.76 Hz), 1.31 (12H, d, J = 6.76 Hz).
^{13}C nmr ($CDCl_3$)	δ 155.9, 134.7, 120.2, 27.5, 22.5.

Preparation of Monocyclopentadienyl Titanium Dichloride Alkoxides, $CpTiCl_2[OR]$.

Two different procedures, outlined below, were employed to synthesise these $CpTiCl_2[OR]$ complexes, table 2.2.1 summarises which method was used for which alcohol substrate and the yields obtained. The most extensively used method of preparation, that using triethylamine, developed from the work reported by Duthaler and co-workers [43], was only replaced by the method involving the sodium salt of the alcohol (from Kalirai et al [ref]) late in the work when it was developed for the preparation of $CpTiCl_2[OC_6H_2(^iPr)(NO_2)]$. Structural illustrations of each of the seven $CpTiCl_2[OR]$ complexes are shown in figure 2.2.1. ^{1}H and ^{13}C nmr data for each complex is also tabulated below along with their mass spectral data. A more detailed discussion on the synthesis of these complexes along with an analysis of their nmr data appears in chapter 3.

A typical experimental procedure is described below. Generally the scales used were of the order 3 - 5 mmol. The literature references for each method refer to the general procedures, not the specific reactants and products.

Moncyclopentadienyl Titanium Dichloride (2,6-di-isopropyl)-phenoxide, $CpTiCl_2[OC_6H_3(^iPr)_2]$

METHOD A [41].

$CpTiCl_3$ (0.66 g, 3 mmol) was dissolved in diethylether (60 ml) giving a clean yellow solution. To this (2,6-di-isopropyl)-phenol, $[(CH_3)_2CH]_2C_6H_3OH$ (0.55 ml, 3 mmol), was added and the resulting solution allowed to stir for approximately 2 minutes, then triethylamine, Et_3N (0.46 ml, 3.3 mmol) was added dropwise. An immediate white precipitate was observed along with a colour change of the solution to orange. The reaction mixture was left stirring overnight then filtered through an in-line glass sinter, the residue washed twice with Et_2O (2 x 20 ml), the washings combined with the filtrate and the solvent removed *in vacuo* leaving an orange/red solid. This was recrystallized from hexane (25 ml) affording the title compound in 70% yield.

METHOD B [16].

Sodium hydride (0.6 g of a 60% suspension in oil, 15 mmol) was washed with petroleum ether (5 ml) to remove the oil, then dried under vacuum. Toluene (40 ml) and (2,6-di-isopropyl)-phenol, $[(CH_3)_2CH]_2C_6H_3OH$ (0.9 ml, 5 mmol) were added to the NaH and the mixture allowed to stir for ½ an hour at 100°C (oil bath). A solution of $CpTiCl_3$ (1.1 g, 5 mmol) in toluene (40 ml) was prepared and added to the reaction vessel, upon which it changed colour from yellow to orange. The reaction was left stirring at 100°C overnight, allowed to cool to room temperature and then filtered through a glass sinter packed with kieselguhr. The toluene was removed *in vacuo* and the resultant orange/red solid recrystallised from hexane (40 ml). $CpTiCl_2[OC_6H_3(^iPr)_2]$ was isolated in 63% yield.

Monocyclopentadienyl Titanium Dichloride (2,6-di-isopropyl-4-nitro)phenoxide, $CpTiCl_2[OC_6H_2(^iPr)_2(NO_2)]$.

This compound was only prepared by method B outlined above, method A was attempted but only starting material could ever be isolated from the reaction mixture. Recrystallizations from hexane were also unsuccessful but a clean sample of the title compound was isolated after washing the crude product in hot iso-octane (to remove any of the starting nitrophenol) then filtering a dichloromethane solution of it through a glass sinter. The dichloromethane was removed by evacuation and the complex obtained in 86% yield.

Compound	Experimental Method	Yield (%)
$CpTiCl_2[OC_6H_3(^iPr)_2]$	A B	70 63
$CpTiCl_2[O^iPr]$	A	50
$CpTiCl_2$[menthoxide]	A	70
$CpTiCl_2[OC_6H_3(Me)_2]$	A	76
$CpTiCl_2[OC_6H_2(^iPr)_2(NO_2)]$	A B	- 86
$CpTiCl_2[OC_6H_2(Me)_2(Br)]$	A B	50 42
$CpTiCl_2[OC_6H_2(Me)_3]$	B	40

Table 2.2.1

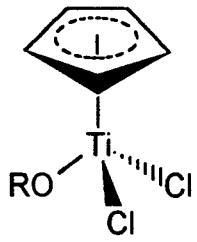

RO =

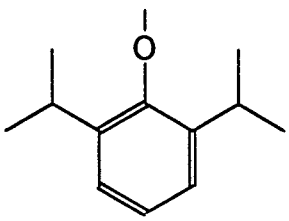

$-OC_6H_3(^iPr)_2$

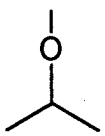

$-O^iPr$

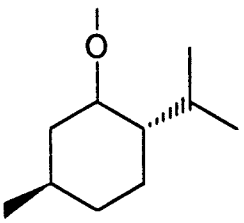

-menthoxide

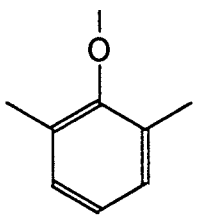

$-OC_6H_3(Me)_2$

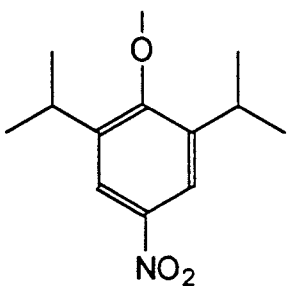

$-OC_6H_2(^iPr)_2(NO_2)$

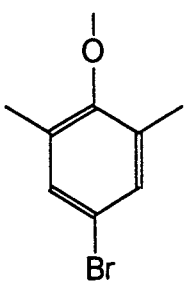

$-OC_6H_2(Me)_2(Br)$

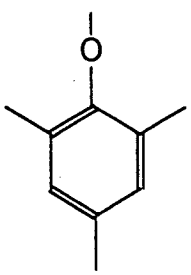

$-OC_6H_2(Me)_3$

Figure 2.2.1

$CpTiCl_2[OR]$ - Analytical Data

$CpTiCl_2[OC_6H_3(^iPr)_2]$

Colour:	orange/red
Melting point:	128-129°C
^1H nmr ($CDCl_3$)	δ 7.04-7.16 (3H, m), 6.72 (5H, s), 3.19-3.30 (2H, septet, J = 6.76 Hz), 1.24-1.26 (12H, d, J = 6.76).
^{13}C nmr ($CDCl_3$)	δ 164.6 s, 138.3 s, 124.7 d, 123.5 d, 120.9 d, 27.1 d, 23.7 q.
EI mass spec.	m/e 360 (M^+, 85%), 345 ($M^+ - CH_3$, 22%), 309 ($M^+ - CH_3$ - HCl, 100%), 288 (M^+ - 2HCl, 70%), 273 (M^+ -2HCl -CH_3, 16%), 183 ($M^+ - C_{12}H_{17}O$, 15%), 177 ($C_{12}H_{17}O^+$, 20%).

$CpTiCl_2[O^iPr]$.

Colour:	yellow
Melting point:	104-105°C
^1H nmr ($CDCl_3$)	δ 6.70 (5H, s), 4.90-5.04 (1H, septet, J = 6.2 Hz), 1.35-1.40 (6H, d, J = 6.2 Hz).
^{13}C nmr ($CDCl_3$)	δ 119.0 d, 87.3 d, 25.0 q.
EI mass spec.	m/e 242 (M^+, 20%), 227 ($M^+ - CH_3$, 100%), 200 ($M^+ - C_3H_6$, 16 %), 183 ($M^+ - C_3H_7O$, 67%), 164 ($M^+ - C_3H_6$ - HCl, 40%), 148 ($M^+ - C_3H_6O$ - HCl, 32%).

$CpTiCl_2$[menthoxide]

Colour:	yellow
Melting point:	89-90°C
^1H nmr ($CDCl_3$)	δ 6.66 (5H, s), 4.44-4.56 (1H, dt, J = 4.2, 10.5 Hz), 2.20-2.35 (1H, double septet, J = 6, 15 Hz), 2.07-2.20 (1H, m), 1.55-1.70 (2H, m), 1.35-1.70 (2H, m), 1.20-1.35 (1H, q, J = 7 Hz), 0.95-0.97 (3H, d, J = 6.4 Hz), 0.91-0.94 (3H, d,

J = 7Hz), 0.90 (2H, m), 0.82-0.84 (3H, d, J = 7 Hz).

^{13}C nmr ($CDCl_3$) δ 119.0 d, 95.9 d, 50.6, 44.6 t, 34.1 t, 32.0, 25.9, 22.8 t, 22.2, 21.0, 15.8.

EI mass spec. m/e 338 (M^+, 12%), 302 (M^+ - HCl, 100%), 266 (M^+ - 2HCl, 18%), 253 (M^+ - 2HCl - CH, 45%), 183 (M^+ - $C_{10}H_{19}O$, 30%).

$CpTiCl_2[OC_6H_3(Me)_2]$

Colour: orange/red

Melting point: 114-115°C

^{1}H nmr ($CDCl_3$) δ 6.90-7.10 (3H, m), 6.73 (5H, s), 2.30 (6H,s).

^{13}C nmr ($CDCl_3$) δ 128.6, 127.6, 124.2, 121.0 d, 17.4 q.

EI mass spec. m/e 405 (M^+, 90%), 268 (M^+ - HCl, 20%), 232 (M^+ - 2HCl, 100%), 203 (M^+ - HCl - Cp, 25%), 183 (M^+ - C_8H_9O, 24%), 148 (M^+ - C_8H_9O - Cl, 23%), 121 ($C_8H_9O^+$, 24%).

$CpTiCl_2[OC_6H_2(^iPr)_2(NO_2)]$

Colour: yellow/orange

Melting point: decomposes above 200°C

^{1}H nmr ($CDCl_3$) δ 8.03 (2H, s), 6.77 (5H, s), 3.16-3.26 (2H, septet, J = 6.76 Hz), 1.27-1.29 (12H, d, J = 6.76 Hz).

^{13}C nmr ($CDCl_3$) δ 167.5 s, 143.6 s, 139.8 s, 121.6 d, 119.9 d, 27.5 d, 23.4 q.

EI mass spec. m/e 405 (M^+, 90%), 390 (M^+ - CH_3, 15%), 354 (M^+ - CH_3 - HCl, 100%), 333 (M^+ - 2HCl, 15%), 304 (M^+ - HCl - Cp, 57%).

$CpTiCl_2[OC_6H_2(Me)_2(Br)]$

Colour:	orange/red
Melting point:	136-138°C
^1H nmr ($CDCl_3$)	δ 7.20 (2H, s), 6.73 (5H, s), 2.25 (6H, s).
^{13}C nmr ($CDCl_3$)	δ 131.2 s, 129.7 s, 122.4 s, 121.2 d, 120.7 d, 17.3 q.
EI mass spec.	m/e 382 (M^+, 100%), 309 (M^+ - 2HCl, 27), 266 (M^+ - Cp - HCl - CH_3, 24%), 182 (M^+ - C_8H_9OBr, 30%).

$CpTiCl_2[OC_6H_2(Me)_3]$

Colour:	red
Melting point:	108-110°C
^1H nmr ($CDCl_3$)	δ 6.81 (2H, s), 6.72 (5H, s), 2.27 (9H, s).
^{13}C nmr ($CDCl_3$)	δ 133.9, 129.1, 127.4, 120.9, 21.0, 17.4.
EI mass spec.	m/e 318 (M^+, 90%), 282 (M^+ - HCl, 12%), 246 (M^+ - 2HCl, 54%), 217 (M^+ - Cp - HCl, 17%), 183 (M^+ - $C_9H_{11}O$, 10%), 135 ($C_9H_{11}O^+$, 100%).

Preparation of 1-undecene-6-yne.

To a magnetically stirred solution of 1-hexyne (3.29 g, 40 mmol) in THF (20 ml) at -30°c was added ^{n}BuLi (22 ml of 1.8 M solution in hexane, 40 mmol). The reaction mixture was left stirring at -30°C for 1 hour, a faint white precipitate was evident throughout. A solution of 5-bromo-pent-1-ene (5.96 g, 40 mmol) in HMPA (30 ml) was prepared and transferred dropwise via canula to the reaction flask at 0°C over ½ an hour. The resulting mixture, a yellow solution, was allowed to warm up to room temperature and left stirring overnight, then poured onto H_2O (100 ml) and extracted with petroleum ether (100 ml + 50 ml). The extracts were combined, washed with water, dried over $MgSO_4$ and

then the solvent removed by rotary evaporation. The crude product was a thick yellow liquid which was purified to a colourless liquid by Kugelrohr distillation. The title compound was obtained in 85% yield.

^{1}H nmr ($CDCl_3$) δ 5.80(1H, ddt, J = 17.2, 10.0, 6.6 Hz), 5.08-4.93 (2H, m), 2.15 (6H, m), 1.70-1.29 (6H, m), 0.91 (3H, t, J = 7.2 Hz).

^{13}C nmr ($CDCl_3$) δ 138.2 d, 115.0 t, 80.6 s, 79.8 s, 33.0 t, 31.4 t, 28.5 t, 22.1 t, 18.6 t, 18.3 t, 13.8 q.

Preparation of 3,3-bis(cyclopentadienyl)-2-^{n}butyl-3-titanabicyclo[3.3.0]-oct-1-ene (6A) [32].

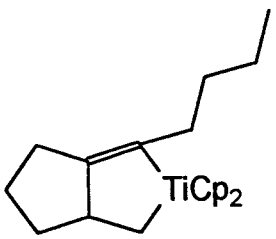

Cp_2TiCl_2 (0.5 g, 2 mmol) was dissolved in THF (10 ml) and cooled -70°C. To this ^{n}BuLi (2.2 ml of a 1.81 M solution in hexane, 2 equivs) and PMe_3 (4 ml of a 1.0 M solution in THF, 2 equivs) were added, the reaction mixture allowed to warm up to room temperature and left stirring for 1 hour. To the resulting brown-black mixture 1-undecen-6-yne (0.3 g, 2 mmol) was added with further stirring for 1 hour. The THF was removed *in vacuo* and the product extracted into hexane (8 ml). The hexane solution was transferred to another flask and the solvent removed *in vacuo* affording the title compound in 75% yield (0.5 g) as dark red crystals.

^{1}H nmr (C_6D_6) δ 6.0 (5H, s), 5.95(5H, s), 2.5-2.0 (7H, m), 1.9-1.7 (1H, m), 1.6-1.3 (5H, m), 1.3-0.9 (5H, m).

^{13}C nmr (C_6H_6) δ 113.5, 111.7, 58.4, 41.2, 40.0, 32.4, 30.3, 23.9, 22.7, 14.4.

Preparation of $Cp_2Ti(PMe_3)_2$ [77].

Cp_2TiCl_2 (0.5 g, 2 mmol), ground magnesium turnings (0.2 g, 8 mmol) and $HgCl_2$ (0.01 g, 0.02 equivalents) were stirred in THF (5 ml) for approximately 5 minutes. Trimethylphosphine as a 1 M solution in THF (8 ml), 8 mmol) was added and the reaction vessel placed in a sonicator until a colour change (red → brown) was observed, then the reaction mixture left stirring at 30°C overnight. The THF was removed from the black-brown mixture *in vacuo*. The residue was extracted with hexane (10 ml + 5 ml), after removal of the hexane *in vacuo* black crystals of $Cp_2Ti(PMe_3)_2$ were obtained in 60% yield.

^1H nmr (C_6D_6) δ 4.69 (10 H, s), 0.98 (18 H, s).

^{13}C nmr (C_6H_6) δ 91.4 d, 23.8 q.

Preparation of $Cp_2TiCl(PMe_3)$

$Cp_2TiCl(PMe_3)$ was prepared by a disproportionation reaction: a solution of Cp_2TiCl_2 in THF (0.05 M) was prepared and added dropwise with stirring to a THF solution of $Cp_2Ti(PMe_3)_2$ until the colour went from brown-black to blue-green. 13 ml (0.65 mmol) of the Cp_2TiCl_2 solution was added, a quantitative yield of the title compound was assumed. The THF was removed *in vacuo* affording blue-green crystals.

EI mass spec. m/e 213 (M^+ - PMe_3, 90%), 178 (Cp_2Ti^+, 22%), 148 ($CpTiCl^+$, 100%).

2.3 ELECTROCHEMICAL PROCEDURES

2.3.1 Cyclic Voltammetry.

Cyclic voltammetry was carried out on THF solutions of the various organotitanium species under investigation. Three different types of cells were used; one for experiments by standard procedures in the laboratory and two for use with a vacuum line to ensure dry conditions, one of these being adapted for controlled potential electrolysis experiments. A more detailed account of the design and utilisation of these cells appears in chapter 4. Basically they consist of three electrodes; a vitreous carbon disc or platinum gauze working electrode, a platinum wire hoop or gauze secondary electrode and a silver wire pseudo reference electrode. The silver wire reference electrode was placed within a Luggin capillary whose tip was placed adjacent to the surface of the working electrode. Ferrocene was added as an internal reference at the end of each experiment.

The THF was distilled under nitrogen from Na/benzophenone before use and transferred to the cell straight from the still. The supporting electrolyte in each case was tetrabutylammonium tetrafluoroborate (Bu_4NBF_4, TBAB). For the 'dry' work this was melted under vacuum before dissolution in THF, its preparation is outlined below.

Cyclic voltammograms at a variety of sweep rates were obtained using a Hi-Tek Instruments potentiostat (model DT 2101) and a waveform generator (model PPR1). The response was recorded on a Gould x-y chart recorder (model 60 000).

The voltammetry of $CpTiCl_2$[OR] complexes was studied using several experimental procedures, the details of which are described in chapter 4, along with a presentation of the results of these procedures using data obtained from the $CpTiCl_2$[menthoxide] system to exemplify the differences

observed in each case.

The procedure developed for voltammetry on a vacuum line was then used in the study of other organotitanium systems; namely the redox behaviour of Cp_2TiCl_2 in the presence of alkylphosphine ligands and a brief look at the voltammetry of a titanocyclo-octene. An account of the apparatus designed for this work also appears in chapter 4.

Preparation of tetrabutylammonium tetrafluoroborate, Bu_4NBF_4 (TBAB).

An aqueous solution of tetrabutylammonium hydrogen sulphate, Bu_4NHSO_4 (200 g, 0.5 mol) was added to an aqueous solution of sodium tetrafluoroborate (55 g, 0.5 mol), a thick white precipitate formed immediately. The aqueous mixture was filtered and the residue heated in a vacuum oven to remove the majority of the water. The white solid was then dissolved in ethyl acetate and the small water layer separated off. The ethyl acetate layer was heated to fully dissolve the crude Bu_4NBF_4 and $MgSO_4$ added while warm to dry the solution then filtered off. Petroleum ether was added to the filtrate which was then cooled to afford light white crystals. These were dried thoroughly in a vacuum oven and stored in a desiccator. Isolated yield - 85%.

Melting point: 160-162°C (literature 162°C)

2.3.2 Controlled Potential Electrolysis.

Controlled potential electrolyses were performed on solutions of the various organotitanium species under dry conditions using a specially designed cell for use on a vacuum line (described in detail in section 4.5). Again THF was the solvent and TBAB the supporting electrolyte. Cyclic voltammograms of the electrolyte solutions were recorded from this cell before and after the

electrolysis using the same instrumentation described above, the charge passed during the electrolysis was measured with a Hi-Tek gated integrator.

CHAPTER 3

THE SYNTHESIS OF $CpTiCl_2[OR]$ COMPLEXES.

With the use of Cp_2TiCl_2 in the coupling of unsaturated hydrocarbons (section 1.2.3) in mind, it was decided that work should concentrate in the synthesis of different organotitanium species that could be used in the same way, but also having the ability to induce some asymmetry into the organic product. The presence of two cyclopentadienyl ligands around the pseudo-tetrahedral titanium centre, although providing stability, do remove the possibility of rendering the titanium centre chiral. Hence monocyclopentadienyl titanium complexes were chosen as a starting point in this project, it was thought that as one cyclopentadienyl anion provides six electrons this would help in stabilising the complex while making available at least three other ligand sites to use for the introduction of some chirality. Asymmetry could be induced in such systems either by making the metal centre itself chiral or by using chiral ligands.

3.1 METHODS OF PREPARATION.

$CpTiCl_3$ was prepared by literature methods [36] and used to make $CpTiCl_2[OR]$ complexes. Riediker and Duthaler reported the synthesis of $CpTiCl[OR^*]_2$ from $CpTiCl_3$, where R^* is a chiral glucose moiety, using triethylamine as the base to remove a proton from the alcohol and to mop up the HCl generated during the reaction [41]. The initial synthesis of $CpTiCl_2[OR]$ complexes in this project was based on this method reported by Riediker and Duthaler.

$CpTiCl_2[OC_6H_3(^iPr)_2]$, $CpTiCl_2$[menthoxide] and $CpTiCl_2[O^iPr]$ had been previously prepared [78] by the Et_3N method. Of these complexes $CpTiCl_2[O^iPr]$ was the only one known to have been made by another method; by a redistribution reaction between the monocyclopentadienyl titanium trialkoxide and $CpTiCl_3$ [79]. A further four new $CpTiCl_2$[OR] complexes were prepared, all seven are illustrated again in figure 3.1.1.

With the Et_3N method of preparation, a 1.1 molar equivalent of Et_3N was added to a 1:1 mixture of $CpTiCl_3$ and the alcohol in diethylether. An immediate precipitate of $Et_3N.HCl$ was observed which could be filtered off. This procedure proved successful for all the alcohols used except the p-nitrophenol, and each $CpTiCl_2$[OR] complex except $CpTiCl_2$-$[OC_6H_2(^iPr)_2(NO_2)]$, could be recrystallised from hexane giving bright yellow, orange or red crystals. $CpTiCl_2[OC_6H_2(^iPr)_2(NO_2)]$ could be prepared by a method introduced by Kalirai et al [16] in their assessment of the anti-tumour activity of some cyclopentadienyl titanium compounds. They introduced nitrophenol and aminophenol ligands into the Cp_2Ti unit by using NaH to make the sodium salt of the alcohol then adding Cp_2TiCl_2 yielding $Cp_2Ti[OR]_2$ complexes. This method was adopted for the preparation of $CpTiCl_2[OC_6H_2(^iPr)_2(NO_2)]$ and proved much more successful than the triethylamine method. Consequently it was decided to try this procedure with a couple of the other aromatic alcohols. Table 3.1.1 is reproduced from chapter 2 and summarizes the isolated yields obtained for each of the $CpTiCl_2$[OR] complexes under the specified experimental procedures.

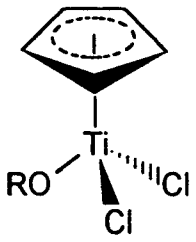

RO =

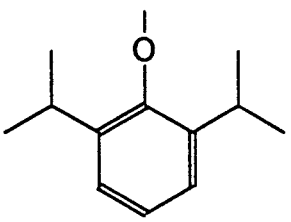

$-OC_6H_3(^iPr)_2$

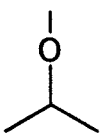

$-O^iPr$

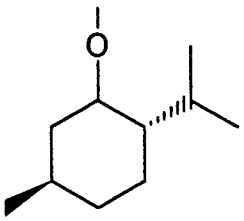

-menthoxide

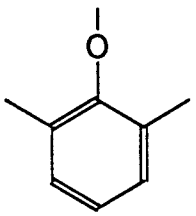

$-OC_6H_3(Me)_2$

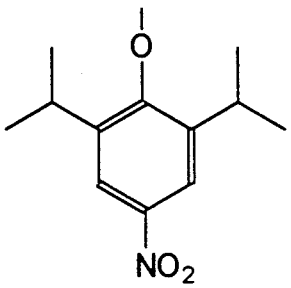

$-OC_6H_2(^iPr)_2(NO_2)$

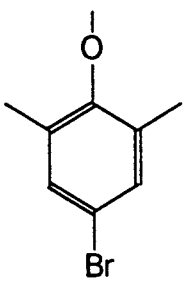

$-OC_6H_2(Me)_2(Br)$

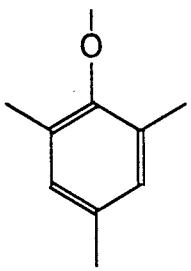

$-OC_6H_2(Me)_3$

Figure 3.1.1

Compound	Experimental Method	Isolated Yield (%)
$CpTiCl_2[OC_6H_3(^iPr)_2]$	Et_3N NaH	70 63
$CpTiCl_2[OC_6H_3(Me)_2]$	Et_3N	76
$CpTiCl_2[OC_6H_2(Me)_2(Br)]$	Et_3N NaH	50 42
$CpTiCl_2[OC_6H_2(Me)_3]$	NaH	40
$CpTiCl_2[OC_6H_2(^iPr)_2(NO_2)]$	Et_3N NaH	- 86
$CpTiCl_2[O^iPr]$	Et_3N	50
$CpTiCl_2$[menthoxide]	Et_3N	70

Table 3.1.1

From this data it would seem that the Et_3N method works better than the NaH method for the two complexes where both methods gave the desired product, namely $CpTiCl_2[OC_6H_3(^iPr)_2]$ and $CpTiCl_2[OC_6H_2(^iPr)_2(Br)]$, although there is not a great deal of difference in the percentage yields; 70% and 50% respectively for the Et_3N method and 63% and 42% for the NaH method. $CpTiCl_2[OC_6H_2(Me)_3]$ was only prepared via its sodium salt (the NaH method) giving an isolated yield of 40% which perhaps, judging by the results with $CpTiCl_2[OC_6H_2(^iPr)_2]$ and $CpTiCl_2[OC_6H_2(^iPr)_2(Br)]$, could have been improved had the other experimental procedure been tried. The lack of success with triethylamine and $HOC_6H_2(^iPr)_2(NO_2)$ with $CpTiCl_3$ must be due somehow to the strong electron withdrawing effects of the nitro group on the aromatic ring, but a detailed investigation into this was not carried out.

3.2 ^{1}H AND ^{13}C NMR DATA.

Some examples of the ^{1}H nmr spectra of the $CpTiCl_2[OR]$ complexes are shown in figures 3.2.1, 3.2.2, and 3.2.3. Figure 3.2.1 shows the ^{1}H nmr spectrum of $CpTiCl_2$[menthoxide], run in a $CDCl_3$ solution on a 270 MHz spectrometer. The single peak of 5H intensity at 6.6 ppm relates to the five equivalent protons on the cyclopentadienyl ring. Another feature is the doublet of triplets around 4.2 ppm. This signal integrates to one proton and a 90° COSY symmetrised spectrum showed it to relate to the proton on the carbon atom next to the oxygen. The three methyl groups all appear as doublets around 1 ppm. All other protons show more complicated signals in the region 1-2.5 ppm.

Figure 3.2.2 shows the ^{1}H nmr spectrum for a $CDCl_3$ solution of $CpTiCl_2[OC_6H_3(^{i}Pr)_2]$. The 5H cyclopentadienyl single peak can be seen at 6.7 ppm and the aromatic protons give a multiplet between 7.0 and 7.2 ppm. The iso-propyl groups on the aromatic ring are equivalent; the methine (CH) protons giving a 2H signal at about 3.2 ppm which appears as a septet (J = 6.76 Hz) since it is split by the six protons of the two methyl groups. The methyl groups give a 12H intensity doublet at about 1.25 ppm (J = 6.76 Hz). Figure 3.2.3 shows the ^{1}H nmr spectrum for $CpTiCl_2[OC_6H_2(^{i}Pr)_2(NO_2)]$ and, as would be expected, is very similar to figure 3.2.2. The main difference is the signal from the aromatic protons, where here the two protons on the aromatic ring are equivalent and show a singlet at about 8.0 ppm. The downfield shift in this proton signal shows that the aromatic ring is more electron deficient because of the presence of the electron-withdrawing nitro group.

The effect of the various alkoxide ligands on the electron density of the cyclopentadienyl group in the $CpTiCl_2[OR]$ complexes would appear minimal since there is no great difference in the nmr signals for either the protons or the carbons of the ring. Table 3.2.1 summarizes the nmr data for the cyclopentadienyl group on each of the $CpTiCl_2[OR]$ complexes. The

complexes with the alkoxy groups, ie $CpTiCl_2$[menthoxide] and $CpTiCl_2[O^iPr]$, do show cyclopentdienyl ^1H and ^{13}C nmr signals slightly more upfield than the complexes containing aryloxy ligands. Otherwise all the analogous signals are in very much the same positions. However all these complexes show cyclopentadienyl nmr signals significantly more upfield compared to the ^1H and ^{13}C nmr data for $CpTiCl_3$, also shown in table 3.2.1.

Complex	^1H nmr signal	^{13}C nmr signal
$CpTiCl_2[OC_6H_3(^iPr)_2]$	6.72	120.9
$CpTiCl_2[OC_6H_3(Me)_2]$	6.73	121.0
$CpTiCl_2[OC_6H_2(Me)_2(Br)]$	6.73	121.2
$CpTiCl_2[OC_6H_2(Me)_3]$	6.72	120.9
$CpTiCl_2[OC_6H_2(^iPr)_2(NO_2)]$	6.77	121.6
$CpTiCl_2[O^iPr]$	6.70	119.0
$CpTiCl_2$[menthoxide]	6.66	119.0
$CpTiCl_3$	7.05	123.6

Table 3.2.1

Showing the ^1H and ^{13}C nmr data in the cyclopentadienyl region for $CpTiCl_2$[OR] and $CpTiCl_3$ complexes in $CDCl_3$, run on a 270 MHz spectrometer.

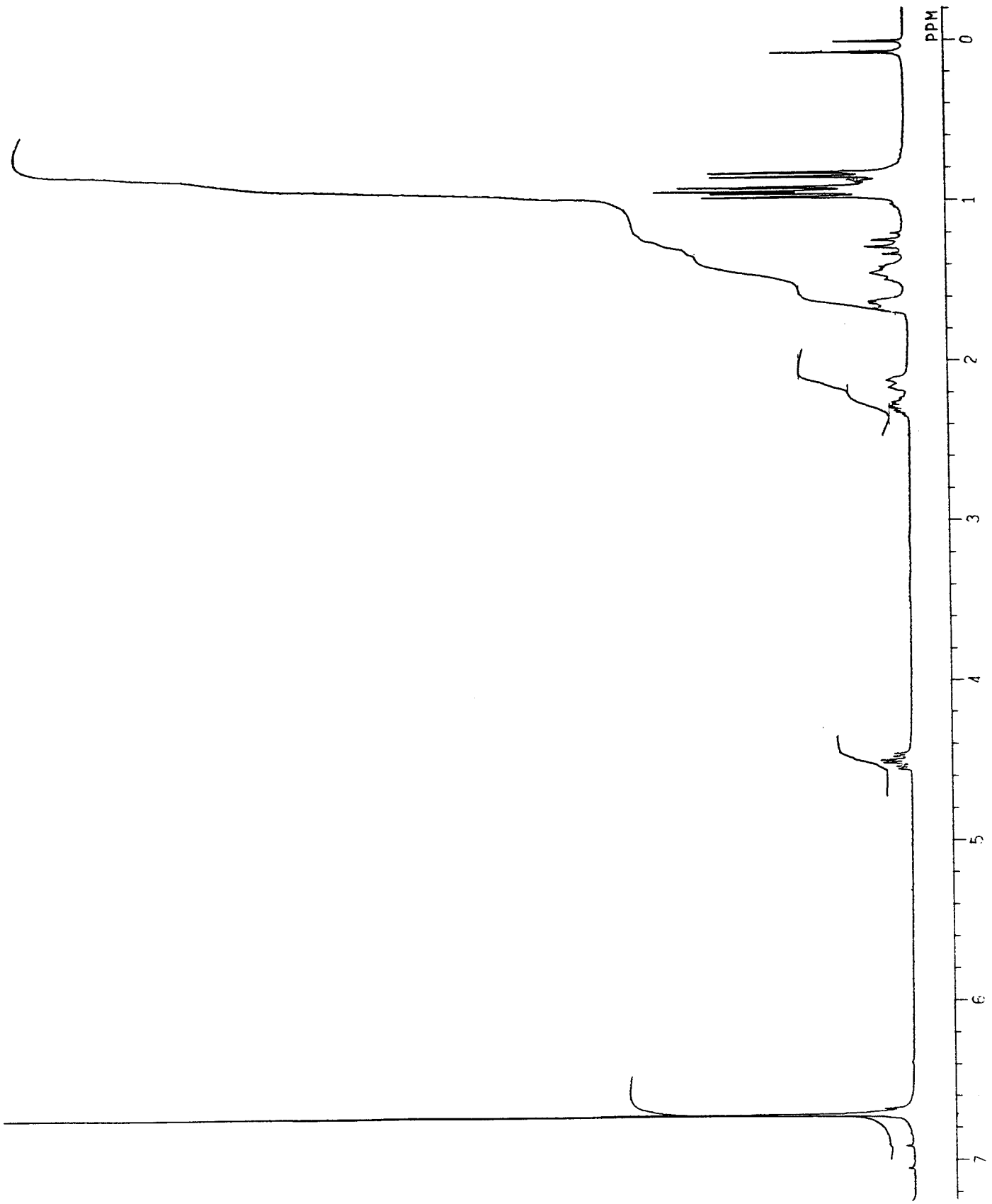

Figure 3.2.1
^{1}H nmr Spectrum ($CDCl_3$) of $CpTiCl_2$[menthoxide]

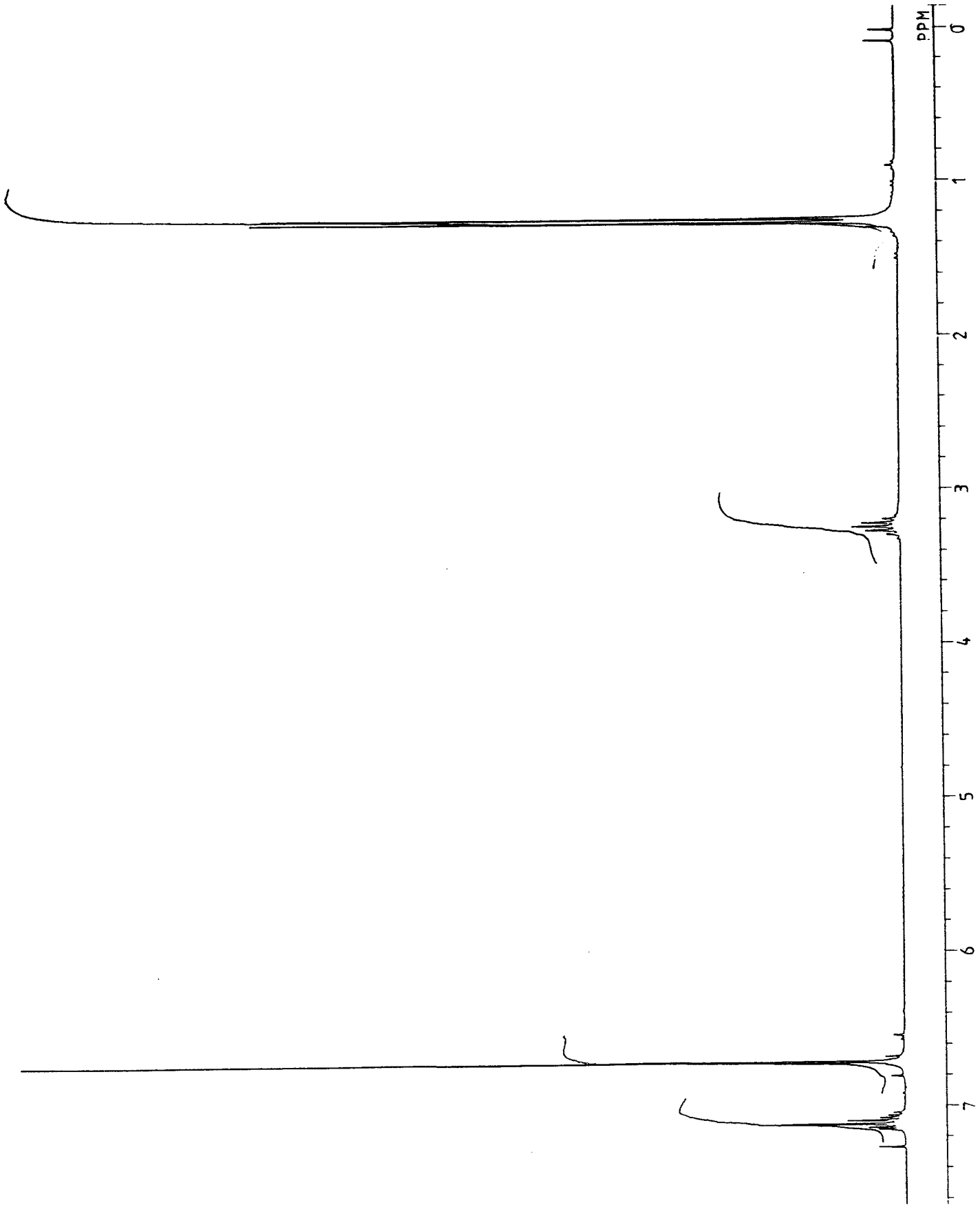

Figure 3.2.2
^{1}H nmr Spectrum ($CDCl_3$) of $CpTiCl_2[OC_6H_3(^iPr)_2]$

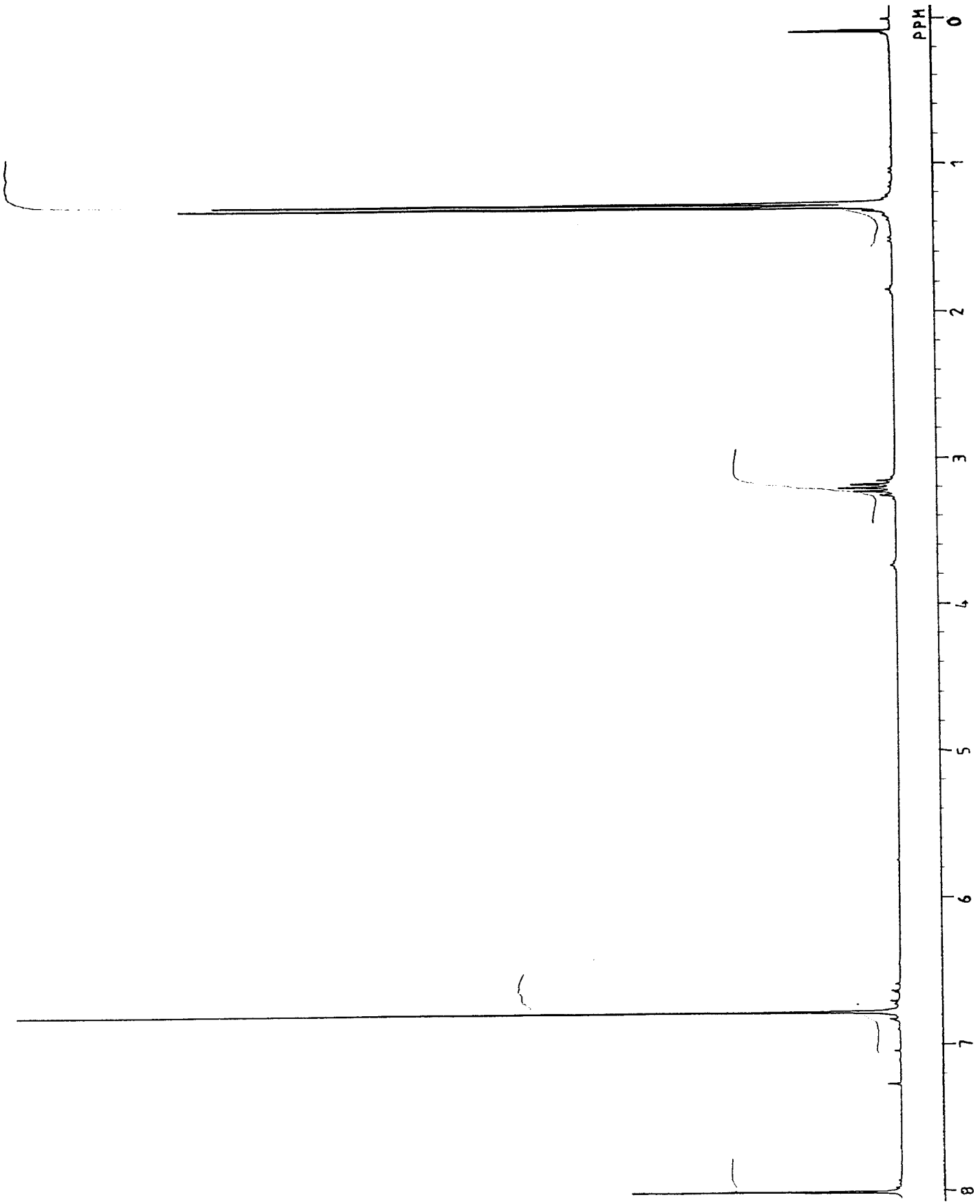

Figure 3.2.3
^{1}H nmr Spectrum ($CDCl_3$) of $CpTiCl_2[OC_6H_2(^iPr)_2(NO_2)]$

3.3 $CpTiCl_2[OR]$ COMPLEXES NOT ISOLATED.

It was the aim to provide an extensive list of $CpTiCl_2[OR]$ complexes incorporating different R groups into the coordination sphere of the titanium. Various alcohols were tried; mainly aromatic systems with differing properties. Highly sterically hindered phenols such as $HOC_6H_3(Me)_2$ and $HOC_6H_3(^iPr)_2$ worked well but the reaction between phenol itself and $CpTiCl_3$ produced a mixture of products. The ^1H nmr spectrum of this mixture did show a large singlet for the cyclopentadienyl protons in a comparable place to the other $CpTiCl_2[OR]$ complexes but other significant peaks were also present indicating that the sample contained more than one compound. One of these compounds was probably the desired $CpTiCl_2[OPh]$ complex but the mixture was a thick orange oil and attempts at recrystallisation were unsuccessful, so a pure compound was not isolated.

Substituted phenols incorporating electron-withdrawing and electron-donating groups were also tried; p-hydroxymethylbenzoate (**3A**) and p-methoxyphenol (**3B**) were both tried, mixing them with $CpTiCl_3$ in the presence of triethylamine. Both reactions however, again provided mixtures of products that could not be easily separated.

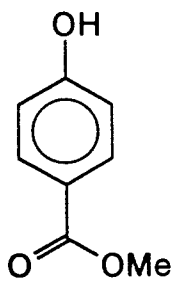

(3A)

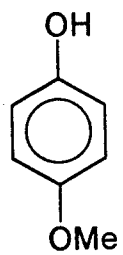

(3B)

Since the sterically hindered phenols worked well the nitrophenol that was chosen was that which had iso-propyl groups in the 2 and 6 positions on the ring. This ligand was prepared by a method reported in an American patent

[76] involving nitration of the phenol using 50% nitric acid in iso-octane, although the yield for this reaction is poor (18% was the best achieved) the product obtained is very clean.

Since the preparation of $CpTiCl_2[OC_6H_2(^iPr)_2(NO_2)]$ via the sodium salt of the phenol was successful, providing a monocyclopentadienyl titanium complex with a strongly electron-withdrawing alkoxide ligand, it was decided to try and make the analogous dimethylaminophenol, thereby providing an electron-donating alkoxide. The dimethylaminophenol was chosen in preference to the aminophenol because it was thought that coordination to the titanium via the nitrogen may occur with the amine since the base used in the reaction with $CpTiCl_3$ could remove a hydrogen from the nitrogen instead of, or as well as, from the oxygen.

Attempts to reduce $HOC_6H_2(^iPr)_2(NO_2)$ were made, the most successful of which involved protection of the hydroxy group by reaction with acetic anhydride in pyridine. This was followed by reduction using 10% palladium on charcoal and $NaBH_4$ in ether [80]. $AcOC_6H_2(^iPr)_2(NH_2)$ was obtained from the reaction but the attempt to methylate the amine using sodium borohydride and formaldehyde [81] was unsuccessful.

3.4 COORDINATING DIOLS TO A MONOCYCLOPENTADIENYL TITANIUM MOIETY.

The synthesis of complexes with a diol as a bidentate ligand coordinated to the titanium centre was also attempted. The same procedure as for most of the monodentate alcohols was adopted, ie the triethylamine method. Duthaler and coworkers had already reported the synthesis by this method, of the monocyclopentadienyl titanocycle shown below (3C), incorporating a diol into

the coordination sphere of the titanium [43].[1]

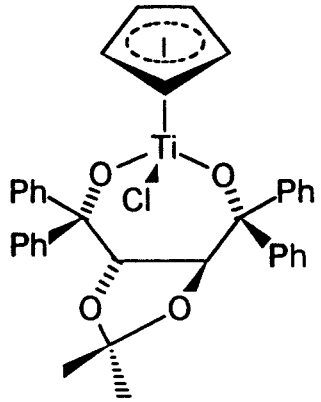

(3C)

Two diols were tried; 2-hydroxyphenethyl alcohol (3D) and 2-hydroxybenzyl alcohol (3E). Aromatic diols were chosen because of the success with the monodentate aromatic alcohols, albeit the more sterically hindered ones, however (3D) and (3E) were fairly inexpensive and readily available. The coordination of (3D) to the titanium centre would create a 6-membered titanocycle and diol (3E) a 7-membered one. Because of the knowledge that it was possible to prepare the threitol derivative (3C) which contains a 7-membered titanocycle, it was thought that the hydroxybenzyl alcohol (3E) would coordinate to the titanium more favourably than the hydroxyphenethyl alcohol (3D).

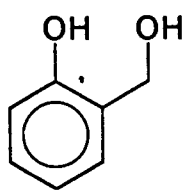

(3D)

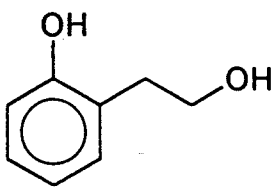

(3E)

[1] A sample of complex 3C was in fact prepared for this project by the method reported in [43] and its cyclic voltammetry investigated (chapter 5). J.Senior is acknowledged for providing the sample.

2.2 equivalents of Et_3N were added to a 1:1 mixture of the diol and $CpTiCl_3$ in Et_2O, in each case the yellow colour of the $CpTiCl_3$ solution darkened to orange on addition of the diol and a precipitate formed when triethylamine was added. This behaviour was similar to that seen for the other alcohols, and hence the reaction looked promising. However, when samples of the crude reaction products (thick red oils in both cases) were taken for nmr analysis the spectra showed a variety of products. Contrary to initial beliefs,the diol which would be expected to form a 7-membered ring with the titanium (**3E**) gave the least promising ^1H nmr spectrum with little evidence for the presence of the desired complex. The ^1H nmr spectrum obtained from the product of the reaction between $CpTiCl_3$ and (**3D**) was more promising (figure 3.4.1) although a mixture of products was still evident. Two sharp single peaks appeared in the cyclopentadienyl region in almost equal intensity and no starting $CpTiCl_3$ was apparent. In the ^1H nmr spectrum of the actual diol (**3D**) the protons of the CH_2 group gave a signal at 4.8 ppm, no signal in this area was seen on the spectrum of the reaction product, instead a multitude of small peaks appeared between 5.0 and 5.7 ppm. Amongst these there does appear to be an AB-quartet which would relate to the CH_2 protons of the doubly coordinated diol. There is of course the possibility that a bimetallic species could form with one diol ligand being shared between two titanium centres, also coordination through only one of the oxygens of the diol molecule is feasible. Recrystallisation of the product mixture from hexane and from CH_2Cl_2/hexane did not prove successful and further attempts at separation and purification were not carried out.

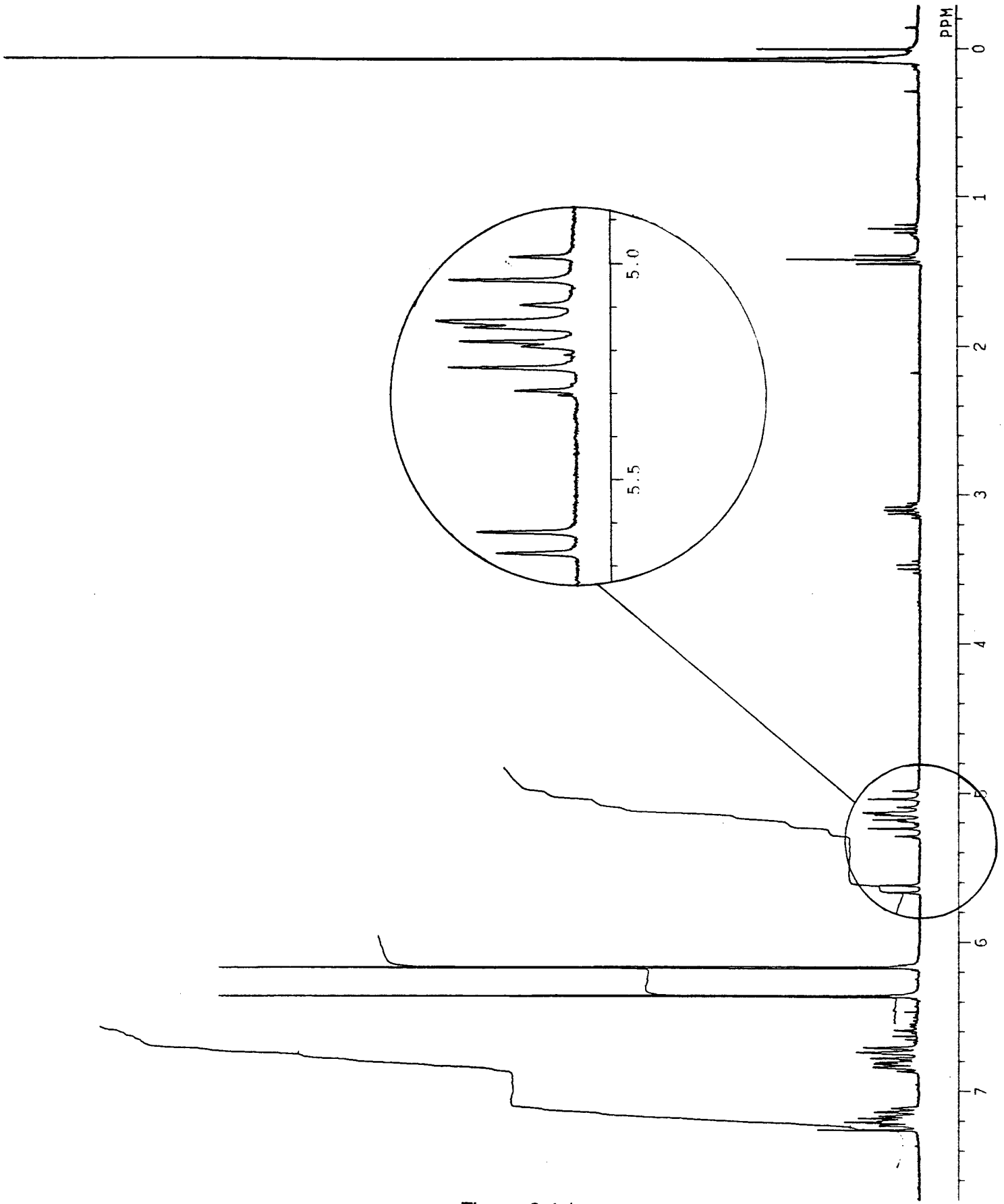

Figure 3.4.1
^{1}H nmr Spectrum ($CDCl_3$) of the product of the reaction between $CpTiCl_3$ and diol (**3D**).

CHAPTER 4

DEVELOPMENT OF AN EXPERIMENTAL TECHNIQUE FOR 'DRY' ELECTROCHEMISTRY.

In the early stages of this project the voltammetry of the $CpTiCl_2[OR]$ complexes was not reproducible; it varied with the concentration of the titanium complex and the care taken in drying the solutions. Hence it was concluded that the ratio of titanium complex to water was critical in determining the experimental response and a considerable effort went into developing techniques where the electrochemical experiments can be carried out under conditions as dry as possible and where the responses are reproducible. This work is presented in this chapter using the complexes $CpTiCl_2$[menthoxide] and $CpTiCl_2[O^iPr]$ to illustrate the results.

In summary, these experimental procedures fall into four categories, brief descriptions of which are outlined below:

1. Using dried solvent and electrolyte, the solutions were prepared as quickly as possible in the open laboratory and the electrochemical experiment was carried out in a cell in the open laboratory; ie the conditions used for most non-aqueous electrochemistry.
2. Using dried solvent and electrolyte, solutions were prepared and the electrochemical experiment carried out in the glove-box.
3. Using dried solvent, the electrolyte was melted under vacuum but the solutions prepared in the open laboratory and the experiment carried out in a cell in the laboratory.
4. Using dried solvent, the electrolyte was melted under vacuum, the solutions were prepared and the experiments carried out under argon

in a closed cell on a vacuum line. The transfer of solvents and solutions was performed using vacuum line techniques and the solvent/electrolyte system was passed through a column of activated alumina into the working compartment of the cell.

Prior to addition of the solvent to the electrolyte, the THF was always distilled from Na/benzophenone and transferred to a flask containing the pre-melted Bu_4NBF_4 under an atmosphere of argon as described in the experimental section.

$CpTiCl_2$ [menthoxide] was chosen to illustrate the influence of experimental procedure on the voltammetric response since the differences in the I-E curves are particularly clear with this complex. $CpTiCl_2[O^iPr]$ is also used to emphasise further the effects of making efforts to remove water from the solutions.

4.1 PROCEDURE 1.

Cyclic voltammetry using dried solvent and electrolyte and carrying out the experiment in a cell in the open laboratory.

The electrochemical cell used for the open cell work was a three electrode, two compartment cell, illustrated in figure 4.1.1. The secondary electrode was a platinum wire hoop, designed to be symmetrically positioned around the working electrode which was a vitreous carbon disc (area = 0.07 cm^2). The reference electrode, a silver wire, was placed inside a Luggin capillary whose tip was placed adjacent to the surface of the working electrode.

Figure 4.1.2 shows a cyclic voltammogram recorded at 300 mV s^{-1} between the limits -0.7 V and -1.7 V vs ferrocene for a THF solution of $CpTiCl_2$[menthoxide] (20 mM) with Bu_4NBF_4 (0.2 M) in an open cell in the laboratory. Two cathodic and two anodic processes can be seen. The major cathodic process appears

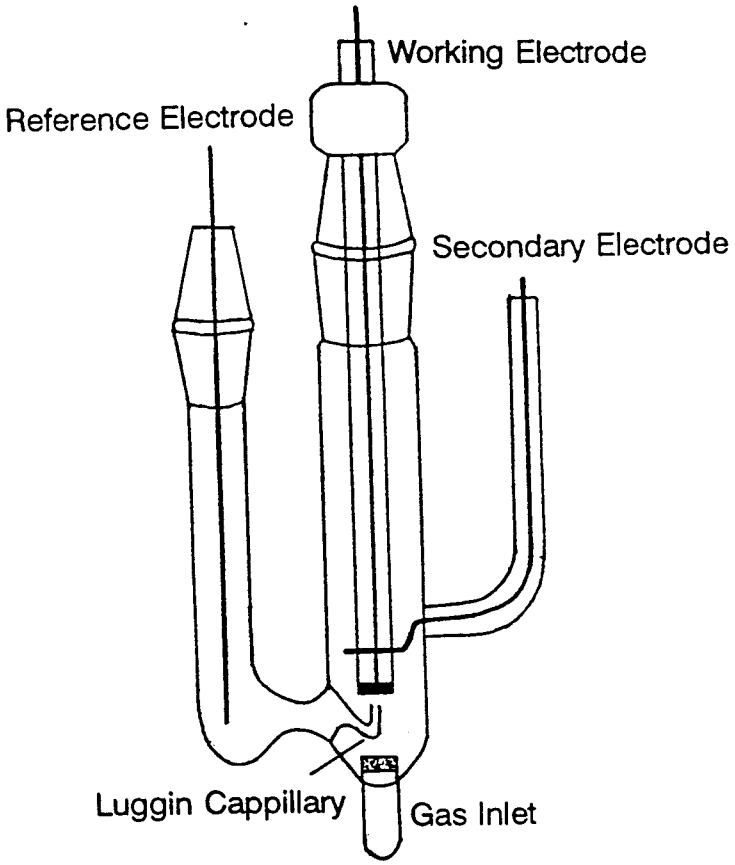

Figure 4.1.1
Electrochemical cell for cyclic voltammetry in the laboratory.

as a peak occurring at $E_{p/2}$ = -1.38 V vs ferrocene (peak A), this has a coupled anodic peak, A´. The peak separation of this couple is 60 mV thereby looking similar to a reversible couple but the ratio of their peak current densities is less than one; $Ip^{A'}/Ip^{A}$ = 0.7. Another much smaller cathodic peak, B, is observed with $E_{p/2}$ = -0.92 V and the second anodic process, evident by the presence of peak C, occurs at about the same potential.

The presence of peak B is an indication that another species, apart from $CpTiCl_2$[menthoxide], exists in solution, albeit in very small concentrations. This species is more easily reduced than $CpTiCl_2$[menthoxide]. Peak C relates to the oxidation of a species that is produced during the reduction of CpTiCl[menthoxide] and may be coupled to B. The presence of peak C along

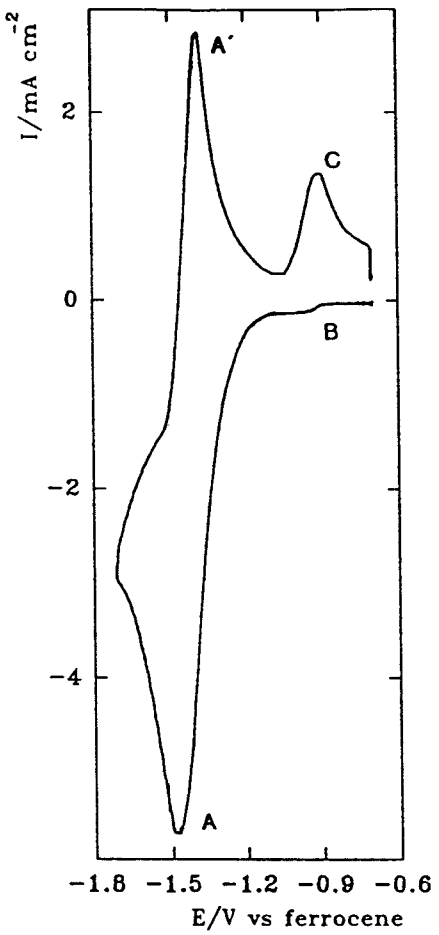

Figure 4.1.2
Cyclic Voltammogram recorded at a vitreous carbon disc at 300 mV s^{-1} for a THF/Bu_4NBF_4 (0.2M) solution of $CpTiCl_2$[menthoxide] (20 mM) (procedure 1).

with the fact that A´ is not as large as A indicates that the reduced species produced at A undergoes a chemical reaction. The product of this chemical reaction is oxidised at C. Since peak A´ is the major anodic peak indicating that oxidation of the initial reduced species does occur, this chemical reaction is not complete under these conditions.

When the concentration of the electroactive species is reduced the cyclic voltammogram obtained through this experimental procedure differs greatly from that obtained at higher concentrations. Figure 4.1.3 shows a cyclic voltammogram recorded at 300 mV s^{-1} between the limits -0.4 V and -1.84 V vs ferrocene for a THF solution of $CpTiCl_2$[menthoxide] (4.3 mM) with Bu_4NBF_4 (0.2M). Peak A remains the major cathodic process and the minor cathodic peak B still exists, however at potentials more negative than A a third cathodic peak is seen, peak D, with a peak potential of about -1.7 V vs ferrocene. Peak

D is not observed with the higher concentration experiments and has no coupled oxidation. On sweeping in the anodic direction the only electron transfer process observed is that represented by peak C. Peak A´ is completely absent, indicating that the chemical reaction undergone by the reduced species produced at A has reached completion under these conditions.

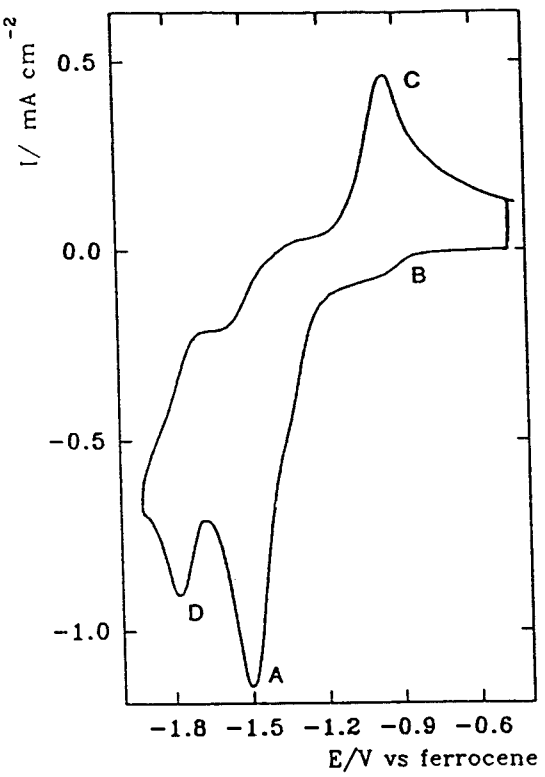

Figure 4.1.3
Cyclic Voltammogram recorded at a vitreous carbon disc at 300 mV s^{-1} for a THF/Bu_4NBF_4 (0.2M) solution of $CpTiCl_2$-[menthoxide] (4.3 mM) (procedure 1).

4.2 PROCEDURE 2.

Cyclic voltammetry using dried solvent and electrolyte and carrying out the experiment in the glove-box.

Figure 4.2.1 shows a cyclic voltammogram recorded at 300 mV s^{-1} between -0.6V and -1.66V vs ferrocene for a THF solution of $CpTiCl_2$[menthoxide] (22 mM) with Bu_4NBF_4 (0.2 M) in the cell shown in figure 4.1.1 placed in a glove-box. The electrolyte solution was added to the cell inside the glove-box and the cell remained there throughout the experiment. This cyclic voltammogram is very similar to that shown in figure 4.1.2; again two cathodic and two anodic

processes can be seen. The major cathodic process, peak A occurring with $E_{p/2}$ = -1.38 V vs ferrocene and a coupled anodic process, peak A´. Peak B has a half-peak potential at -0.92 V and the second anodic process, peak C is still evident. The only difference between this voltammogram and the one shown in figure 4.1.2 is the relative size of the anodic peaks A´ and C. Peak C appears slightly larger here in relation to A´ than in the previous case. This is reflected in the peak current density ratio ($Ip^{A'}/Ip^{A}$) since for this couple it is 0.6, whereas it was 0.7 in the previous example. These slight differences however, were within the limits of reproducibility, and the use of the glove-box did not change the response. It was, therefore concluded that, if the cause of the irreproducibility of the voltammetry results was water, it was present in the solvent and/or the electrolyte.

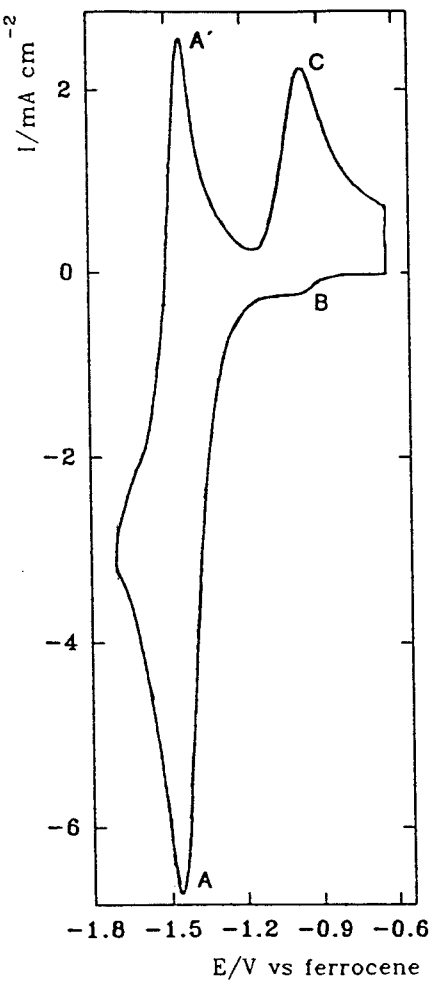

Figure 4.2.1
Cyclic Voltammogram recorded at a vitreous carbon disc at 300 mV s^{-1} for a THF/Bu_4NBF_4 (0.2M) solution of $CpTiCl_2$[menthoxide] (22 mM) (procedure 2).

4.3 PROCEDURE 3.

Cyclic voltammetry using dried solvent, melting the electrolyte under vacuum and carrying out the experiment in the laboratory.

Figure 4.3.1 shows a cyclic voltammogram recorded at 400 mV s^{-1} between -0.7 V and -1.66 V vs ferrocene for a THF solution of $CpTiCl_2$[menthoxide] (22 mM) with Bu_4NBF_4 previously melted under vacuum, in an open cell in the laboratory. Melting the TBAB under vacuum before dissolution involves adding it to a Schlenk flask connected to the vacuum line and heating with a hot air blower until all the crystals have melted. This is a more effective way of drying Bu_4NBF_4, rather than just evacuation at room temperature since it removes any water molecules that may be coordinated to the Bu_4NBF_4 crystals [82].

The cyclic voltammogram in figure 4.3.1 has the same general characteristics as those presented in figures 4.1.2 and 4.2.1, but here the peak current density ratio for the A´/A couple ($Ip^{A'}/Ip^{A}$) has increased to nearly 0.9 and consequently peak C is much smaller relative to A´. This shows that the chemical reaction undergone by the reduced species produced at A occurs to a lesser extent in this case compared to the two previous examples (figs. 4.1.2 & 4.2.1). However, at the end of the experiment when the cell has sat around in the laboratory for a while, peak C grows in size relative to A´ indicating that the extent of the chemical reaction is increasing with time.

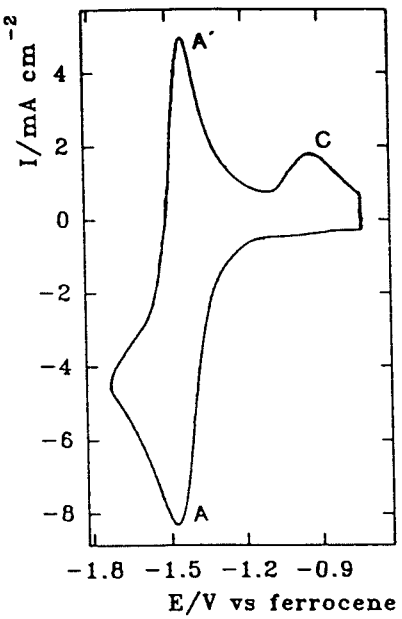

Figure 4.3.1
Cyclic Voltammogram recorded at a vitreous carbon disc at 400 mV s^{-1} for a THF/Bu_4NBF_4 (0.2M) solution of $CpTiCl_2$[menthoxide] (22 mM) (procedure 3).

4.4 PROCEDURE 4

Cyclic voltammetry using dried solvent, melting the electrolyte under vacuum and carrying out the experiment in a closed cell on a vacuum line.

The electrochemical cell used for work on the vacuum line is shown in figures 4.4.1a and 4.4.1b and was designed specifically to enable cyclic voltammetry to be run on solutions in a closed system under an inert atmosphere, with conditions as dry as possible.

In this closed, dry cell a vitreous carbon disc (area = 0.05 cm^2) sealed in a glass tube acted as the working electrode. The counter electrode, a platinum wire hoop, was again designed so that, as far as possible, it was placed symmetrically about the working electrode. A silver wire placed inside the Luggin capillary was used as a pseudo reference electrode, the Luggin tip was placed close to, but not touching, the working electrode. Both the working electrode and the Luggin capillary could be adjusted and removed for cleaning by means of Young's greaseless sliding joints. The pear-shape of the main body of the cell was chosen in order to minimize the volume of electrolyte solution, hence decreasing the amount of complex needed for the experiment. A pressure equalizing funnel was fitted to the top of the cell, this was part-filled with alumina (Woelm neutral, super 1 grade [71, 72]) through which the electrolyte solution was passed. A rotatable, bent, sealed glass tube was fitted to one side of the cell, this was used to add ferrocene to the electrolyte solution at the end of an experiment as an internal reference. Attachment to the vacuum line was via a vacuum tap connected on the other side of the cell. Elastic bands were used to hold all the quick-fit joints tightly together.

All cell parts were dried in an oven at 150°C for at least 12 hours prior to use, the cell was assembled hot, a known amount of the active compound added along with a magnetic stirrer bead and the whole apparatus evacuated for 3-5 hours, refilling with argon at intervals. The supporting electrolyte was melted

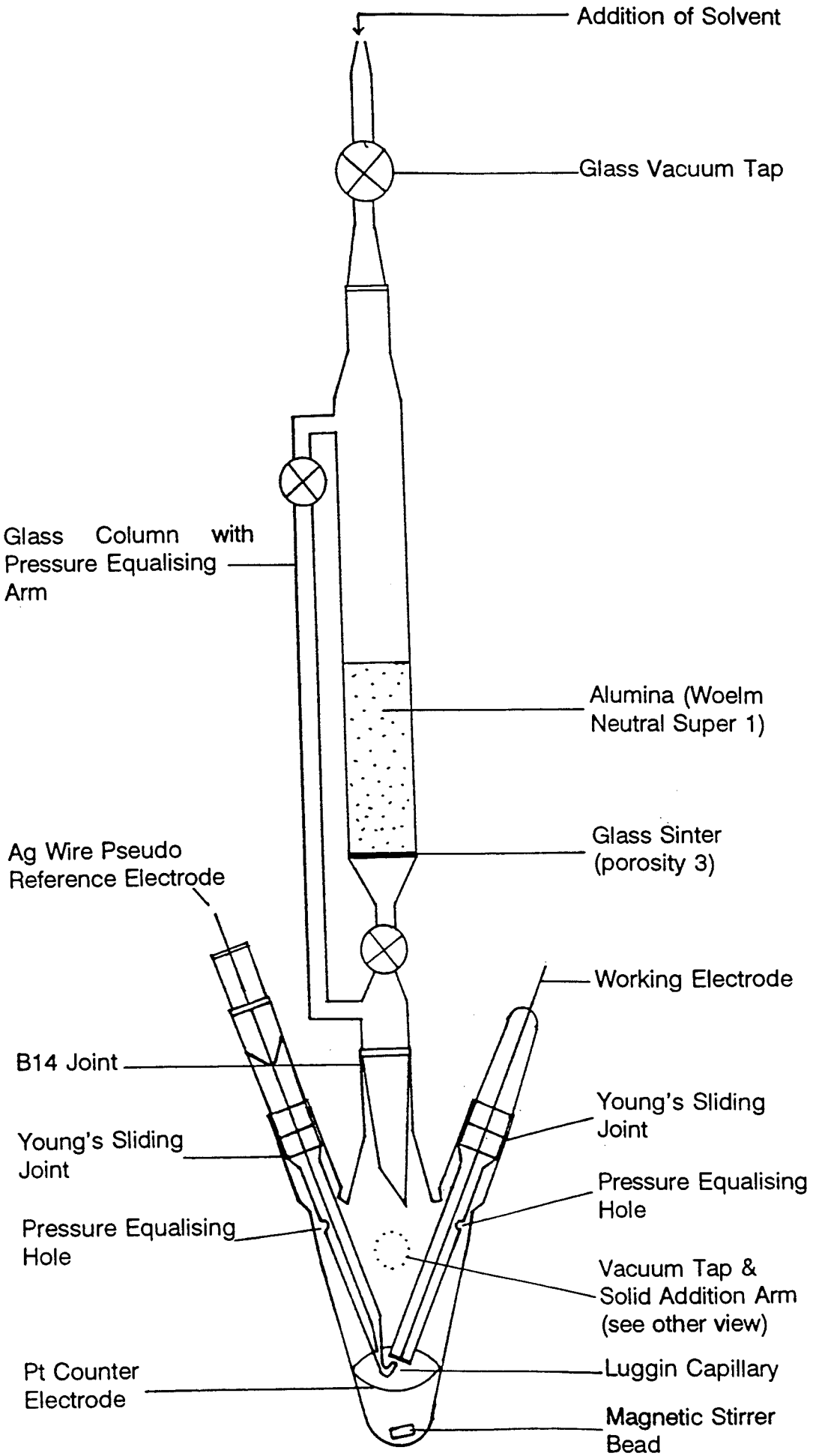

Figure 4.4.1a
Cyclic Voltammetry Cell for use on a Vacuum Line

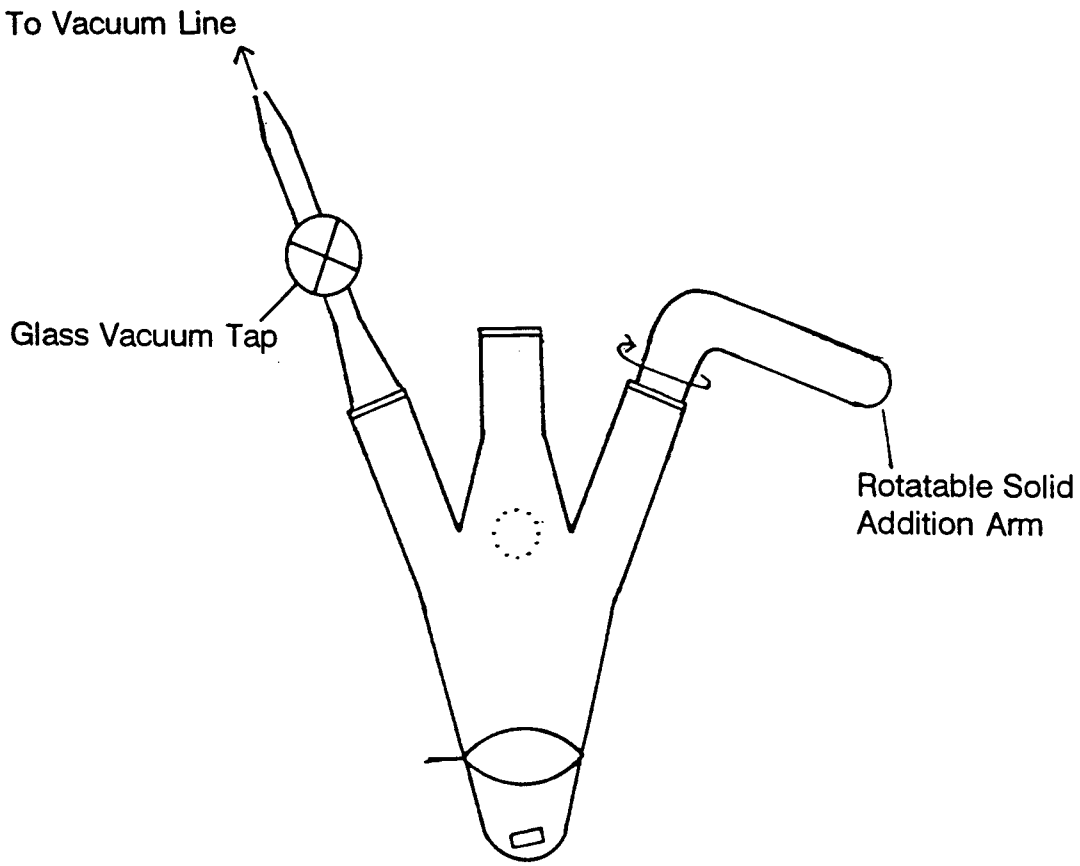

Figure 4.4.1b
Cyclic Voltammetry Cell for use on a Vacuum Line - Side View

in a separate flask under vacuum, THF transferred straight from the still to this flask via a canula then, once the TBAB had dissolved, a canula was again used to transfer the solution to the drying column of the cell. The electrolyte solution passed through the alumina and into the working compartment, stirring was applied until all the solid active compound had dissolved. Ferrocene was added from the solid addition arm at the end of the experiment. After dismantling the apparatus the volume of the electrolyte solution was measured to obtain an accurate concentration of the electro-active species.

An example of the results obtained using this cell and the vacuum line is shown in figure 4.4.2 which displays a cyclic voltammogram recorded at 300 mV s^{-1} between the limits -0.74 V and -1.74 V vs ferrocene for a THF solution of $CpTiCl_2$[menthoxide] (12 mM) with Bu_4NBF_4 (0.2 M) in a closed cell connected to the vacuum line. This cyclic voltammogram does have similar

characteristics to those obtained by the other different experimental procedures, but here the response is less complex even though the concentration of the titanium complex is relatively low. The major electron transfer process is again shown by the reversible couple A/A´. The formal potential of the A/A´ couple is -1.38 V vs ferrocene and the ratio of the current densities of peaks A and A´, $Ip^{A'}/Ip^{A}$, is now equal to one indicating that the reduced species produced at A is stable under these conditions and hence undergoes no chemical change. Peaks B and C are just visible on this cyclic voltammogram and unlike the previous cases are now of equal size (see section 5.4).

The effectiveness of this procedure for simplifying the voltammetry of the $CpTiCl_2[OR]$ complexes and enabling reproducible results to be obtained is further exemplified by the cyclic voltammograms for $CpTiCl_2[O^iPr]$ shown in figures 4.4.3 and 4.4.4. The first voltammogram, figure 4.3.3, was recorded in the laboratory from the cell illustrated in figure 4.1.1 (procedure 1) for a 19 mM solution of $CpTiCl_2[^iOPr]$ with Bu_4NBF_4 (0.2 M) between -0.5 V and -1.7 V vs ferrocene at 300 mV s^{-1}. Although peak A still represents the major cathodic process, peak B is much more significant in size and a third cathodic process is evident from the presence of peak D. Peak A does not have a coupled anodic peak since no peak A´ can be observed, thereby suggesting that the reduced species produced at A is unstable and is completely removed by a chemical reaction. The only anodic process is represented by peak C. Comparing this with the cyclic voltammogram in figure 4.4.4 which was run on a lower concentration of $CpTiCl_2[O^iPr]$ (7.4 mM) at 400 mV s^{-1} by the vacuum line procedure (procedure 4), it can be seen that the chemical reaction responsible for the disappearance of the major reduced species occurs to a much lesser extent. This is evident from the presence of the anodic peak A´ and the smaller size of peak C. In this voltammogram peak B is also less significant in size and there is no evidence of peak D, the third cathodic peak.

The results in this chapter indicate that the ratio of titanium complex to water

is an important factor in the study of the electrochemistry of such species and hence was taken into consideration in the ensuing investigation (chapter 5).

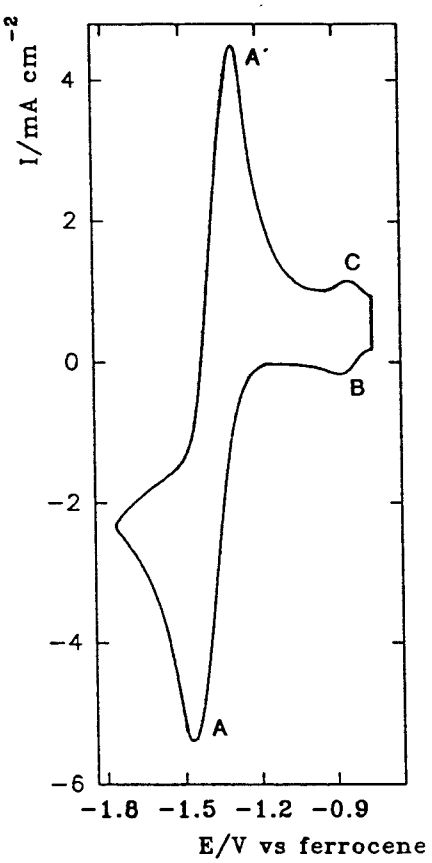

Figure 4.4.2
Cyclic Voltammogram recorded at a vitreous carbon disc at 300 mV s^{-1} for a THF/Bu_4NBF_4 (0.2M) solution of $CpTiCl_2$[menthoxide] (12 mM) (procedure 4).

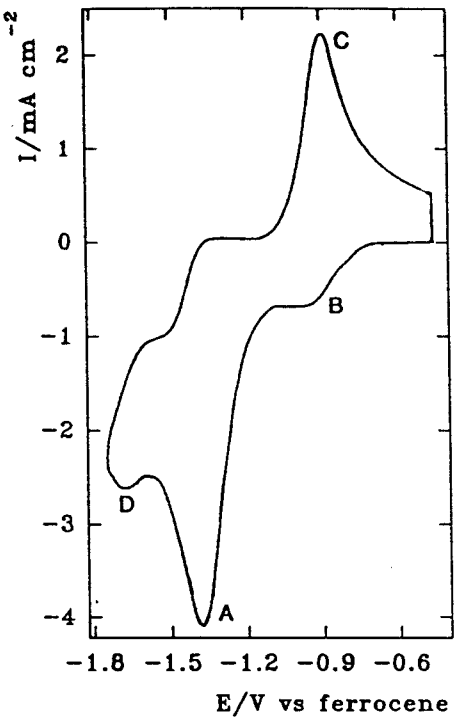

Figure 4.4.3
Cyclic Voltammogram recorded at a vitreous carbon disc at 300 mV s^{-1} for a THF/Bu_4NBF_4 (0.2M) solution of $CpTiCl_2[O^iPr]$ (19 mM) (procedure 1).

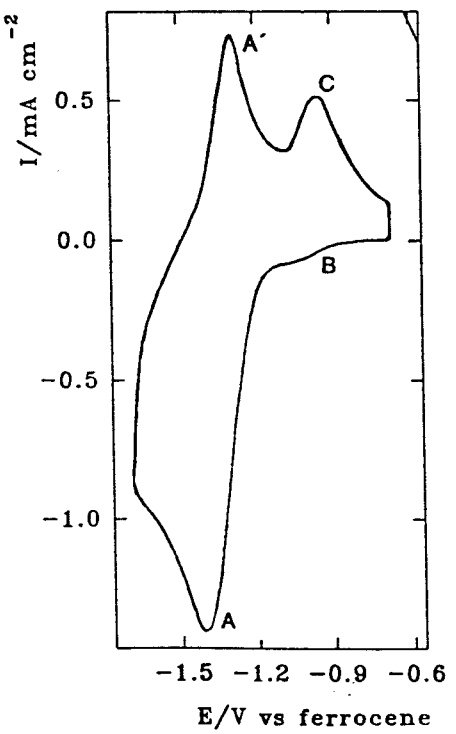

Figure 4.4.4
Cyclic Voltammogram recorded at a vitreous carbon disc at 400 mV s^{-1} for a THF/Bu_4NBF_4 (0.2M) solution of $CpTiCl_2[O^iPr]$ (7.4 mM) (procedure 4).

4.5 CONTROLLED POTENTIAL ELECTROLYSIS.

In order to help identify the reduction products of some of the electron transfers seen in the voltammetry of $CpTiCl_2[OR]$ complexes and other moisture sensitive organotitanium species, it was necessary to perform controlled potential electrolysis on their THF solutions.

The cell shown in figure 4.5.1 was developed to carry out these bulk electrolysis experiments under dry conditions similar to those for the 'dry' cyclic voltammetry. The considerations involved in its design were based on a wish to perform a controlled potential electrolysis as quickly as possible (ideally between ½ and 1 hour), hence a small volume for the working compartment and electrodes with high surface area. It was also desirable to be able to obtain cyclic voltammograms of the electrolyte solution before and after electrolysis so a Luggin capillary was made to fit close to the working electrode. The reference electrode was again a silver wire placed inside the Luggin capillary. The counter electrode, a cylindrical platinum gauze, was placed in a glass column separated from the working compartment by a glass sinter. To minimise resistance between the working and counter electrodes they were designed to be parallel to each other and as close as possible. Both electrodes were smaller than the glass sinter separating them in order to promote a uniform potential distribution. A magnetic stirrer bead was placed in the working compartment to aid dissolution and to enhance mass transport during the electrolysis, again helping to decrease the duration of the experiment.

The same alumina-filled drying column as designed for the closed, dry cyclic voltammetry cell (figure 4.1.2) was fitted to this electrolysis cell and the procedure for adding the THF/TBAB solution the same as before, melting the TBAB under vacuum before dissolution. The active solid compound was added to the cell prior to evacuation. Once the THF/TBAB solution had passed through the alumina into the working compartment of the cell, a vacuum was

applied briefly to the counter electrode column by means of the tap on the arm at the top whilst argon was applied through the tap on the main body of the cell, thus drawing up the required amount of solution into the counter electrode compartment. No mixing of the solutions between the two compartments during the electrolysis experiments was observed. The volume of solvent added was measured at the end of the experiment.

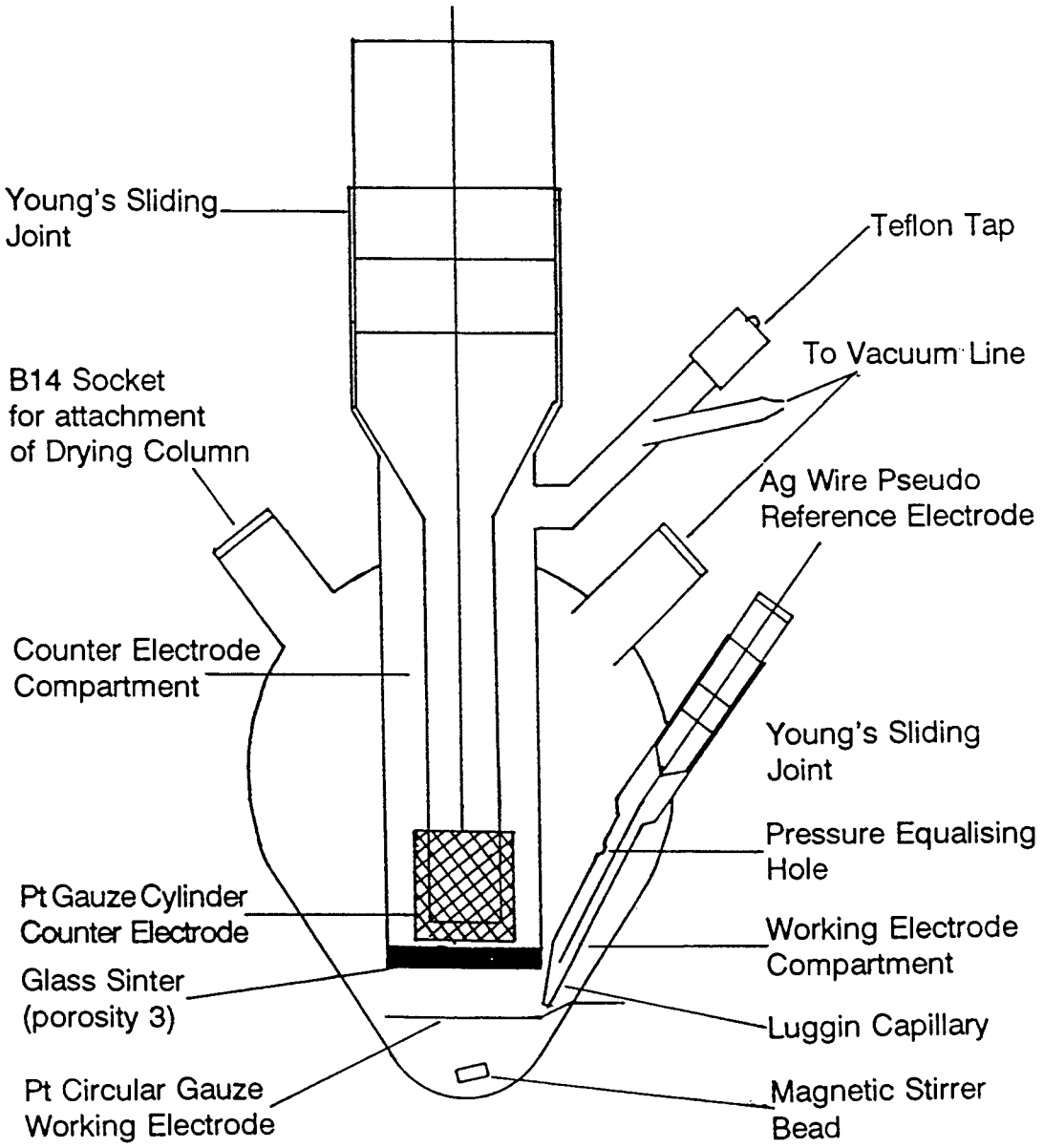

Figure 4.5.1
Electrolysis Cell for use on a Vacuum Line

To test the performance of this cell a controlled potential electrolysis was performed on a solution of the ferricyanide, knowing that this displays a one electron reduction. An aqueous solution of $K_3Fe(CN)_6$ (1.5 mM) with KOH (0.1 M) was held at -0.1 V vs Ag wire for about half an hour, the charge passed and the cell current were recorded at regular intervals. Cyclic voltammograms were taken of the solution before and after electrolysis, both showed a reversible electron transfer. Extrapolation of a plot of current (mA) against charge passed (C) gave a value for q^{∞}, the total charge consumed during the experiment. q^{∞} is related to n, the number of electrons involved in the overall reaction by the following equation:

$$q^{\infty} = nFcV$$

where c is the concentration of the electroactive species and V is the volume of the solution in the working electrode compartment. The value for q^{∞} obtained in the experiment with the reduction of ferricyanide led to n = 1 and, hence, with aqueous solutions, the cell behaviour performed well. However when controlled potential electrolyses were performed using this cell and non-aqueous systems, the n values obtained from the coulometry were consistently low; this was the case even with model systems such as the oxidation of ferrocene. Therefore in later work, electrolyses in this cell were used to investigate products and changes to both voltammetry and spectroscopy during oxidation/reduction but the coulometry was not interpreted.

CHAPTER 5

THE ELECTROCHEMICAL BEHAVIOUR OF $CpTiCl_2[OR]$ (R = alkyl, aryl) COMPLEXES IN THF.

This chapter describes the study of the electrochemistry of the $CpTICl_2[OR]$ complexes in THF/Bu_4NBF_4 solutions carried out under rigorously dried conditions (chapter 4, procedure 4). The influence of water on the results is also discussed.

5.1 $CpTiCl_2[OAr]$

Ar = $-C_6H_3(^iPr)_2$, $-C_6H_3(Me)_2$, $-C_6H_2(Me)_2(Br)$, $-C_6H_2(Me)_3$

Figure 5.1.1 shows a cyclic voltammogram recorded at a vitreous carbon disc electrode at 400 mV s^{-1} between the potential limits -0.6 V and -1.6 V vs ferrocene for a THF solution of $CpTiCl_2[OC_6H_3(^iPr)_2]$ (15 mM) with Bu_4NBF_4 (0.2 M) in the closed cell. This voltammogram shows a reduction process, peak A with $E_{p/2}$ = -1.18 V vs ferrocene, and a coupled oxidation, peak A´. The peak separation for this couple is 60 mV and the ratio of the peak current densities, $Ip^{A'}/Ip^{A}$, is equal to one. Another small cathodic process, represented by peak B, can just about be seen at potentials less negative than peak A but no further reduction or oxidation processes are evident within the potential range limited by the solvent/electrolyte reactions. From figure 5.1.2 it can be seen that there is no significant change to the shape of the response as the sweep rate is decreased. At 36 mV s^{-1} $Ip^{A'}/Ip^{A}$ is still equal to one, showing that the reduced species produced at A is stable even at very slow sweep rates. The form of the response suggests that this electron transfer is a

simple reversible one electron process.

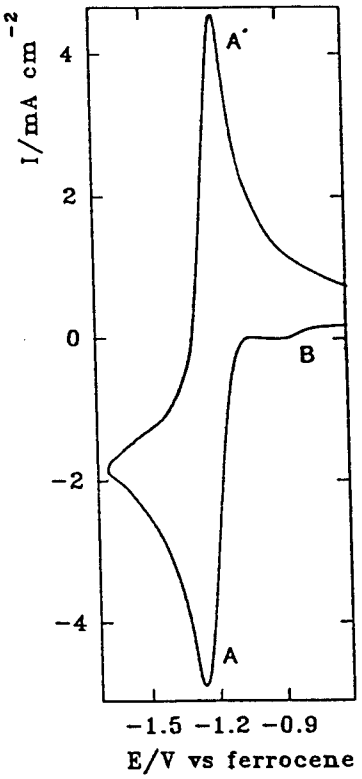

Figure 5.1.1

Cyclic Voltammogram recorded at a vitreous carbon disc at 400 mV s^{-1} for a THF/Bu_4NBF_4 (0.2M) solution of $CpTiCl_2[OC_6H_3(^iPr)_2]$ (15 mM) in a closed cell.

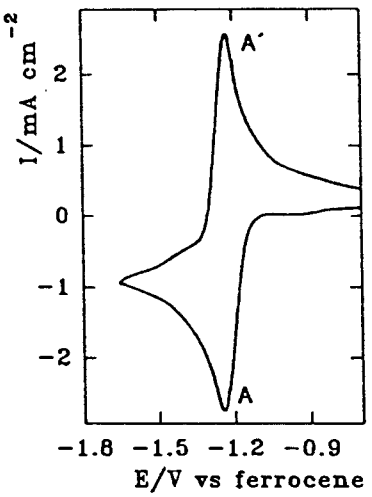

Figure 5.1.2

Cyclic Voltammogram recorded at a vitreous carbon disc at 100 mV s^{-1} for a THF/Bu_4NBF_4 (0.2M) solution of $CpTiCl_2[OC_6H_3(^iPr)_2]$ (15 mM) in a closed cell.

For a lower concentration solution of $CpTiCl_2[OC_6H_3(^iPr)_2]$ (7 mM) in THF with Bu_4NBF_4 (0.2 M) the cyclic voltammogram recorded at 25 mV s^{-1} between -0.8 V and -1.6 V vs ferrocene again displays a reversible one electron transfer (figure 5.1.3).

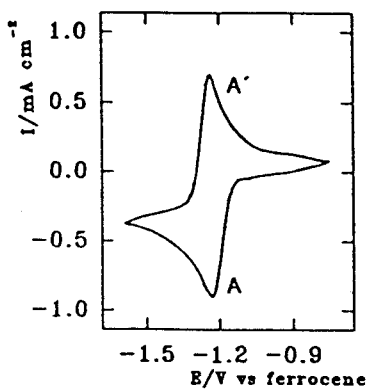

Figure 5.1.3

Cyclic Voltammogram recorded at a vitreous carbon disc at 25 mV s^{-1} for a THF/Bu_4NBF_4 (0.2M) solution of $CpTiCl_2[OC_6H_3(^iPr)_2]$ (7 mM) in a closed cell.

Cyclic voltammograms were recorded for the other $CpTiCl_2[OAr]$ complexes and all showed similar responses. The reversibility of the A/A´ couple for the $CpTiCl_2[OAr]$ complexes in THF is further illustrated in figure 5.1.4 which shows a series of cyclic voltammograms recorded at varying sweep rates between the potential limits -0.64 V and -1.64 V vs ferrocene for a 10.7 mM solution of $CpTiCl_2[OC_6H_2(Me)_2(Br)]$ with Bu_4NBF_4 (0.2 M) as the supporting electrolyte. A plot of Ip^A (the current density of the major reduction process) against $\nu^{1/2}$ is shown in figure 5.1.5 and displays a straight line passing through the origin. This was also the case for similar plots for all the aryloxy complexes.

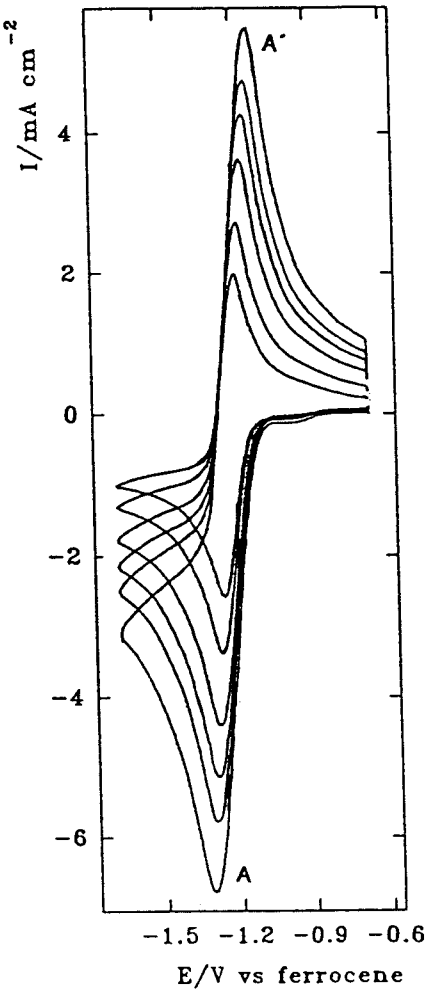

Figure 5.1.4
Cyclic Voltammogram recorded at a vitreous carbon disc at 50, 100, 200, 300, 400 & 600 mV s^{-1} for a THF/Bu_4NBF_4 (0.2M) solution of $CpTiCl_2[OC_6H_2(Me)_2(Br)]$ (10.7 mM) in a closed cell.

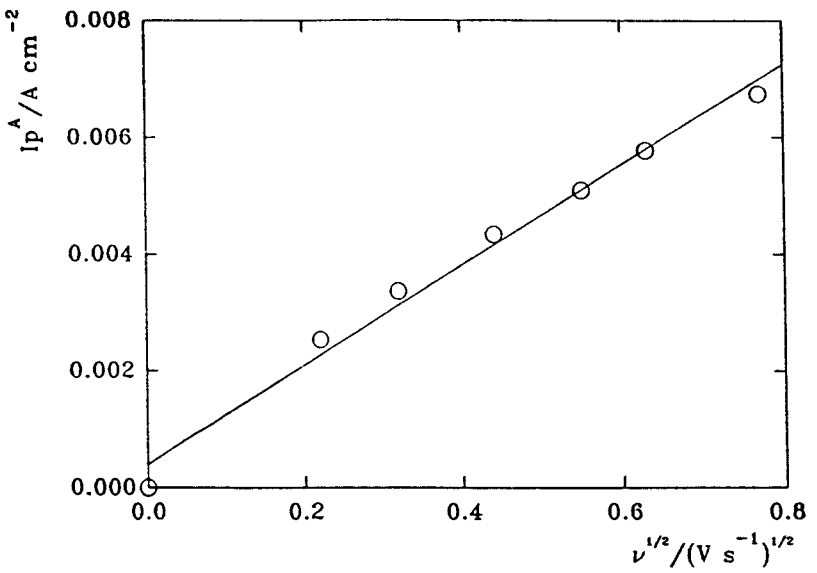

Figure 5.1.5

Showing data obtained from the cyclic voltammetry recorded at a vitreous carbon disc of a THF/Bu_4NBF_4 (0.2 M) solution of $CpTiCl_2[OC_6H_2(Me)_2(Br)]$ (10.7 mM) in a closed cell.

To further confirm that the reduction of these complexes involved the addition of one electron, voltammetry was performed using a Pt microdisc electrode (diameter 10 μm). Figure 5.1.6 shows the well-formed S-shaped reduction wave recorded for a THF solution of $CpTiCl_2[OC_6H_2(Me)_2(Br)]$ (10.7 mM) where the half-wave potential occurs at -1.22 V vs ferrocene. The backward scan follows almost exactly that of the forward scan and $E_{¾} - E_{¼}$ = 56 mV, confirming the reversibility of the electron transfer. The value of *nD* was obtained for this voltammogram from equation 5.1a below where, *i* is the mass transport controlled limiting current in amps, *c* is the concentration of the electroactive species (mol cm^{-3}) and *a* is the radius of the microdisc (cm) [83].

$$i = 4nFDca \qquad (5.1a)$$

The value of n^3D for this system was calculated from the Randles-Sevčik equation (5.1b) [84]:

$$Ip^A = -(2.7 \times 10^5)(n^{½})^3 cD^{½}\nu^{½} \qquad (5.1b)$$

Where Ip^A is in A cm^{-2}, *D*, the diffusion coefficient, is in cm^2 s^{-1}, ν is in V s^{-1} and *c*, the concentration of the electroactive species, is in mol cm^{-3}. The value of

$Ip^A/\nu^{1/2}c$ was calculated from the slope of the plot of Ip^A vs $\nu^{1/2}$ in figure 5.1.5. From these two measurements independent values for n and D can be calculated; n = 1.1 and D = 1.1 x 10^{-5} cm^2 s^{-1}.

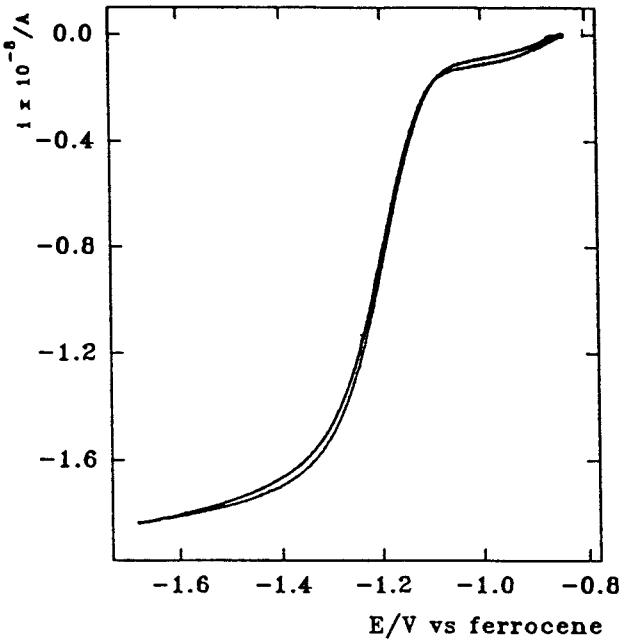

Figure 5.1.6
Cyclic Voltammogram recorded at a Pt microdisc electrode (diameter = 10 μm) at 20 mV s^{-1} for a THF/Bu_4NBF_4 (0.2M) solution of $CpTiCl_2[OC_6H_2(Me)_2(Br)]$ (10.7 mM) in a closed cell.

The values for n^3D were calculated from Ip^A vs $\nu^{1/2}$ plots for each of the $CpTiCl_2[OAr]$ complexes and are tabulated along with the half-peak potentials (table 5.1.1). With the value of n = 1, it can be seen that three of the complexes gave diffusion coefficients similar to those expected in THF solutions. In aqueous solutions, D for most species falls in the range 0.5 - 0.7 x 10^{-5} cm^2 s^{-1}. The viscosities for THF and water are 0.46 cp and 1.0 cp respectively, hence the diffusion coefficients in THF would be expected to be in the range 1.0 - 1.5 x 10^{-5} cm^2 s^{-1}. $CpTiCl_2[OC_6H_3(^iPr)_2]$, whose diffusion coefficient came out to be rather low, would not be expected to be any different from the other complexes and hence it was thought that this low D value resulted from uncertainties in the concentration of the solution prepared using vacuum line techniques.

Complex	cencentration (mM)	ν (mV s^{-1})	$E_{p/2}$* (V)	n^3D† (cm^2 s^{-1})
$CpTiCl_2[OC_6H_3(^iPr)_2]$	15.0 7.0	36 - 400 25 - 600	-1.18	0.6 x 10^{-5}
$CpTiCl_2[OC_6H_3(Me)_2]$	5.3	36 - 400	-1.20	1.0 x 10^{-5}
$CpTiCl_2[OC_6H_2(Me)_2(Br)]$	10.7	50 - 600	-1.20	1.1 x 10^{-5}
$CpTiCl_2[OC_6H_2(Me)_3]$	11.5	25 - 600	-1.18	1.1 x 10^{-5}

Table 5.1.1

Showing the data obtained from the cyclic voltammetry, recorded at a vitreous carbon disc electrode, of THF solutions of $CpTiCl_2[OAr]$ complexes with Bu_4NBF_4 (0.2 M) as the supporting electrolyte. All experiments were performed using the vacuum line techniques described by procedure 4 (section 4.4).

* All potentials are quoted against ferrocene as an internal reference.

† Calculated from the Randles-Sevčik equation using the slope of the plot of Ip^A vs $\nu^{1/2}$ for each experiment.

The electrolysis cell shown in figure 4.5a was used to perform a controlled potential electrolysis on a 14 mM solution of $CpTiCl_2[OC_6H_3(^iPr)_2]$ in THF with Bu_4NBF_4 (0.2 M). The cyclic voltammogram shown in figure 5.1.7 was recorded using this cell prior to the electrolysis and, although the response is degraded at this large electrode, it again shows one reversible electron transfer. The potential was then switched to -1.0 V vs Ag wire for half an hour. Figure 5.1.8 shows the cyclic voltammogram run on the solution in the cell after the electrolysis, this time commencing the sweep from -1.0 V vs Ag wire in the positive direction. Although a couple of small bumps in the voltammogram are now evident and the major peaks are slightly smaller, a reversible electron transfer process can still be seen at the same potential as before, indicating that the Ti(III) species produced by the reduction is stable in solution on a 30 minute timescale. It should be noted that a colour change occurs during the controlled potential electrolysis; initially the solution is orange, at the end of the electrolysis, it is green.

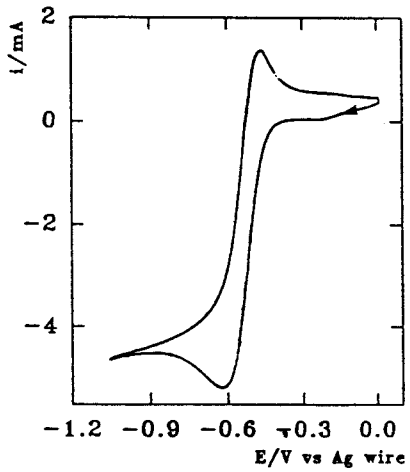

Figure 5.1.7

Cyclic Voltammogram recorded prior to an electrolysis at a Pt gauze electrode at 25 mV s^{-1} for a THF/Bu_4NBF_4 (0.2M) solution of $CpTiCl_2[OC_6H_3(^iPr)_2]$ (14 mM) in a closed cell.

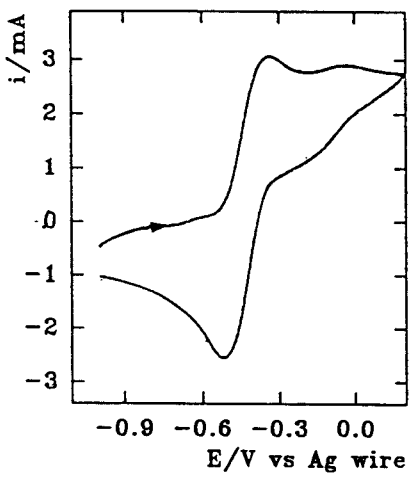

Figure 5.1.8

Cyclic Voltammogram recorded at a Pt gauze electrode at 25 mV s^{-1} for a THF/Bu_4NBF_4 (0.2M) solution of $CpTiCl_2[OC_6H_3(^iPr)_2]$ (14 mM) after a controlled potential electrolysis at -1.0 V vs Ag wire for ½ hour in a closed cell.

A similar electrolysis was performed on a THF solution of $CpTiCl_2$-$[OC_6H_2(Me)_2(Br)]$ (12 mM) which again showed a colour change from orange to green/blue after one hour at -1.0 V vs Ag wire. Cyclic voltammograms

recorded after the electrolysis again showed the reversible oxidation of the Ti(III) species giving further evidence for the stability of this species in dry THF, even over the period of one hour. Ti(III) complexes are commonly green or blue in solution and so the colour changes observed here are a further indication of the reduction being a one electron transfer, facilitating the transformation Ti(IV) to Ti(III) suggesting that the chemistry of these complexes is limited to the electron transfer reaction:

$$CpTiCl_2[OAr] + e^- \rightleftharpoons [CpTiCl_2[OAr]]^-$$

The different substituents on the aromatic ring appear to have no influence on the reduction potentials of these complexes as can be seen by the great similarity in their $E_{p/2}$ values. That is, the substituents do not exert a significant effect on the electron density at the titanium centre. This is also observed with the proton and carbon nmr shifts for the cyclopentadienyl ring, where there is no significant difference in δ between the complexes (section 3.2).

5.2 $CpTiCl_2[OR]$

R = $-OCH(CH_3)_2$ or menthoxide

Figure 5.2.1 shows a cyclic voltammogram recorded at a vitreous carbon disc at 400 mV s^{-1} between the potential limits -0.6 V and -1.6 V vs ferrocene for a THF solution of $CpTiCl_2[O^iPr]$ (7.4 mM) with Bu_4NBF_4 (0.2 M) in the closed cell. A major reduction peak, A, can be seen with $E_{p/2}$ = -1.28 V vs ferrocene which has a coupled oxidation, peak A´. The $Ip^{A'}/Ip^{A}$ ratio for this couple however, is less than one and another important anodic peak (peak C) occurs at -0.86 V. Peak B, the small cathodic peak at about -0.9 V is also evident. The reversibility of the major reduction increases at higher scan rates. As the scan rate is lowered peak C gradually becomes the most significant anodic peak while peak A´ diminishes in size relative to it (figure 5.2.2) until at 36 mV s^{-1} (figure 5.2.3) when it has disappeared completely. At 36 mV s^{-1} peak C is the

only anodic process observed. The peak current density of the major reduction peak, A, varies proportionally with the square root of the potential scan rate and its size is comparable with that of a one electron transfer. The small cathodic peak B at about -0.9 V must be due to an electroactive species present in solution in very small quantities and also appears in the voltammetric responses from other complexes so will be discussed in more detail later. Peak B may or may not be coupled to peak C although the size of peak B does not increase on second potential cycle.

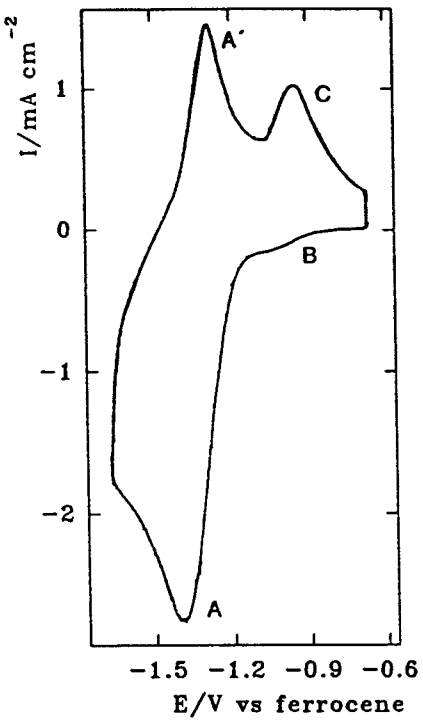

Figure 5.2.1
Cyclic Voltammogram recorded at a vitreous carbon disc electrode at 400 mV s^{-1} for a THF/Bu_4NBF_4 (0.2M) solution of $CpTiCl_2[O^iPr)]$ (7.4 mM) in a closed cell.

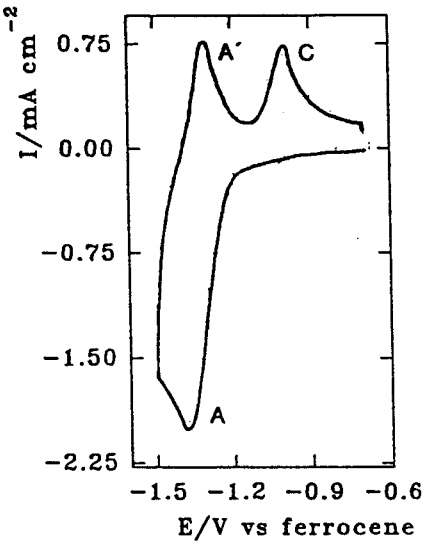

Figure 5.2.2
Cyclic Voltammogram recorded at a vitreous carbon disc electrode at 225 mV s^{-1} for a THF/Bu_4NBF_4 (0.2M) solution of $CpTiCl_2[O^iPr)]$ (7.4 mM) in a closed cell.

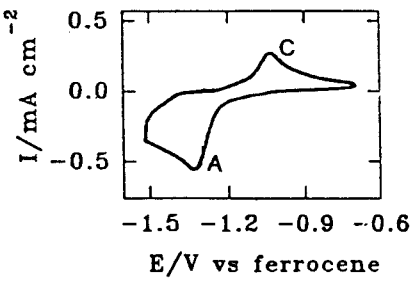

Figure 5.2.3
Cyclic Voltammogram recorded at a vitreous carbon disc electrode at 36 mV s^{-1} for a THF/Bu_4NBF_4 (0.2M) solution of $CpTiCl_2[O^iPr)]$ (7.4 mM) in a closed cell.

It is deduced from this data that the product of the one electron reduction of $CpTiCl_2[O^iPr]$ undergoes a chemical reaction removing it from solution and producing a species that is oxidised at -0.86 V (peak C). The rate constant, k, for this reaction may be calculated from a plot of Ip^a/Ip^c vs log $k\tau$ assuming a first order decay. τ is the time taken to scan from $E_{p/2}$ for the cathodic peak to the sweeping potential [84]. k was found to be 0.2 s^{-1}.

The voltammetry of the $CpTiCl_2$[menthoxide] exhibits some similarities with that of $CpTiCl_2[O^iPr]$ although it is evident that the chemistry of the major reduced species is much slower. Figure 5.2.4 shows a cyclic voltammogram recorded at 400 mV s^{-1} between -0.80 V and -1.80 V vs ferrocene for a THF solution of $CpTiCl_2$[menthoxide] (12 mM) with Bu_4NBF_4 (0.2 M) in the closed cell. One cathodic process, peak A, and one anodic process, peak A´, are evident with $E_{p/2}$ = -1.38 V vs ferrocene. Figures 5.2.5 and 5.2.6 show cyclic voltammograms recorded under the same conditions but with varying sweep rates and in both a second anodic peak can just about be seen at around -0.9 V.

Peaks A and A´ appear to exhibit the behaviour for a reversible electron transfer process. The ratio of their peak current densities, $Ip^{A'}/Ip^A$, is equal to one and even at slow sweep rates when peak C is just evident, $Ip^{A'}/Ip^A$ is close to one indicating that the reduced species is almost completely stable on the timescale of this cyclic voltammetry.

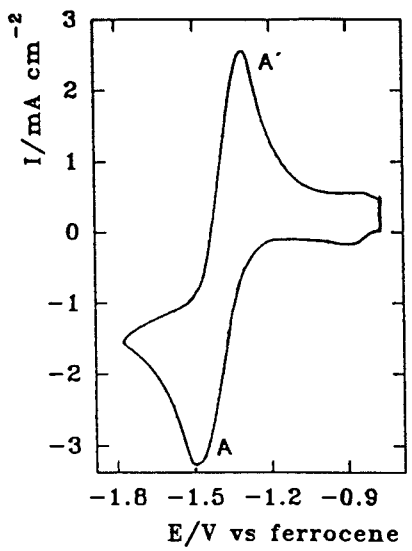

Figure 5.2.4
Cyclic Voltammogram recorded at a vitreous carbon disc electrode at 400 mV s^{-1} for a THF/Bu_4NBF_4 (0.2M) solution of $CpTiCl_2$[menthoxide] (12 mM) in a closed cell.

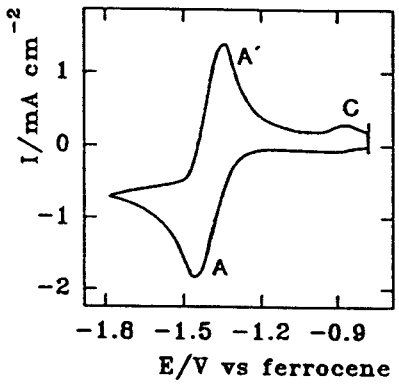

Figure 5.2.5
Cyclic Voltammogram recorded at a vitreous carbon disc electrode at 100 mV s^{-1} for a THF/Bu_4NBF_4 (0.2M) solution of $CpTiCl_2$[menthoxide] (12 mM) in a closed cell.

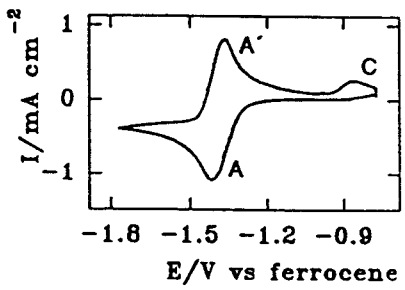

Figure 5.2.6
Cyclic Voltammogram recorded at a vitreous carbon disc electrode at 36 mV s^{-1} for a THF/Bu_4NBF_4 (0.2M) solution of $CpTiCl_2$[menthoxide] (12 mM) in a closed cell.

When the concentration of the electroactive species is decreased, the stability of the reduced species diminishes slightly as can be seen in figure 5.2.7 and the response tends towards that for $CpTiCl_2[O^iPr]$. Figure 5.2.7 shows a cyclic voltammogram recorded at 100 mV s^{-1} between -0.74 V and -1.74 V vs ferrocene for a THF solution of $CpTiCl_2$[menthoxide] (8 mM) with Bu_4NBF_4 in the closed cell. The ratio $Ip^{A'}/Ip^{A}$ is now about 0.8 and peak C has increased relative to A′ showing that the reduced species produced at A is not entirely stable under these conditions and undergoes a chemical change producing a species that is oxidised at C. Making the same assumption as before, the rate constant for this chemical change was calculated to be 0.01 s^{-1}. Peak B, the small cathodic peak at about -0.9 V is also evident in this cyclic voltammogram. When the potential limits are extended further in both positive and negative directions no additional peaks are observed. The dependence of the response on the substrate concentration suggests that the coupled chemistry involves impurities in solution, this is discussed further below.

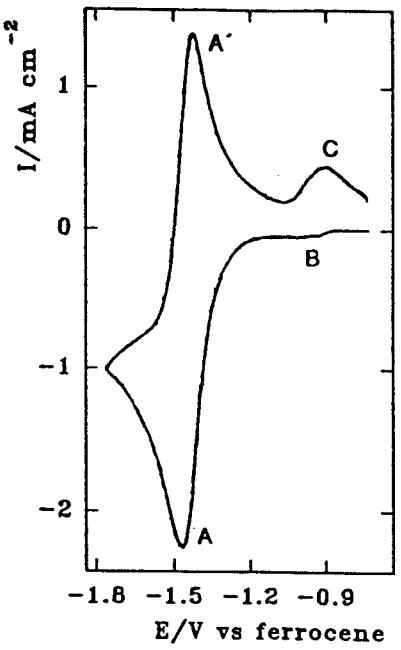

Figure 5.2.7
Cyclic Voltammogram recorded at a vitreous carbon disc electrode at 100 mV s^{-1} for a THF/Bu_4NBF_4 (0.2M) solution of $CpTiCl_2$[menthoxide] (8 mM) in a closed cell.

Table 5.2.2 summarizes the data obtained from the cyclic voltammetry of the alkoxide complexes. The n^3D values were again obtained from the Randles-Sevčik equation (5.1b) using plots of Ip^A vs $\nu^{½}$ and with n = 1 the expected values of D for $CpTiCl_2$[menthoxide] were obtained. $CpTiCl_2$[O^{i}Pr] gave a rather low n^3D value, again probably reflecting uncertainties in concentration measurements since no great variation between the diffusion coefficients of the $CpTiCl_2$[OR] (R = alkyl or aryl) complexes is expected.

The $CpTiCl_2$[OR] complexes, where R is an alkyl group, proved more difficult to reduce than the $CpTiCl_2$[OAr] analogues by between 80 and 180 mV.

Assuming the addition of an electron to be centred on the titanium, the less negative value for those complexes containing the aryloxy ligands is a reflection of the lower electron density around the titanium centre compared to the two alkoxy analogues. This trend is also observed in the ^1H and ^{13}C nmr data for the cyclopentadienyl group in the complexes. That data, presented in section 3.2, shows that the cyclopentadienyl ring is deshielded in the aromatic complexes giving ^1H and ^{13}C nmr δ values more downfield to the corresponding values for the aliphatic analogues. These observations are quite

Complex	concentration (mM)	ν (mV s^{-1})	$E_{p/2}$* (V)	$Ip^{A'}/Ip^{A}$	n^3D† (cm^2 s^{-1})	k (s^{-1})
$CpTiCl_2[O^iPr]$	7.4 7.4	400 225	-1.28	0.50 0.35	0.4×10^{-5}	0.2
$CpTiCl_2$[menthoxide]	12 8	36 -625 100	-1.38	1.0 0.8	1.2×10^{-5} 0.9×10^{-5}	- 0.01
$CpTiCl_3$‡	15	25 - 600	-0.86	1.0	0.9×10^{-5}	-

Table 5.2.1

Showing the data obtained from the cyclic voltammetry, recorded at a vitreous carbon disc electrode, of THF solutions of $CpTiCl_2[OR]$ complexes with Bu_4NBF_4 (0.2 M) as the supporting electrolyte. All experiments were performed using the vacuum line techniques described by procedure 4 (section 4.4).

* All potentials are quoted against ferrocene as an internal reference.

† Calculated from the Randles-Sevčik equation using the slope of the plot of Ip^A vs $\nu^{1/2}$ for each experiment.

‡ Data obtained under the same conditions as for the other complexes and provided for comparison.

expected since with the aryloxides the lone pairs on the oxygen are tied up in the aromatic π-cloud and hence are less able to donate electron density to the titanium centre. With the alkoxides the oxygen lone pairs are free to contribute to the electron density around the metal centre.

The first one electron reduction of $CpTiCl_3$ occurs some 300-500 mV less negative than any of the $CpTiCl_2[OR]$ complexes (R = alkyl or aryl). So replacement of a chloride ligand by an alkoxide or aryloxide makes the titanium(IV) centre in these complexes more difficult to reduce.

THF solutions of $CpTiCl_3$ display two one electron reduction processes; the first at -0.86 V vs ferrocene, is completely reversible whereas the second, at -2.80 V displays only slight reversibility. Figure 5.2.8 shows a cyclic voltammogram recorded at a vitreous carbon disc at 25 mV s^{-1} for a THF solution of $CpTiCl_3$ (15 mM) with Bu_4NBF_4 (0.2 M). The diffusion coefficient for $CpTiCl_3$ in THF was calculated (table 5.2.1) and proved to be within the expected range of values.

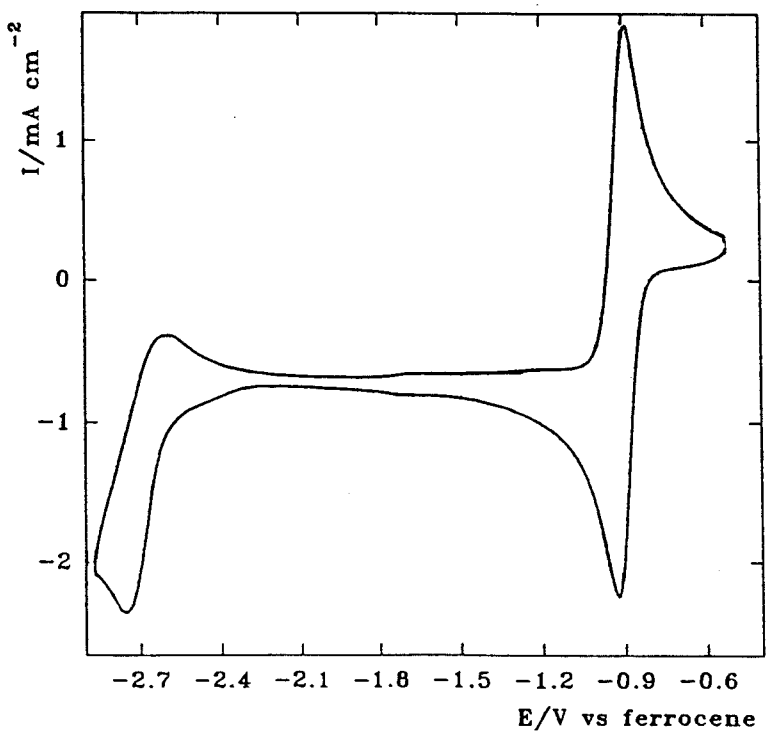

Figure 5.2.8
Cyclic Voltammogram recorded at a vitreous carbon disc electrode at 25 mV s^{-1} for a THF/Bu_4NBF_4 (0.2M) solution of $CpTiCl_3$ (15 mM) in a closed cell.

5.3 THE EFFECT OF RESIDUAL WATER ON THE VOLTAMMETRIC RESPONSES OF $CpTiCl_2[OR]$ (R = alkyl, aryl) COMPLEXES IN THF.

There is a change in the voltammetric response from the $CpTiCl_2[OAr]$ complexes when less effort has been made to perform the experiments under very dry conditions. Figure 5.3.3 shows a cyclic voltammogram recorded at 150 mV s^{-1} between -0.44 V and -1.64 V vs ferrocene for a THF solution of $CpTiCl_2[OC_6H_3(^iPr)_2]$ (23 mM) with Bu_4NBF_4 in a cell in the open laboratory (procedure 1). Although peaks A and A´ still represent the major electron transfer process and appear as a reversible couple, another two peaks are evident. These two peaks, one cathodic at -0.92 V and one anodic at -0.86 V, occur at the same potentials as peaks B and C in the voltammograms of the alkoxide complexes and so have been labelled as such. Comparing this voltammogram with that in figure 5.1.1 shows that although peak B is observed under drier conditions it is then only a small fraction of the size of peak B in this case, albeit peak B is still much smaller than peak A. In figure 5.3.1 it can be seen that peaks B and C probably have equal current densities, which is the case at all scan rates (18 - 800 mV s^{-1}). The current density of peak B is proportional to the square root of the scan rate thereby indicating that this couple could represent a reversible electron transfer occurring with a species in solution of lower concentration than the major complex. There does not appear to be any interchange between this species and the $CpTiCl_2[OAr]$ complex or their reduced forms on the voltammetric timescale. Since peak B for the $CpTiCl_2[OAr]$ complexes occurs to a much greater extent under wetter conditions it is reasonable to suggest that it arises from the substitution of a ligand in $CpTiCl_2[OAr]$ in a reaction involving water. The addition of Cl^-, by adding anhydrous Bu_4NCl, does not change the voltammetric response.

The voltammetric response of the alkoxide complexes under less dry conditions also varies from that in drier solutions in that the extent of the chemical change undergone by the major reduced species is greater the

wetter the solution. This is reflected in a greater loss of the reversibility of the addition of an electron to the $CpTiCl_2[OR]$ complex and hence an increase in the peak representing the oxidation of the product of that chemical change (peak C). When small amounts of water are added to a THF solution of $CpTiCl_2$[menthoxide] and cyclic voltammograms recorded after each addition, the gradual loss in the reversibility of the major reduction process and the increase in the size of peak C as more water is added can be observed. This is shown in figure 5.3.2 where all the cyclic voltammograms are recorded at 300 mV s^{-1} between -0.80 V and -1.88 V vs ferrocene for a THF/Bu_4NBF_4 (0.2 M) solution of $CpTiCl_2$[menthoxide] (72 mM). Voltammogram (a) shows the response prior to the addition of any extra water; peak C is in evidence although it is very small compared to A´. As more water is added it can be seen that peak C grows in significance while peak A´ diminishes until in voltammogram (e), peak C is by for the most prominent anodic peak. No significant increase in peak B was observed with the addition of water.

When the potential limits are extended in the negative direction past peak A for the alkoxide complex solutions a further cathodic peak at about -1.7 V vs ferrocene is observed on the cyclic voltammogram if peak A´ is completely absent (figures 4.1.3 and 4.4.3 in chapter 4).

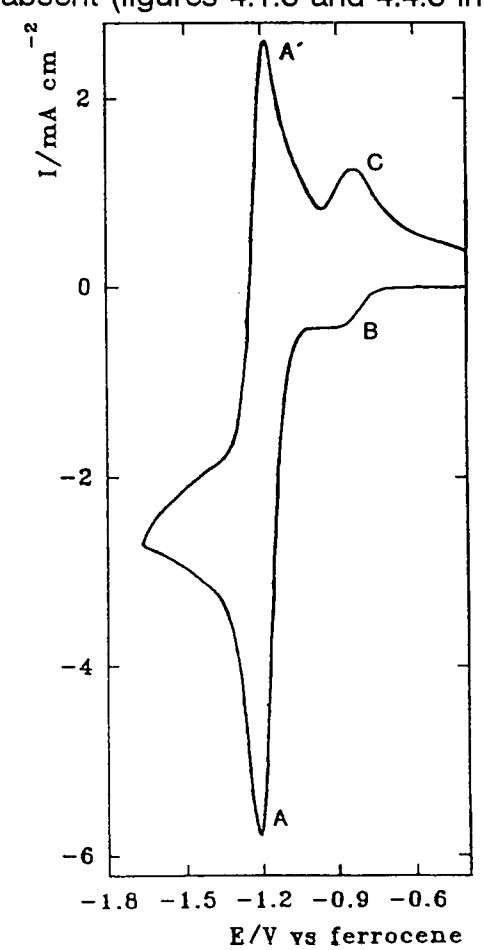

Figure 5.3.1
Cyclic Voltammogram recorded at a vitreous carbon disc electrode at 150 mV s^{-1} for a THF/Bu_4NBF_4 (0.2M) solution of $CpTiCl_2[OC_6H_3(^iPr)_2]$ (23 mM).

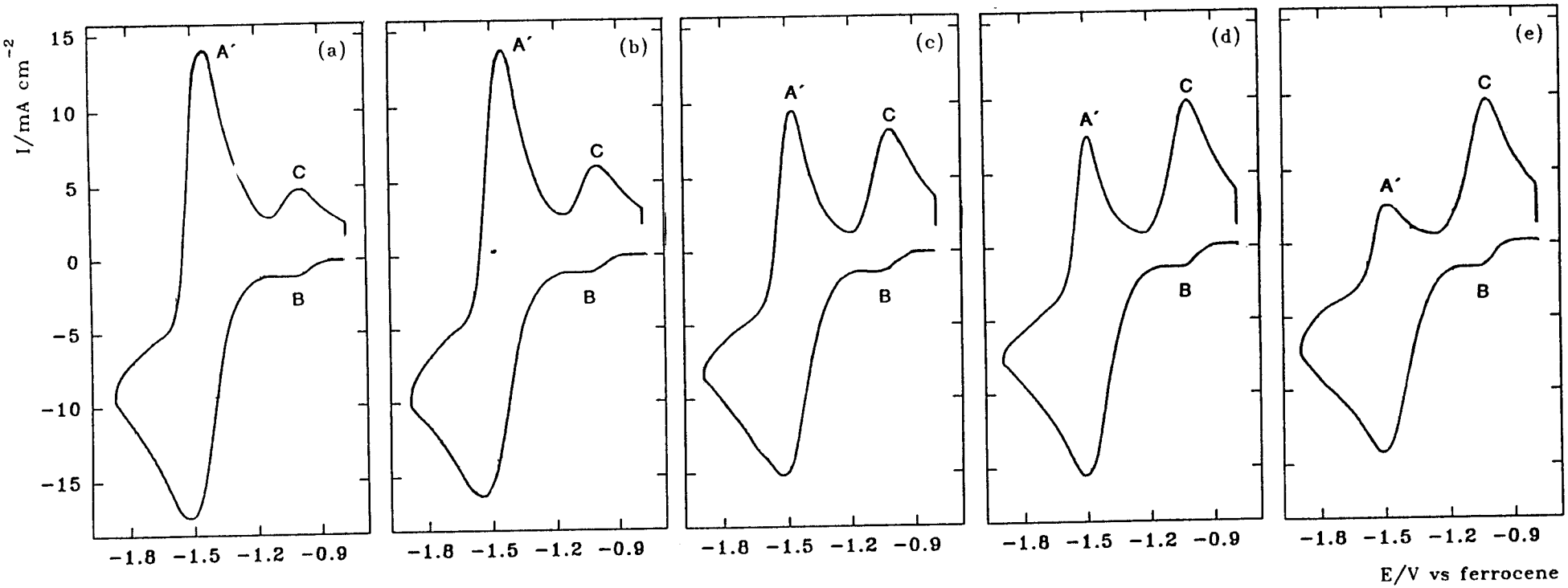

Figure 5.3.2

A series of cyclic voltammograms recorded at a vitreous carbon disc electrode at 300 mV s^{-1} for a THF/Bu_4NBF_4 (0.2 M) solution of $CpTiCl_2$[menthoxide] (72 mM) with inoreasing amounts of water added (a → e).

5.4 THE MECHANISM OF REDUCTION OF $CpTiCl_2[OR]$ (R = alkyl, aryl) COMPLEXES IN THF.

From the evidence in section 5.3 and the previous comparison of experimental procedures in chapter 4 it is clear that the concentration of water in the electrolyte solution affects the voltammetric response quite significantly. This effect is different for the aryloxide and alkoxide complexes although the same peaks arising from the reduction and oxidation of the products of reactions with water are evident in both cases. Peak B, at -0.92 V, has been attributed to the reduction of a species present in lower concentrations than the major complex but whose concentration increases the wetter the solution. It has been suggested that this arises from the substitution of a ligand in a reaction with water and since the reduction occurs at the same potential for both classes of complex it is reasonable to propose that it is the -OAr or -OR group that is displaced. The fact that no change in the response is observed on the addition of free chloride ions to solution supports this proposal. Hence a likely reaction is:

$$CpTiCl_2[OR] + H_2O \rightleftharpoons CpTiCl_2[OH] + ROH$$

Where R can be alkyl or aryl. One can imagine that this replacement of the -OR ligand by a hydroxy group proceeds via the protonation of the alkoxide (or aryloxide) oxygen followed then by the exchange of ligands. Peaks B and C then relate to the process:

$$CpTiCl_2[OH] + e^- \rightleftharpoons [CpTiCl[OH]]^-$$

This reaction with water occurs with all the complexes even in the cases where considerable effort has gone into trying to make the experimental conditions as dry as possible. However the very small size of peak B in the voltammograms of $CpTiCl_2[OAr]$ complexes recorded using the vacuum line and alumina drying column procedure indicates that these solutions are considerably drier than those of the other experimental procedures. This is especially noticeable in figure 5.1.3 where vacuum line techniques have been employed for a low concentration solution of a $CpTiCl_2[OAr]$ complex (the

higher the complex concentration the more masked the reactions with water become) and peak B is barely visible. By all accounts if peak B is evident then peak C, of equal magnitude, ought also to be present. It is difficult tell whether this is the case or not in the voltammograms where peak B is very small because the large current density of peak A´ conceals any contribution from the process represented by peak C.

For the alkoxide complexes however, peak C is almost always greater than peak B when the potentials are swept past the major reduction peak A. The only occasion when this is not the case is when the voltammetry is recorded on a solution with a relatively high concentration of $CpTiCl_2$[menthoxide], a fast sweep rate and rigorously dried conditions; figure 5.2.4 shows an example where this is the case. The more irreversible the major cathodic peak A is, the larger peak C appears. Peak C also grows steadily at the expense of the other anodic peak A´, on the addition of increasing amounts of water. When the potential sweep is reversed before the commencement of peak A it can be seen that peaks B and C represent a reversible electron transfer, as has previously been cited for the aryloxide complexes, and is shown in figure 5.4.1 which displays a number of cyclic voltammograms at varying scan rates for a 19 mM THF/Bu_4NBF_4 (0.2 M) solution of $CpTiCl_2[O^iPr]$ recorded under incompletely dried conditions. The larger size of peak C compared to peak B in the voltammograms where peak A is present can then only be explained by the electroactive species oxidised at peak C also being formed as a decomposition product of the major reduced species. That is, the reaction between the major anion and water produces the species that is oxidised at peak C, hence the reaction mechanism for the behaviour of the alkoxide complexes can be represented by a 'scheme of squares' shown below in scheme 5.4.1.

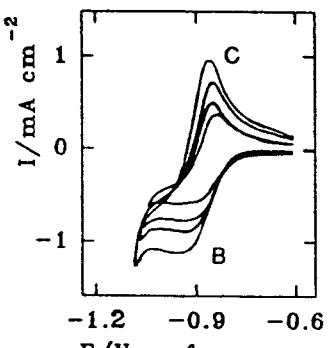

Figure 5.4.1
Cyclic Voltammogram recorded at a vitreous carbon disc electrode at 600, 300, 150 & 75 mV s^{-1} for a THF/Bu_4NBF_4 (0.2M) solution of $CpTiCl_2[O^iPr]$ (19 mM).

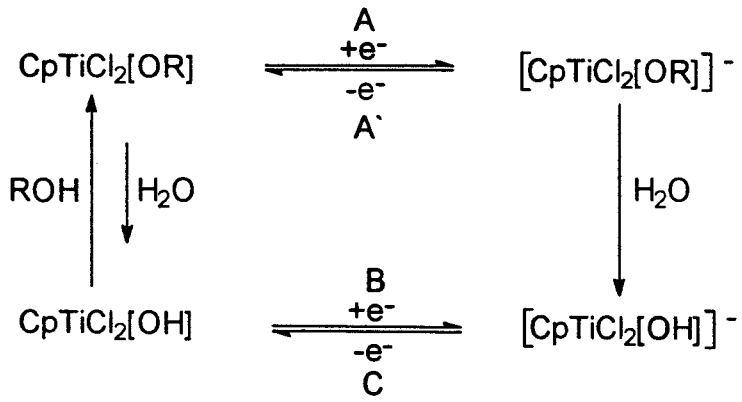

R = alkyl

Scheme 5.4.1

Scheme 5.4.1 describes the one electron reduction of the $CpTiCl_2[OR]$ complex that would appear as a completely reversible electron transfer but for the presence of water in the solution. If even trace amounts of water are present side reactions occur involving water with both the neutral titanium complex and its reduced form. The product of these reactions also form a redox couple.

Peak B does not grow to the size of peak C on a second potential cycle as might be expected since more $CpTiCl_2[OH]$ is being produced. This shows that the Ti(IV) complex interacts more strongly with the -OR ligand than with the -OH, ie the equilibrium between $CpTiCl_2[OR]$ and $CpTiCl_2[OH]$ lies well to the side of the $CpTiCl_2[OR]$ complex and re-establishes itself faster than the time it takes the potential to be swept to the reduction potential of $CpTiCl_2[OR]$ again. However, with the $[CpTiCl_2[OR]]^-$ anion, where the titanium is formally Ti(III), the competition between -OR and -OH favours the -OH, the degree of which depends on the water concentration and the structure of the R group.

It is also worth noting that in the voltammograms of the $CpTiCl_2[OR]$ complexes, when the chemical reaction between the $[CpTiCl_2[OR]]^-$ anion and water appears complete, ie no peak A´ is observed, a third cathodic peak is observed at potentials more negative than peak A. This peak can be seen in figures 4.1.3 and 4.4.3 (chapter 4) at about -1.7 V vs ferrocene and is labelled

peak D. Peak D is evident when significant amounts of $[CpTiCl_2[OH]]^-$ are produced and probably relates to the further reduction of this anion, the product of which has fast chemistry since no coupled anodic process is observed.

The mechanism proposed in scheme 5.4.1 reflects the behaviour of the aryloxide complexes only in part: residual water in solution does remove a limited amount of the starting complex forming the hydroxide species $CpTiCl_2[OH]$. This is clear from the presence of two redox couples, of unequal sizes, in the incompletely dried solutions. However since peak C never appears any larger than peak B no reaction between the anion $[CpTiCl_2[OR]]^-$ and water forming more $[CpTiCl_2[OH]]^-$ than is generated at peak B, is occurring. It is unclear why the Ti(III) aryloxide anion does not appear to react with water to any extent whereas the neutral Ti(IV) complex does. It may just be an effect of kinetics; the Ti(III) anion does not exist in solution for long enough to react significantly with water while the Ti(IV) complex is, of course, in solution for a considerable time. After the generation of the $[CpTiCl_2[OAr]]^-$ anion in a controlled potential electrolysis experiment there maybe some evidence for its consumption by reaction with water. A reaction with water could explain why the peaks in figure 5.1.8 representing the reversible one electron oxidation of $[CpTiCl_2[OAr]]^-$ after its generation by bulk electrolysis, are smaller than those representing the reversible reduction of $CpTiCl_2[OAr]$ before the electrolysis (figure 5.1.7). The cyclic voltammmogram in figure 5.1.8 also shows a couple of bumps occurring at potentials in the region of peaks B and C.

It is clear however, that whether in reduced form or not, the aryloxide complexes are more stable in the presence of water than the alkoxides. One reason for this could be the steric hindrance around the oxygen atom. All the aryloxide complexes prepared and isolated had bulky groups in the 2 and 6 positions on the aromatic ring thereby, to some extent, shielding the oxygen

atom from attack by other species. It is perhaps significant that the attempts to react aromatic groups without 2,6-substitution with $CpTiCl_3$ in the same way as all the other $CpTiCl_2[OR]$ complexes were made, were unsuccessful. The alkoxide complexes studied were not so sterically hindered at the oxygen atom and certainly in $CpTiCl_2[O^iPr]$ the oxygen is very open to attack and this complex is by far the most sensitive to water. If reaction with water does occur via protonation of the oxygen as suggested, another reason for the greater stability of the aryloxide complexes could of course, be the reduced electron density at an oxygen attached to a benzene ring, thus supporting the trend observed for the reduction potentials of the two groups of complexes and the cyclopentadienyl ^1H and ^{13}C nmr data (section 5.2).

5.5 THE ELECTROCHEMICAL REDUCTION OF $CpTiCl_2[OC_6H_2(^iPr)_2(NO_2)]$ IN THF.

The voltammetry of $CpTiCl_2[OC_6H_2(^iPr)_2(NO_2)]$ differs greatly from that of the other $CpTiCl_2[OR]$ complexes which is perhaps not surprising since it contains two centres of possible reduction; the titanium centre and the nitro group. One reduction peak is observed at -1.00 V vs ferrocene as shown in figure 5.5.1 which displays a cyclic voltammogram recorded at a vitreous carbon disc at 100 mV s^{-1} between -0.66 V and -1.46 V vs ferrocene for a THF solution of $CpTiCl_2[OC_6H_2(^iPr)_2(NO_2)]$ (14.5 mM) with Bu_4NBF_4 (0.2M) in the vacuum line cell. At slow sweep rates this reduction appears totally irreversible, but at sweep rates greater than 300 mV s^{-1} there is some evidence of a coupled oxidation peak, seen in figure 5.5.2 where the scan rate is 800 mV s^{-1}. The reduction peak is of a comparable size to those for the other $CpTiCl_2[OR]$ complexes in very dry medium indicating that this too is a one electron transfer. A second reduction process is observed at -2.06 V, this is also irreversible and appears smaller than the first cathodic peak (figure 5.5.3). There is not a great deal of variation in the voltammetric response between

'wet' and dry experiments, the only difference being the presence of a small cathodic peak at about -0.9 V in the voltammograms obtained from the less rigorously dried solutions (figure 5.5.4). This peak occurs at the same potential as peak B in the other $CpTiCl_2[OR]$ voltammograms indicating that the -OAr group in $CpTiCl_2[OC_6H_2(^iPr)_2(NO_2)]$ is also substituted by -OH to some extent. The low stability of the major reduced species was also reflected in a controlled potential electrolysis experiment where a potential of -1.4 V vs Ag wire was applied to a stirred solution of this complex in a vacuum line cell. The voltammogram recorded on the solution after complete reduction showed no anodic or cathodic processes and the resulting solution was dark red in colour.

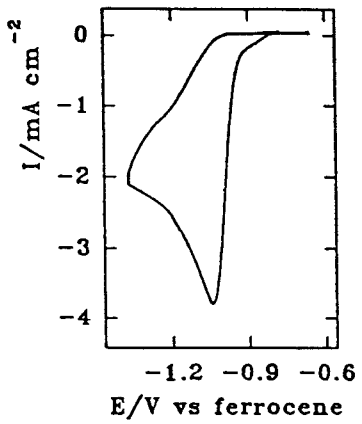

Figure 5.5.1
Cyclic Voltammogram recorded at a vitreous carbon disc electrode at 100 mV s^{-1} for a THF/Bu_4NBF_4 (0.2M) solution of $CpTiCl_2[OC_6H_2(^iPr)_2(NO_2)]$ (14.5 mM) in a closed cell.

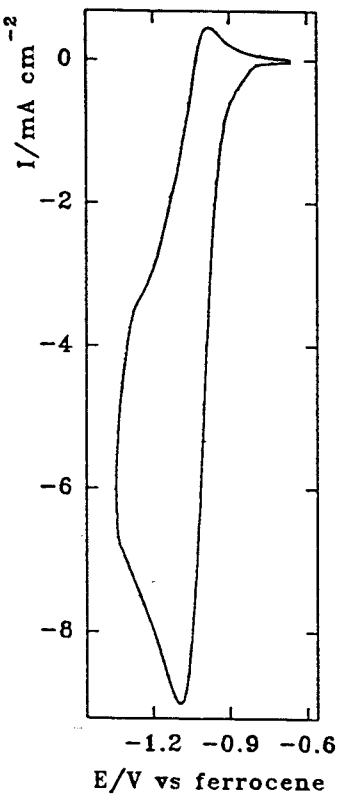

Figure 5.5.2
Cyclic Voltammogram recorded at a vitreous carbon disc electrode at 800 mV s^{-1} for a THF/Bu_4NBF_4 (0.2M) solution of $CpTiCl_2[OC_6H_2(^iPr)_2(NO_2)]$ (14.5 mM) in a closed cell.

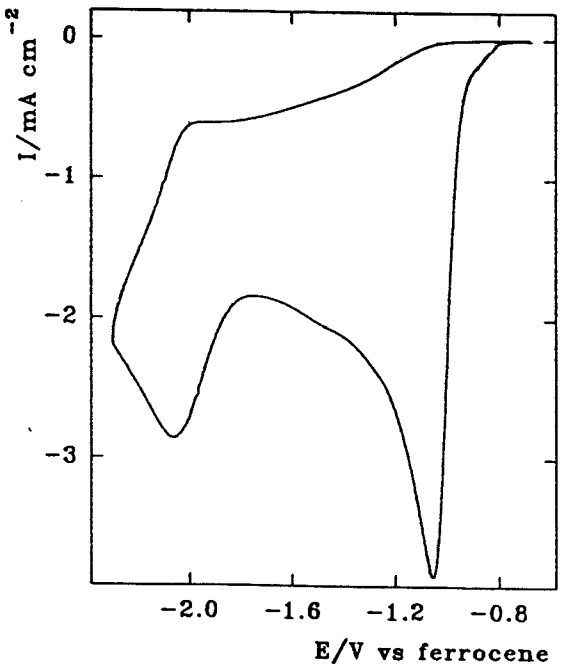

Figure 5.5.3
Cyclic Voltammogram recorded at a vitreous carbon disc electrode at 100 mV s^{-1} for a THF/Bu_4NBF_4 (0.2M) solution of $CpTiCl_2[OC_6H_2(^iPr)_2(NO_2)]$ (14.5 mM) in a closed cell.

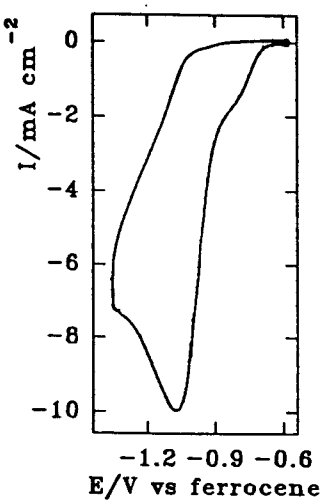

Figure 5.5.4
Cyclic Voltammogram recorded at a vitreous carbon disc electrode at 100 mV s^{-1} for a THF/Bu_4NBF_4 (0.2M) solution of $CpTiCl_2[OC_6H_2(^iPr)_2(NO_2)]$ (25 mM).

The large shift in reduction potential, 200 - 300 mV, for the $CpTiCl_2$-$[OC_6H_2(^iPr)_2(NO_2)]$ complex compared to the other $CpTiCl_2[OR]$ complexes, together with the fact that after a complete one electron reduction the solution was not an expected colour for a Ti(III) species indicates that the reduction observed does not occur at the titanium centre but perhaps at the nitro group of the aryloxy ligand. Nitro groups are known to be readily reduced in aprotic media and the anion radicals produced, especially for nitroaromatic molecules, are normally very stable. In this case however a very unstable anion radical is produced. One explanation for this could be that, following the addition of an electron, cleavage of the Ti-O bond occurs forming the phenoxide and $CpTiCl_2$ (a known compound) or its dimer. The formation of the phenoxide could also explain the red colour observed after the electrolysis and not the green or blue of a Ti(III) species. The scope of this project did not extend to an exact determination of the reduction product in this case.

5.6 THE CYCLIC VOLTAMMETRY OF 3C IN THF.

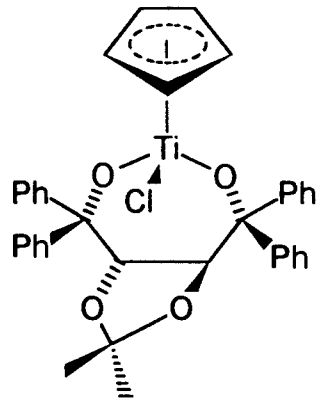

3C

As reported previously the complex **3C**, containing a threitol derivative as a bidentate ligand (section 3.4), has been prepared [43]. It was decided to investigate its cyclic voltammetry in the same way as the $CpTiCl_2[OR]$ complexes to see if any comparisons could be drawn between the responses.

A cyclic voltammogram of a THF solution of **3C** (11 mM) recorded under rigorously dry conditions shows two major reduction processes (figure 5.6.1). The first reduction occurs at -1.80 V vs ferrocene and shows almost complete reversibility; the peak separation is 60 mV, a plot of peak current density against the square root of the sweep rate is a straight line passing through the origin, however the ratio of peak current densities for this couple does not equal unity at slower sweep rates. A small anodic peak is observed at -1.16 V possibly explaining the incomplete reversibility although there is no noticeable increase in the size of this peak when the major reduction becomes less reversible but it does not occur if the first major reduction is not swept. The reversibility of the first electron transfer increases with faster sweep rates. A second irreversible reduction, of a comparable size to the first is evident at -2.6 V.

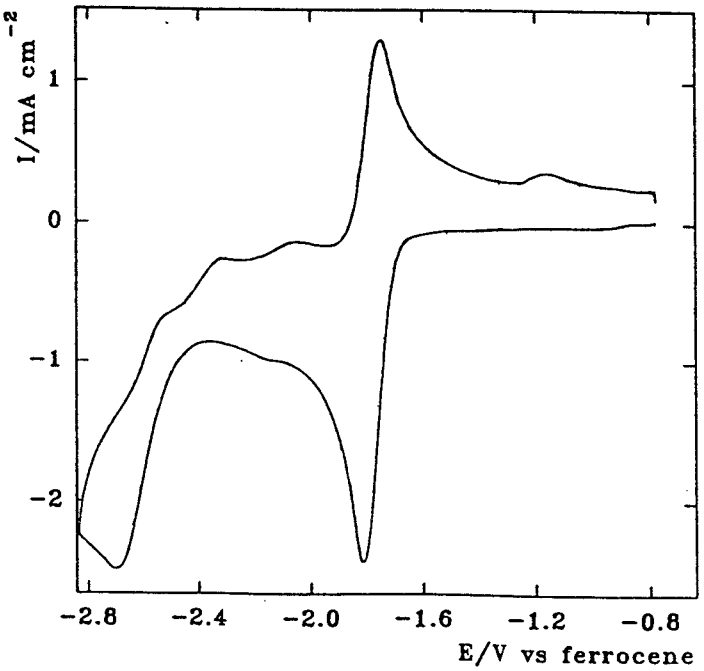

Figure 5.6.1
Cyclic Voltammogram recorded at a vitreous carbon disc electrode at 300 mV s^{-1} for a THF/Bu_4NBF_4 (0.2M) solution of **3C** (11 mM).

There are distinct differences between the voltammetric responses for this diol complex compared to the monodentate alkoxide complexes, not least that the formal potential for the Ti(IV)/Ti(III) couple occurs at a substantially more negative potential (500 - 600 mV more negative) than the $CpTiCl_2[OR]$ complexes. However a reduction from Ti(III) to Ti(II) is observed for this compound whereas with the $CpTiCl_2[OR]$ species it was not seen within the potential limits of the electrolyte solution, although with the less dry solutions, a reduction of the Ti(III) species, $[CpTiCl_2[OH]]^-$ was sometimes evident (peak D). Also it is worth noting that no cathodic peak equivalent to peak B at -0.92 V was ever observed in the cyclic voltammetry of complex **3C**. No further investigation into the redox behaviour of 3C was performed and the small bumps evident on the voltammogram in figure 5.6.1 are not explained except that they could well be attributed to impurities in the solution.

5.7 CONCLUSIONS

The data in this chapter and its ensuing discussion has highlighted the sensitivity of $CpTiCl_2[OR]$ (R = alkyl or aryl) to water levels in solution. Unlike many such systems, the chemistry that occurs between both the neutral $CpTiCl_2[OR]$ complexes and their anions, and water, produces species with well defined electrochemistry. Because of the clarity of this electrochemistry it can be seen that even solutions deemed to be 'dry' contain some level of water, sometimes this level is significant enough to drastically affect the chemistry of $CpTiCl_2[OR]$ complexes. For this reason it was necessary to work with higher concentrations of the electroactive species (> 5 mM); higher than the 0.5 - 2 mM solutions generally used in electrochemical studies. The lessons learnt here could perhaps be applied to non-aqueous chemistry in fields outside electrochemistry.

CHAPTER 6

THE ELECTROCHEMICAL REDUCTION OF Cp_2TiCl_2 IN THE PRESENCE OF PHOSPHINE LIGANDS.

In chapter one (section 1.2.3), the role of titanocene dichloride in catalysing various organic transformations was reviewed and the importance of the lower oxidation states of titanium was stressed. It was also noted that low-valent titanium species were stabilised by alkylphosphine ligands. In this chapter the electrochemistry of Cp_2TiCl_2 in the presence of PR_3 compounds and of $Cp_2TiCl(PR_3)$ and $Cp_2Ti(PR_3)_2$ is explored.

Although there have been reports of the cyclic voltammetry of titanocene dichloride in the presence of alkylphosphine compounds [50,59-61] and mechanisms postulated to account for the behaviour observed, these have been limited in their scope. A detailed examination of the intermediates involved and the products formed in these experiments has not yet been reported. It was felt valuable to extend these investigations further for three reasons: a) the desire to determine the exact nature and stability of the lower valent titanium species involved in synthetic organic transformations, b) the possibility of developing an alternative route by which low-valent titanium species can be generated and then used in synthesis, c) the reduction of Cp_2TiCl_2 remains of interest because of the continuing uncertainty concerning the stablility of $[Cp_2TiCl_2]^-$ to loss of chloride.

All experiments were carried out using procedure 4 described in chapter 4 since low valent organotitanium species have proved to be exceptionally sensitive to residual water in solution. Ferrocene has generally been used as an internal reference during this work but in the case of solutions containing

alkylphosphine compounds, the response for ferrocene was distorted and variable. Unfortunately the potential of the silver wire reference electrode also shifted significantly (up to 400 mV) when the phosphine was present in solution. Other compounds known to show reversible one electron transfers in aprotic media were tried but a redox couple suitable as a reference point could not be identified for the system under study. It was decided that the primary one electron reduction peak of Cp_2TiCl_2, which in a solution without phosphine, has a peak potential of -1.32 V vs ferrocene, would where possible be used as a potential reference. It is recognised that the occurence of chemical reactions between the reduced titanium species and the alkylphosphine may have the effect of shifting this potential to some extent. However, this was the best procedure available for comparison of the peak potentials.

6.1 THE CYCLIC VOLTAMMETRY OF Cp_2TiCl_2.

An example of the voltammetric response of Cp_2TiCl_2 in a THF solution (7.3 mM) with Bu_4NBF_4 (0.2 M) as the supporting electrolyte, at a vitreous carbon disc can be seen in figure 6.1.1. Two reduction processes can be seen at -1.32 V (peak Q) and -2.52 V (peak T) vs ferrocene, and there are coupled anodic processes (peaks Q´ and T´ respectively). The first redox couple (Q/Q´) displays all the characteristics of a reversible one electron transfer. The peak separation is 60 mV and the ratio of peak current densities, $Ip^{Q´}/Ip^{Q}$, is equal to unity at all scan rates. A plot of Ip^{Q} against the square root of the scan rate gives a straight line passing through the origin. Taking the slope of this plot and using it to calculate n^3D from the Randles-Sevčik equation gave a value of 1.3×10^{-5} cm^2s^{-1} which, with $n = 1$, is comparable to the other titanium complexes (section 5.1). The second reduction, represented by peak T, is only partially reversible; the anodic peak, T´ being smaller than peak T, although peak T´ does get larger with increasing scan rate. Peak T, because of its irreversibility, is more drawn out than peak Q. Using equation 6.1a where

$\alpha_c n_\alpha$ = 48/| Ep-$Ep_{½}$| in mV, which makes some allowance for the different peak shape, and D = 1.3 x 10^{-5} cm^2 s^{-1}, it may be shown that n = 1 for this process.

$$Ip^T = -(2.99 \times 10^5)n(\alpha_c n_\alpha)^{½}cD^{½}v^{½} \qquad (6.1a)$$

The behaviour observed here is in keeping with the literature although some authors have reported the existence of a third cathodic process [50,55]. No further electron transfer processes were evident in this study. Of course, it still remains uncertain whether the $[Cp_2TiCl_2]^-$ anion reversibly loses Cl^-.

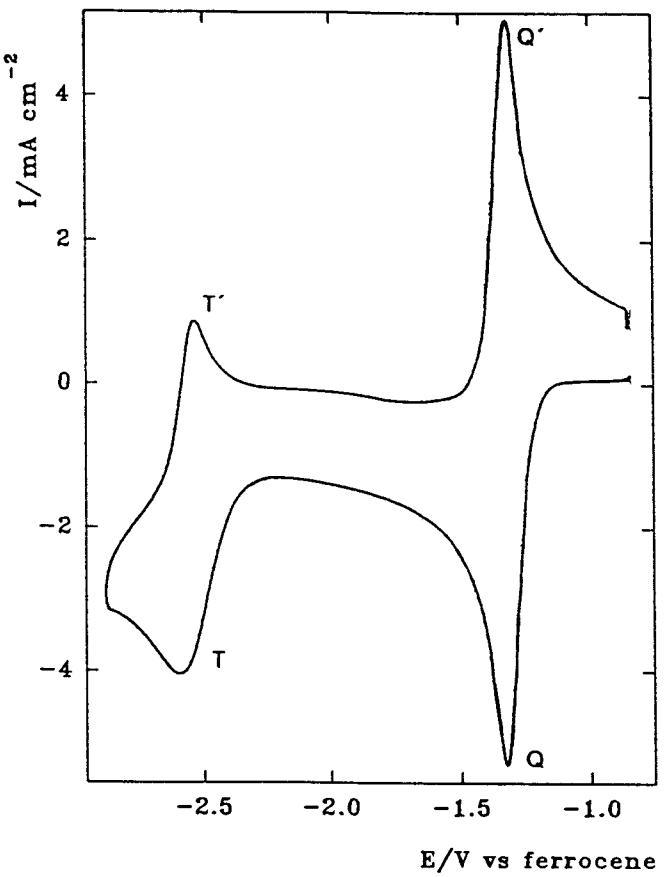

Figure 6.1.1
Cyclic Voltammogram recorded at a vitreous carbon disc electrode at 600 mV s^{-1} for a THF/Bu_4NBF_4 (0.2M) solution of Cp_2TiCl_2 (7.3 M).

6.2 THE CYCLIC VOLTAMMETRY Cp_2TiCl_2 AND TRIMETHYLPHOSPHINE IN THF.

Figure 6.2.1 shows a cyclic voltammogram recorded at a vitreous carbon disc at 100 mV s^{-1} for a THF solution of Cp_2TiCl_2 (9 mM) and excess trimethylphosphine, PMe_3 (50 mM) with Bu_4NBF_4 (0.2 M) as the supporting electrolyte. The first reduction represents the addition of an electron to Cp_2TiCl_2 and has been identified as peak Q_1 and assigned a peak potential of -1.32 V vs ferrocene. The potential limits of the cyclic voltammogram in figure 6.2.1 are therefore -0.70 V and -3.30 V vs ferrocene. On the first sweep, two reduction peaks are observed; peak Q_1 at -1.32 V and peak P at -2.78 V vs ferrocene. Peak P occurs 260 mV more negative than the second reduction seen with Cp_2TiCl_2 without phosphine present (peak T, figure 6.1.1) and has no reverse oxidation peak. Furthermore, peak T is totally absent. On the backward sweep two anodic peaks are evident; peak R´ at -1.92 V and peak S´ at -0.92 V. The wave, labelled Q_1´´, is merely the reduction process Q_1 ceasing to occur as the potential is scanned towards positive values. The shape of the voltammogram on the first sweep does not change at different sweep rates (25 - 300 mV s^{-1}). Reversing the potential after peak Q_1 shows it to be completely irreversible, although the anodic peak S´ appears to be coupled to it (figure 6.2.2). A plot of Ip^{Q1} for the first reduction, against the square root of the potential sweep rate gives a straight line passing through the origin. Using the slope of this line a value for n^2D was calculated from equation 6.1a. The value of n^2D was 1.1 x 10^{-5} cm^2 s^{-1}, implying that the reduction of Cp_2TiCl_2 in the presence of PMe_3 remains a one electron process. Peak P, the other reduction peak seen on the first scan, is slightly more drawn out than peak Q_1; but again, using equation 6.1a to take this into account, n^2D again came out to be 1.1 x 10^{-5} cm^2 s^{-1} indicating that this process too involves a one electron transfer. The anodic peak R´ only appears on the first sweep if the potential is swept past peak P.

On the second sweep for both the voltammograms shown, it can be seen that

the oxidation process represented by peak S´ is completely irreversible and peak Q_1 still represents the only reduction process in this potential region. A third cathodic process is now evident at -1.98 V which only ever appears on the second and subsequent scans, it has been labelled peak R as the reverse of the oxidation represented by peak R´. At slower scan rates peak R is not evident even when R´ is present.

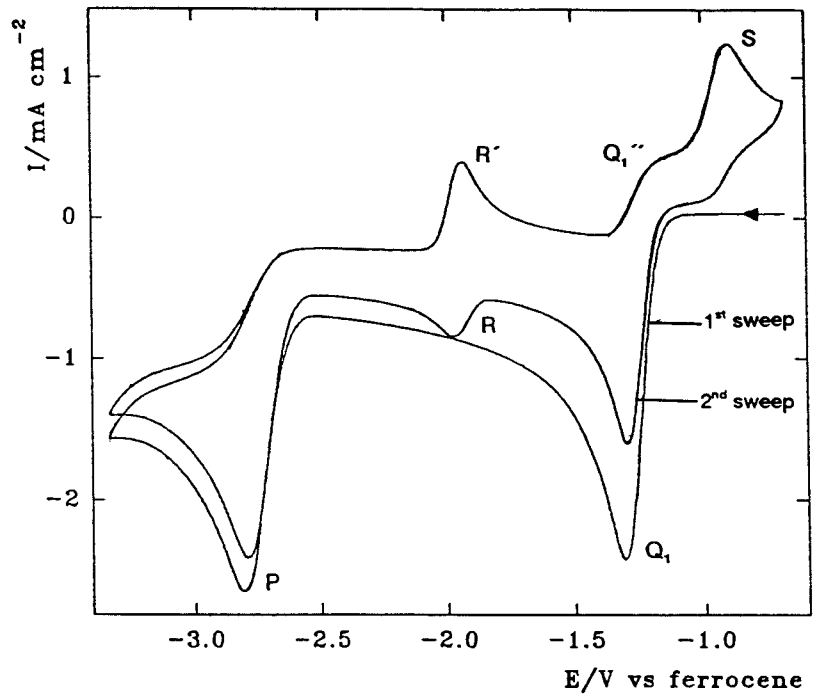

Figure 6.2.1

Cyclic Voltammogram recorded at a vitreous carbon disc electrode at 100 mV s^{-1} for a THF/Bu_4NBF_4 solution (0.2M) of Cp_2TiCl_2 (9m M) + PMe_3 (50 mM).

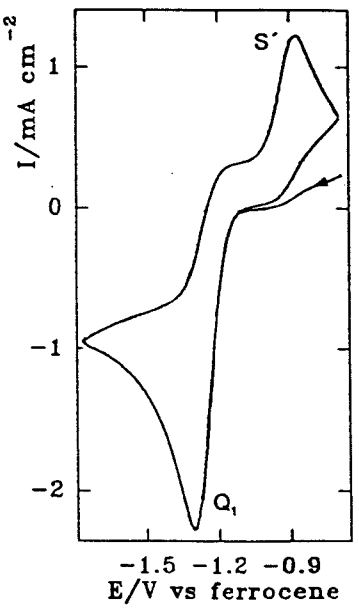

Figure 6.2.2

Cyclic Voltammogram recorded at a vitreous carbon disc electrode at 100 mV s^{-1} for a THF/Bu_4NBF_4 (0.2M) solution of Cp_2TiCl_2 (9m M) + PMe_3 (50 mM).

This voltammetry is compatible with the mechanism set out in scheme 6.2.1. The addition of the first electron to titanocene dichloride (peak Q_1) produces the Ti(III) anion, $[Cp_2TiCl_2]^-$. In the presence of trimethylphosphine, rapid substitution of Cl^- by PMe_3 occurs to produce the neutral Ti(III) species, $Cp_2TiCl(PMe_3)$. $Cp_2TiCl(PMe_3)$ then undergoes a one electron reduction at -2.78 V vs ferrocene (peak P). The resulting anion again undergoes rapid substitution of Cl^- by PMe_3 to give the neutral Ti(II) species, $Cp_2Ti(PMe_3)_2$. $Cp_2Ti(PMe_3)_2$ displays an oxidation process at -1.92 V (peak R´) along with a

coupled reduction (peak R), which is not however evident at slow scan rates or on the first sweep. On the second sweep peak Q_1 is again seen. This partly results from the diffusion of Cp_2TiCl_2 from the bulk solution, but the chemistry undergone by the $[Cp_2TiCl(PMe_3)]^+$ cation produced at S´ may involve reformation of Cp_2TiCl_2. Such chemistry involves another ligand substitution reaction, this time PMe_3 being substituted by Cl^-, which is entirely reasonable since free Cl^- ions are produced near the electrode throughout the potential cycle right up to the point where this reaction occurs (during theoxidation represented by peak S´). A similar reaction is not seen for the Ti(III) cation, $[Cp_2Ti(PMe_3)_2]^+$ (forming $Cp_2TiCl(PMe_3)$ if it did occur) since no increase in peak S´ is observed when peak R´ appears. The decreased size of peak R, or its complete absence , at slow scan rates must be due to the increased diffusion of $[Cp_2Ti(PMe_3)_2]^+$ away from the electrode at long times. The absence of the reduction of $[Cp_2Ti(PMe_3)_2]^+$ on the first scan is, of course because peak P has to be swept to form $[Cp_2TiCl(PMe_3)]^-$ before $Cp_2Ti(PMe_3)_2$ can be formed and subsequently oxidised at peak R´.

The electron transfer labelled U´ in scheme 6.2.1 and referring to the further oxidation of $[Cp_2TiCl_2]^+$ is discussed later in the next section but is not shown in figure 6.2.1 since the potentials were not swept far enough.

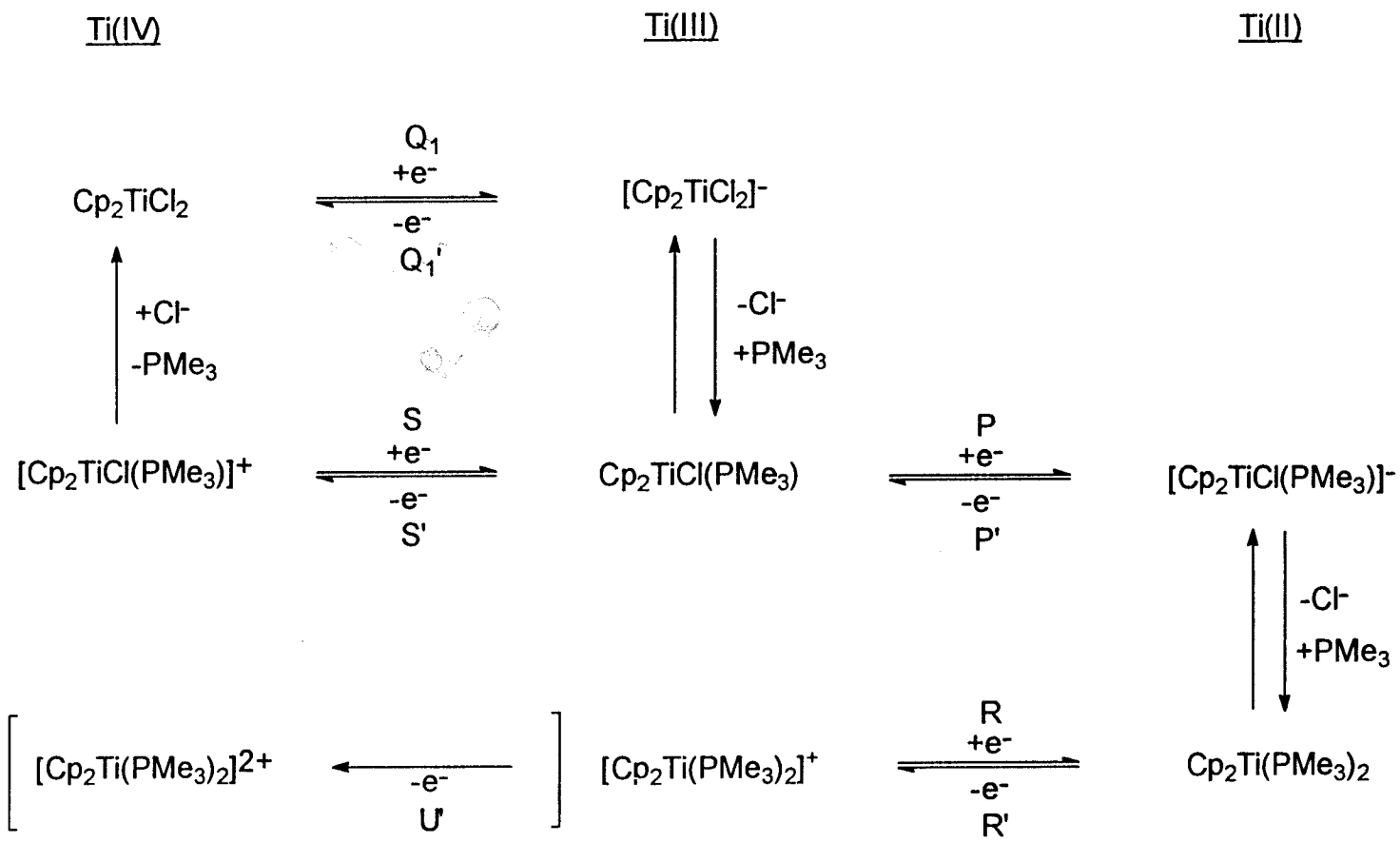

Scheme 6.2.1
(Cp_2TiCl_2 + PMe_3)

6.3 THE CYCLIC VOLTAMMETRY OF $Cp_2Ti(PMe_3)_2$.

The mechanism proposed in scheme 6.2.1, describing the electrochemistry of Cp_2TiCl_2 in the presence of trimethylphosphine, involves the formation of two neutral species during the reduction; $Cp_2TiCl(PMe_3)$ and $Cp_2Ti(PMe_3)_2$. $Cp_2TiCl(PMe_3)$ is formally a Ti(III) species and $Cp_2Ti(PMe_3)_2$ a Ti(II) species, both have previously been prepared and characterised [77].

A sample of $Cp_2Ti(PMe_3)_2$ was prepared and its cyclic voltammetry investigated. An example of the response obtained is shown in figure 6.3.1. Two oxidation processes can be seen, the first possessing a coupled cathodic peak but the second, which is slightly smaller, appearing completely irreversible. It is difficult to assign potential limits to this voltammogram since there is no titanocene dichloride present, but one can imagine that the first oxidation peak seen relates to the electron transfer process:

$$Cp_2Ti(PMe_3)_2 - e^- \rightleftharpoons [Cp_2Ti(PMe_3)_2]^+$$

In previous voltammograms, where Cp_2TiCl_2 is present this process is labelled R´/R and occurs at -1.95 V vs ferrocene hence it has been assigned as such in this case. The R´/R couple here appears to represent an almost reversible electron transfer, becoming more reversible at faster sweep rates indicating that the cation $[Cp_2Ti(PMe_2)]^+$ is quite stable under these conditions. It therefore follows that the second oxidation, labelled peak U´, and occuring at -0.44 V vs ferrocene relates to the further oxidation of this cation:

$$[Cp_2Ti(PMe_3)_2]^+ - e^- \rightleftharpoons [Cp_2Ti(PMe_3)_2]^{2+}$$

The dication is unstable and undergoes rapid chemistry since no reduction process relating to it is seen.

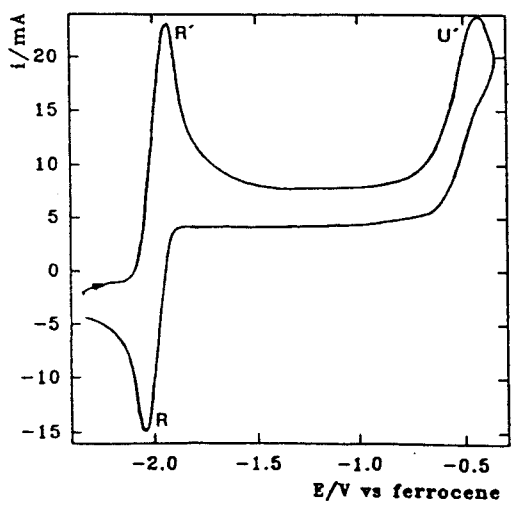

Figure 6.3.1
Cyclic Voltammogram recorded at a Pt gauze electrode at 50 mV s^{-1} for a THF/Bu_4NBF_4 (0.2M) solution of $Cp_2Ti(PMe_3)_2$.

6.4 THE CYCLIC VOLTAMMETRY OF $Cp_2TiCl(PMe_3)$ IN THF.

The method of preparation of $Cp_2TiCl(PMe_3)$ reported in [77], proved unsuccessful when it was tried. Nevertheless, a straightforward method for its preparation was developed involving a disproportionation reaction between Cp_2TiCl_2 and $Cp_2Ti(PMe_3)_2$. On mixing THF solutions of these two complexes, a bright red solution of Cp_2TiCl_2 and a dark brown/black solution of $Cp_2Ti(PMe_3)_2$, in equimolar proportions a blue solution of $Cp_2TiCl(PMe_3)$ was obtained. The blue/green crystals left after evaporation of the solvent were characterised by mass spectrometry (chapter 2).

The cyclic voltammetry of $Cp_2TiCl(PMe_3)$ was recorded by adding a portion of its THF solution straight from the reaction vessel to the electrochemical cell. This procedure, whilst clean and convenient, made it difficult to determine the exact concentration of the electroactive species in the cell. The response obtained was noticeably more complex than that for $Cp_2Ti(PMe_3)_2$.

Figure 6.4.1 shows a cyclic voltammogram recorded at a vitreous carbon disc at 100 mV s^{-1} for a THF/Bu_4NBF_4 (0.2 M) solution of $Cp_2TiCl(PMe_3)$. Starting the scan at -1.72 V vs ferrocene (a potential where no oxidation or reduction processes are occurring) and sweeping towards more negative potentials, switching at -3.14 V and sweeping all the way to -0.34 V, then back to the starting potential again creates a voltammogram with similar characteristics to that for Cp_2TiCl_2 plus PMe_3 in THF. On the first scan, from -1.72 V in the negative direction, a reduction peak can be seen at -2.78 V which has been labelled peak P. Coupled to this is an oxidation represented by peak R´ at -1.92 V. Peak R´ does not occur unless peak P is swept. Continuing on the scan to less negative potentials shows an anodic peak S´ at -0.8 V, which has a reverse cathodic peak S. Another cathodic peak, Q_1, which is smaller than S, is observed with a peak potential of -1.32 V. The reverse of the oxidation process represented by peak R´ can only just be seen at the start of the second sweep. If the potential is swept from a point between peak P and R´

in the positive direction (figure 6.4.2) no peak R´ is seen, the couple S´/Ṡ are present as is peak Q_1 on the backward sweep. No peak corresponding to R is observed either.

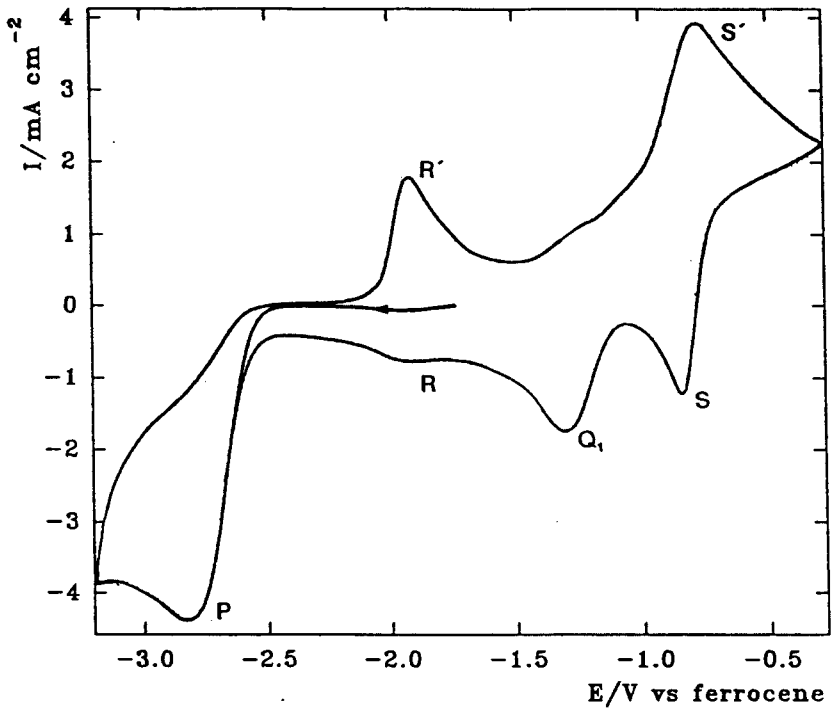

Figure 6.4.1

Cyclic Voltammogram recorded at a vitreous carbon disc electrode at 100 mV s^{-1} for a THF/Bu_4NBF_4 (0.2M) solution of $Cp_2TiCl(PMe_3)$.

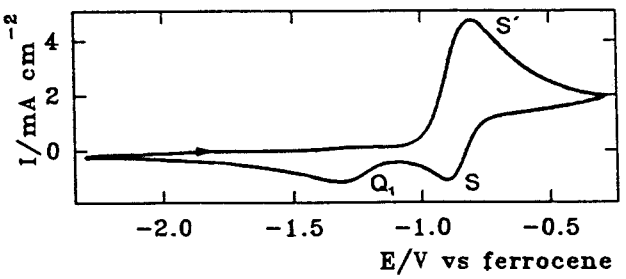

Figure 6.4.2

Cyclic Voltammogram recorded at a vitreous carbon disc electrode at 50 mV s^{-1} for a THF/Bu_4NBF_4 (0.2M) solution of $Cp_2TiCl(PMe_3)$.

The most immediate difference between the voltammetric responses of solutions of $Cp_2TiCl(PMe_3)$ and Cp_2TiCl_2/PMe_3 is the presence of peak S in the

$Cp_2TiCl(PMe_3)$ case. According to scheme 6.2.1 the couple S´/S represent the reversible oxidation of $Cp_2TiCl(PMe_3)$:

$$Cp_2TiCl(PMe_3) - e^- \rightleftharpoons [Cp_2TiCl(PMe_3)]^+ \qquad S'/S$$

So the fact that peak S appears here in the absence of any free chloride is not surprising; when Cl^- is present it has been suggested that the cation $[Cp_2TiCl(PMe_3)]^+$ reacts quickly to form titanocene dichloride (scheme 6.2.2). What is perhaps surprising here, although the solution prepared contains no free chloride ions or phosphine ligands, is the presence of peaks R/R´ and Q_1 relating to the species $Cp_2Ti(PMe_3)_2$ and Cp_2TiCl_2 respectively. Mugnier et al reported on the oxidation of $Cp_2TiCl(PPhMe_2)$ in THF and proposed that after the loss of an electron from this complex the resulting cation, $[Cp_2TiCl(PPhMe_2)]^+$ reacted rapidly with the neutral starting complex yielding Cp_2TiCl_2 and $[Cp_2Ti(PPhMe_2)_2]^+$ [60]. The oxidation of $Cp_2TiCl(PPhMe_2)$ therefore was reported to involve 0.5 electrons since this ligand exchange reaction causes half of the starting species to disappear.

If just the oxidation of $Cp_2TiCl(PMe_3)$ is considered first, a similar scheme to Mugnier's can be written to account for the observations made (scheme 6.4.1).

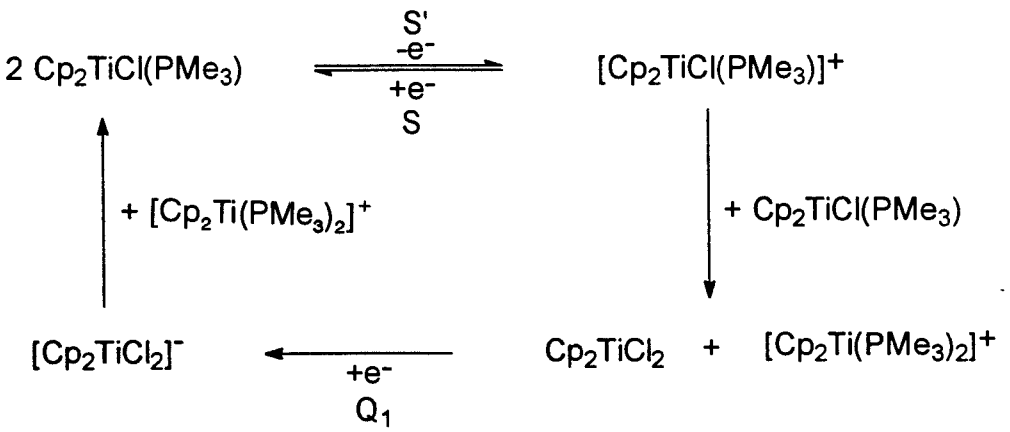

Scheme 6.4.1
($Cp_2TiCl(PMe_3)$ - oxidation)

$Cp_2TiCl(PMe_3)$ is oxidised to the Ti(IV) cation $[Cp_2TiCl(PMe_3)]^+$ which is consumed in a ligand exchange reaction with the starting complex forming

titanocene dichloride and the Ti(III) cation $[Cp_2Ti(PMe_3)_2]^+$. At a scan rate of 50 mV s^{-1} this reaction has not quite gone to completion since peak S, representing the reverse of the oxidation of the starting species, is evident. In this case, the number of electrons transferred in the first oxidation should be between 0.5 and 1 depending on the extent of the ligand exchange reaction. A more precise value of *n* cannot be calculated from the voltammetry since the exact concentration of the $Cp_2TiCl(PMe_3)$ is unknown. The reduction of titanocene dichloride can be seen by the presence of peak Q_1. Since $[Cp_2Tl(PMe_3)_2]^+$ is also formed in the ligand exchange reaction mentioned above it would be logical to expect to see its reduction peak at about -2.0 V (peak R) on the first scan of the voltammogram in figure 6.4.2. This, however, is not the case and can be explained by another ligand redistribution reaction occurring between the $[Cp_2TiCl_2]^-$ anion formed at peak Q_1 and the $[Cp_2Ti(PMe_3)_2]^+$ cation, the product of which is the initial Ti(III) complex, $Cp_2TiCl(PMe_3)$.

When the reduction of $Cp_2TiCl(PMe_3)$ is studied, similar arguments involving ligand exchange reactions can be made and are outlined in scheme 6.4.2 below.

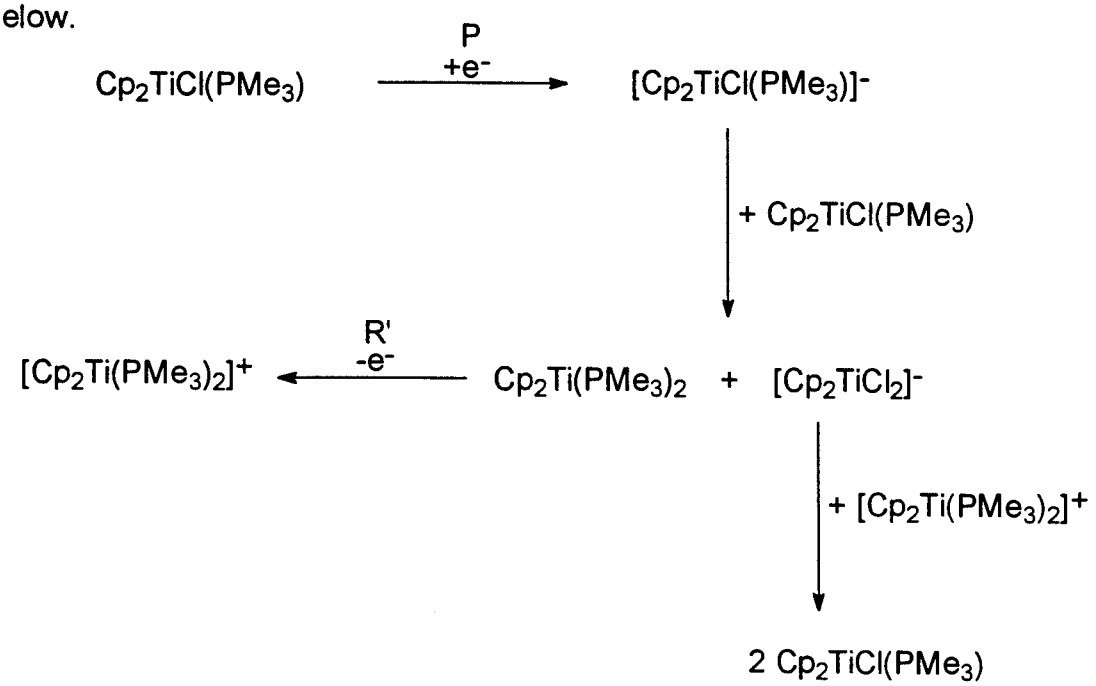

Scheme 6.4.2
($Cp_2TiCl(PMe_3)$ - reduction)

The one electron reduction of $Cp_2TiCl(PMe_3)$ occurs at -2.78 V vs ferrocene (peak P) and generates the Ti(II) anion $[Cp_2TiCl(PMe_3)]^-$ which is unstable in the presence of the neutral starting complex since these two species react by exchanging ligands forming $Cp_2Ti(PMe_3)_2$ and $[Cp_2TiCl_2]^-$. $Cp_2Ti(PMe_3)_2$ can then be oxidised at -1.94 V (peak R´) forming the Ti(III) cation $[Cp_2Ti(PMe_3)_2]^+$. $[Cp_2Ti(PMe_3)_2]^+$ displays a reduction peak at about -2.0 V (peak R), this however, is not large at slow sweep rates because $[Cp_2Ti(PMe_3)_2]^+$ is consumed in another ligand redistribution reaction with $[Cp_2TiCl_2]^-$ and the starting species is reformed.

Both schemes 6.4.1 and 6.4.2 are quite complex but do explain, at least in qualitative terms, the voltammetric response obtained from a THF solution of $Cp_2TiCl(PMe_3)$. Because of the complexity of the chemistry and the experimental conditions it was impossible to examine quantitatively whether rate parameters could be determined for the various steps in the mechanism. A controlled potential electrolysis experiment was performed on $Cp_2TiCl(PMe_3)$ and the cyclic voltammogram obtained after electrolysis at a potential just past peak S´ is shown in figure 6.4.3. Although the response is again degraded at the large Pt gauze electrode, a one reversible electron transfer process can be seen at about -1.3 V vs ferrocene. This has been attributed to the reversible reduction of Cp_2TiCl_2 which is the only species present in solution displaying any electroactivity in this potential area. The mechanism in scheme 6.4.1 would predict that Cp_2TiCl_2 is the only reducible species within this potential range after a bulk electrolysis in which the electron transfer process is $Cp_2TiCl(PMe_3) - e^- \rightarrow [Cp_2TiCl(PMe_3)]^+$, since this cation undergoes a ligand exchange process with $Cp_2TiCl(PMe_3)$ forming titanocene dichloride and $[Cp_2Ti(PMe_3)_2]^+$. $[Cp_2Ti(PMe_3)_2]^+$ does not display any electroactivity in the potential range of the voltammogram in figure 6.4.3. The colour change observed during the electrolysis supports the formation of titanocene dichloride in that the solution is initially blue/green and has turned red by the end of the experiment.

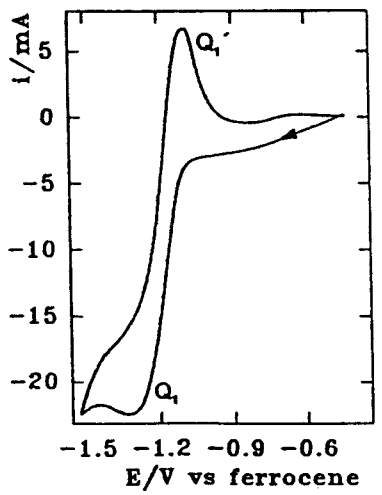

Figure 6.4.3
Cyclic Voltammogram recorded at Pt gauze electrode at 50 mV s^{-1} for a THF/Bu_4NBF_4 (0.2M) solution of $Cp_2TiCl(PMe_3)$ after a controlled potential electrolysis at -0.3 V vs ferrocene.

6.5 THE ADDITION OF Cl^- TO $Cp_2Ti(PMe_3)_2$ AND $Cp_2TiCl(PMe_3)_2$ IN THF.

The addition of excess free chloride ions (as anhydrous Bu_4NCl) to the THF/Bu_4NBF_4 solutions of $Cp_2Ti(PMe_3)_2$ and $Cp_2TiCl(PMe_3)$ was carried out as a way of probing the ligand exchange and redistribution reactions cited in the mechanistic accounts of the electrochemical behaviour of these complexes and that of Cp_2TiCl_2 in the presence of PMe_3.

Figure 6.5.1 shows a cyclic voltammogram recorded at a vitreous carbon disc at 25 mV s^{-1} for a THF solution of $Cp_2Ti(PMe_3)_2$ in the presence of excess Cl^- ions. Comparing this voltammogram with that shown in figure 6.3.1 where only $Cp_2Ti(PMe_3)_2$ was present, it can be seen that the complexity of the response has increased dramatically. Starting the scan at -1.2 V vs Ag wire where no current flows and sweeping in the positive direction gives, in total, four anodic processes, one of these having a coupled oxidation. Then a further cathodic peak is seen at potentials more negative than the switching potential. The first anodic peak has been assigned as peak R´ at -1.98 V vs ferrocene representing the oxidation of the complex $Cp_2Ti(PMe_3)_2$. This process no longer has a reverse reduction (peak R) at this scan rate (at 100 mV s^{-1} a peak representing R is visible). The second anodic peak occurs at -1.24 V vs

ferrocene (peak Q_1') and has a coupled cathodic peak (peak Q_1) at -1.32 V. Peaks Q_1' and Q_1 are the same size indicating that they represent a reversible electron transfer. The third and fourth anodic peaks, S′ at -0.94 V and U′ at -0.56 V, are both smalland irreversible. Continuing the sweep past the switching potential gives peak P at -2.76 V, an irreversible cathodic peak.

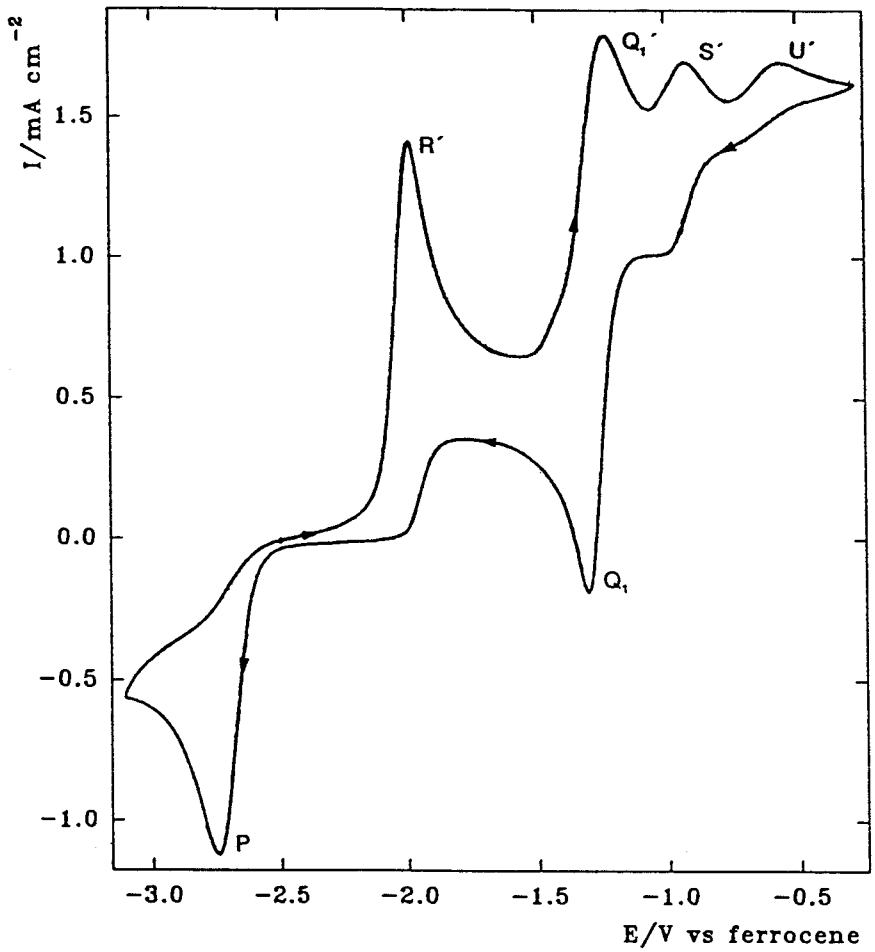

Figure 6.5.1

Cyclic Voltammogram recorded at vitreous carbon disc electrode at 25 mV s^{-1} for a THF/Bu_4NBF_4 (0.2M) solution of $Cp_2Ti(PMe_3)_2$ with an excess of Bu_4NCl.

Scheme 6.5.1 sets out a mechanism accounting for the voltammetric response obtained. As previously explained (section 6.3) $Cp_2Ti(PMe_3)_2$ undergoes a one electron oxidation at about -1.9 V (peak R′), but with Cl^- present in excess this oxidation is no longer reversible. The cation it produces, $[Cp_2Ti(PMe_3)_2]^+$ reacts quickly with Cl^- forming the neutral Ti(III) species $Cp_2TiCl(PMe_3)$. In the

absence of excess chloride ions the $Cp_2TiCl(PMe_3)$ is quite stable and shows a partially reversible redox couple represented by peaks S and S´ (figure 6.4.1). In this case however the peak S´ is very small and irreversible and it is the redox processes represented by peaks Q_1 and Q_1´ that dominate. The implication here could be that further reaction of $Cp_2TiCl(PMe_3)$ with Cl^- occurs producing the anion $[Cp_2TiCl_2]^-$ which is subsequently oxidised at peak Q_1´. Since $Cp_2TiCl(PMe_3)$ appears to be perfectly stable in solution by itself and the fact that no subsequent reduction of $[Cp_2TiCl_2]^-$ is seen, ie peak T at -2.52 V is not evident, it is unlikely that further reaction of $Cp_2TiCl(PMe_3)$ with Cl^- occurs without any further redox behaviour. It is more likely that the reaction of $Cp_2TiCl(PMe_3)$ and Cl^- is accompanied by an electron transfer (equation 6.5a) which then appears as peak Q_1´:

$$Cp_2TiCl(PMe_3) + Cl^- - e^- \rightleftharpoons Cp_2TiCl_2 + PMe_3 \qquad (6.5a)$$

Probably the reaction occurs via the sequence:

$$Cp_2TiCl(PMe_3) - e^- \rightleftharpoons [Cp_2TiCl(PMe_3)]^+ \overset{Cl^-}{\rightleftharpoons} Cp_2TlCl_2 + PMe_3 \qquad (6.5b)$$

But provided all the coupled chemistry is rapid, only a reversible couple is seen (the response is determined by thermodynamic factors and hence is independant of mechanism). Once Cp_2TiCl_2 has been reduced again to $[Cp_2TiCl_2]^-$ (peak Q_1) a ligand exchange reaction occurs and $Cp_2TiCl(PMe_3)$ is immediately formed, this is evident from the presence of peak P which represents the reduction of the neutral Ti(III) species. This gives further evidence that $Cp_2TiCl(PMe_3)$ is a more stable Ti(III) species than the titanocene dichloride anion, even in the presence of excess chloride ions, hence equation 6.5a is an accurate depiction of the chemistry producing peak Q_1´ under these conditions. The fourth anodic process represented by peak U´ at about -0.5 V vs ferrocene is completely irreversible and could relate to the further oxidation of the $[Cp_2Ti(PMe_3)_2]^+$ cation produced during peak R´.

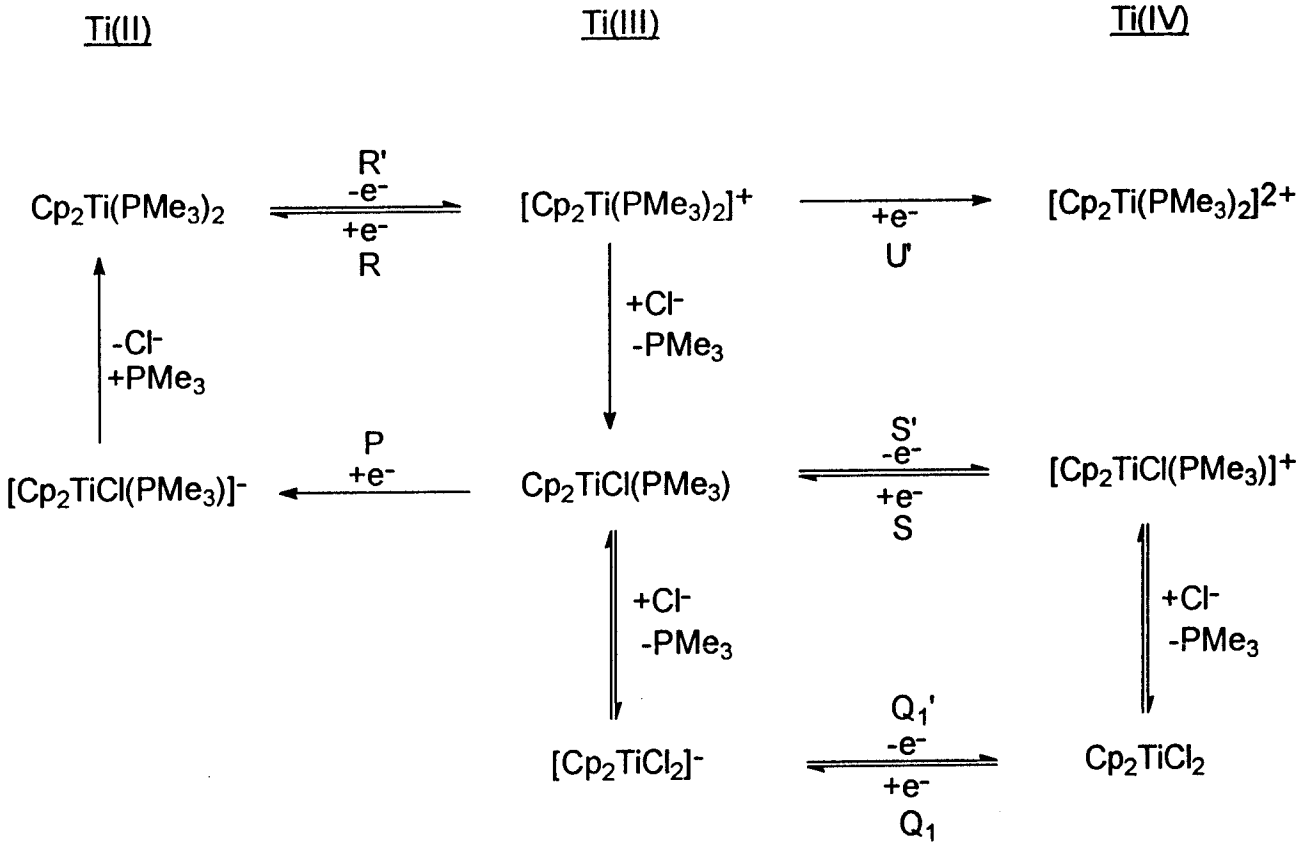

Scheme 6.5.1
($Cp_2Ti(PMe_3)_2$ + Cl^-)

Free chloride ions were also added to a $Cp_2TiCl(PMe_3)$ solution and the voltammetry recorded both before and after a controlled potential electrolysis experiment. Figure 6.5.2 shows the voltammetric response obtained for a THF/Bu_4NBF_4 (0.2 M) solution of $Cp_2TiCl(PMe_3)$ recorded at 50 mV s^{-1} from the electrolysis cell prior to the application of a constant potential. It displays a major reduction peak which has been attributed to the one electron reduction of $Cp_2TiCl(PMe_3)$ and hence labelled peak P and assigned a peak potential of -2.78 V vs ferrocene. Coupled to this is peak R´ at around -2.0 V which appears quite small. Continuing on the backward scan shows the reversible couple Q_1'/Q_1 to be present but no sign of the process related to the couple S´/S. If the potential is cycled from -1.66 V in the positive direction (figure 6.5.3) only the redox couple Q_1'/Q_1 is seen.

The one electron reduction of $Cp_2TiCl(PMe_3)$ and the subsequent chemistry was illustrated by the mechanism in scheme 6.4.2 and involves reactions between the ions produced and the parent complex. In the case here, where there is an excess of chloride ions in solution those reactions still appear to occur but not to such a great extent. That is, the anion $[Cp_2TiCl(PMe_3)]^-$ still undergoes a ligand redistribution reaction with $Cp_2TiCl(PMe_3)$;

$$[Cp_2TiCl(PMe_3)]^- + Cp_2TiCl(PMe_3) \rightarrow Cp_2Ti(PMe_3)_2 + [Cp_2TiCl_2]^-$$

evident because the oxidation of $Cp_2Ti(PMe_3)_2$ is observed at peak R´, but peak R´ is fairly small suggesting that this reaction is slower in the presence of excess Cl^-. The fact that the peaks Q_1' and Q_1 appear as a completely reversible couple suggests that with the high concentration of chloride ions in solution the coupled reactions are fast.

The voltammetric response recorded after a solution of $Cp_2TiCl(PMe_3)$ and excess Cl^- had been held at -0.6 V vs ferrocene for ½ hour (figure 6.5.4) displayed the reversible couple Q_1/Q_1' along with peak P but no other redox processes. There was no change in the size of the peaks after the electrolysis indicating that the electron transfer and chemical reaction were complete in this time limit.The colour change during the electrolysis was again from

blue/green at the start to red at the end. This data confirms that the oxidation of $Cp_2TiCl(PMe_3)$ in the presence of excess chloride ions produces titanocene dichloride. The voltammogram shown in figure 6.5.4 is then that for Cp_2TiCl_2 in the presence of a limited amount of trimethylphosphine. There is a difference between this and the response obtained from Cp_2TiCl_2 with excess PMe_3 which can be seen by comparing figures 6.5.4 and 6.2.1. In figure 6.5.4 the ratio of titanium complex to PMe_3 is 1 : 1 so there is only enough PMe_3 near the electrode surface to form the $Cp_2TiCl(PMe_3)$ complex and when this is subsequently reduced the formation of $Cp_2Ti(PMe_3)_2$ cannot occur hence no peak R´ is observed.

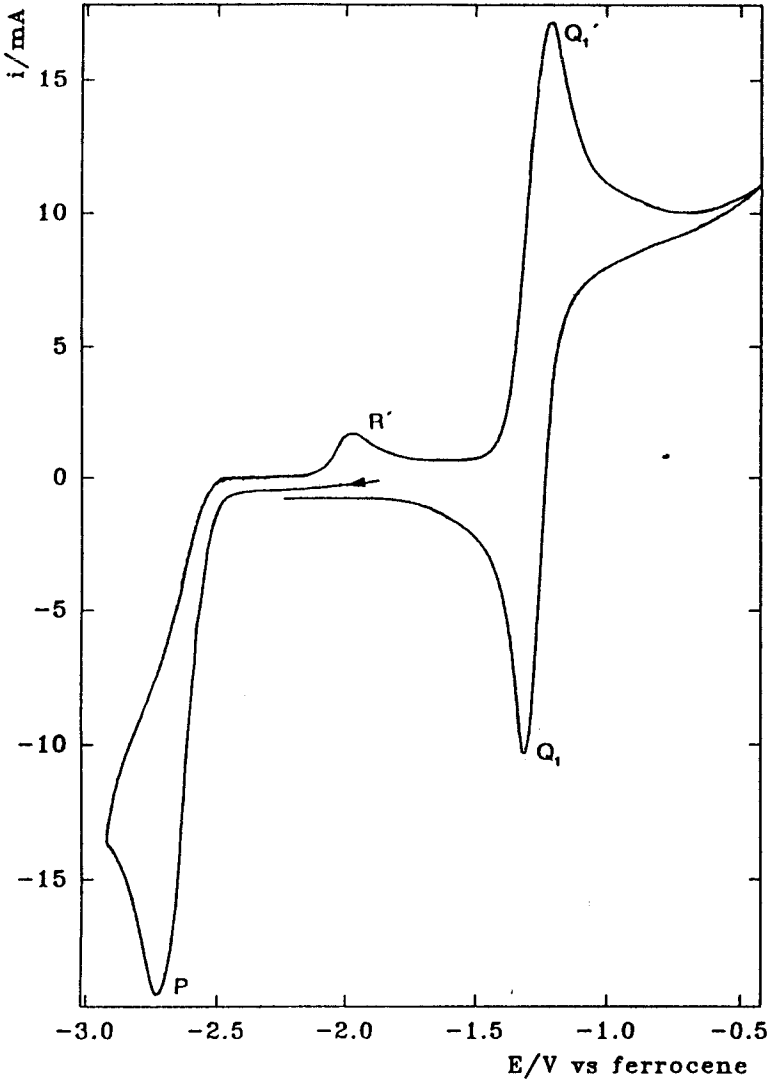

Figure 6.5.2

Cyclic Voltammogram recorded at a Pt gauze electrode at 50 mV s^{-1} for a THF/Bu_4NBF_4 (0.2M) solution of $Cp_2TiCl(PMe_3)$ with excess Bu_4NCl.

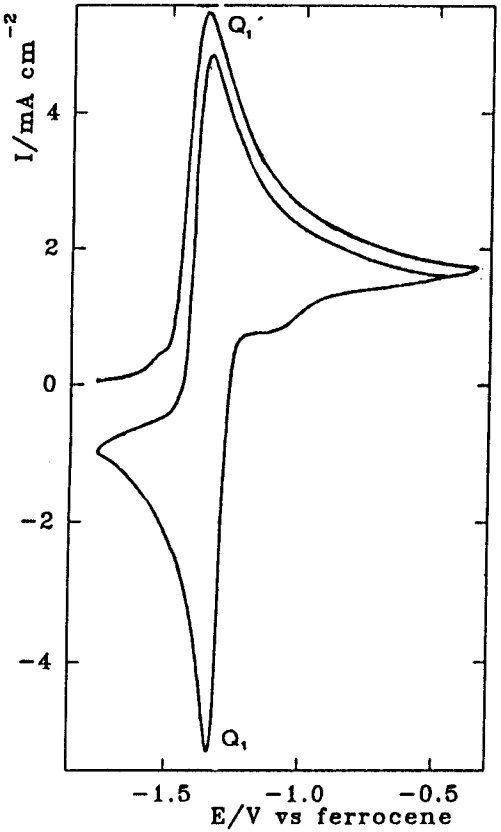

Figure 6.5.3

Cyclic Voltammogram recorded at a vitreous carbon disc electrode at 100 mV s^{-1} for a THF/Bu_4NBF_4 (0.2M) solution of $Cp_2TiCl(PMe_3)$ with excess Bu_4NCl.

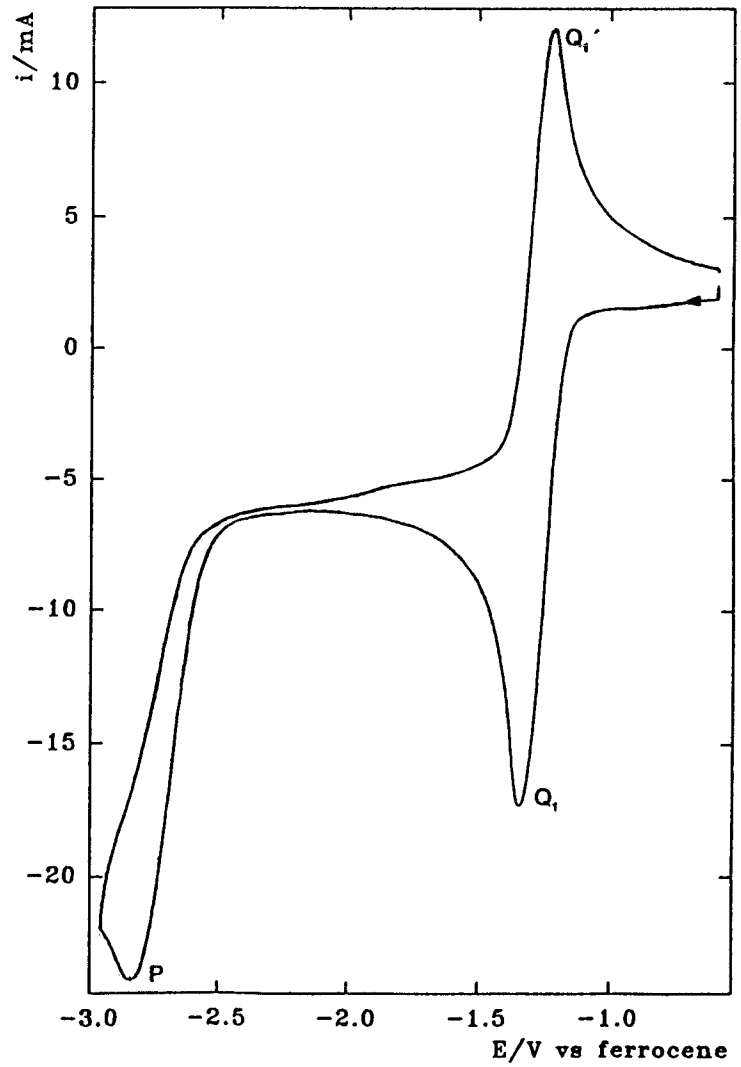

Figure 6.5.4

Cyclic Voltammogram recorded at a Pt gauze electrode at 50 mV s^{-1} for a THF/Bu_4NBF_4 (0.2M) solution of $Cp_2TiCl(PMe_3)$ with excess Bu_4NCl after a conrolled potential electrolysis at -0.6 V vs ferrocene.

6.6 THE CONTROLLED POTENTIAL ELECTROLYSIS OF Cp_2TiCl_2/PMe_3 SOLUTIONS.

The cyclic voltammetry recorded from a THF solution of Cp_2TiCl_2 plus excess PMe_3 after a controlled potential electrolysis at -1.6 V vs ferrocene (just passed peak Q_1) for 40 minutes is shown in figure 6.6.1. The potential has been swept from the electrolysis potential in the negative direction then back to more positive potentials and finally switching again to return to the starting point. Although the peaks are a little more drawn out, this voltammogram is very similar to that obtained for Cp_2TiCl_2/PMe_3 before electrolysis and hence similar peaks have been labelled accordingly.

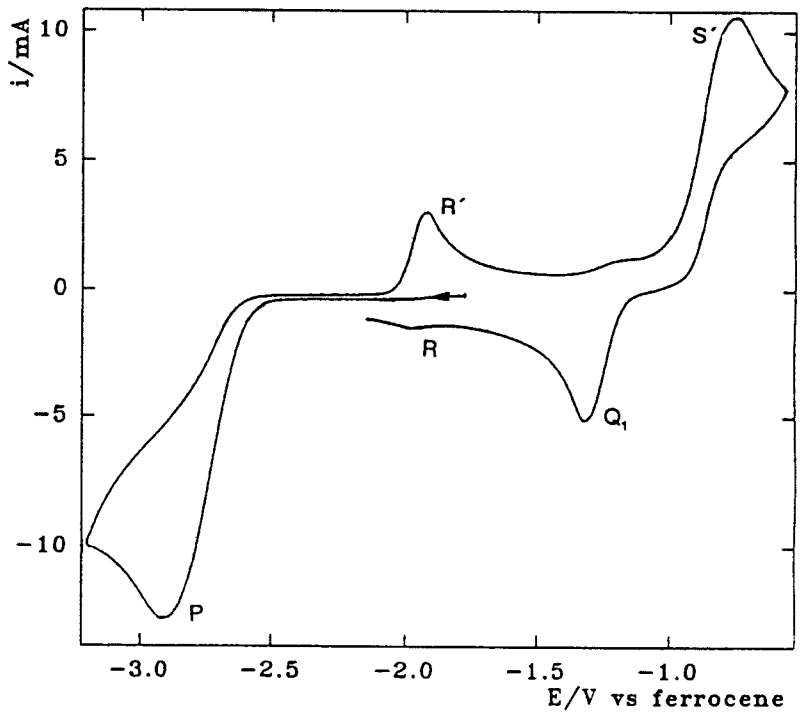

Figure 6.6.1

Cyclic Voltammogram recorded at a Pt gauze electrode at 50 mV s^{-1} for a THF/Bu_4NBF_4 (0.2M) solution of Cp_2TiCl_2 with PMe_3 after a conrolled potential electrolysis at -1.6 V vs ferrocene.

Since it has been postulated (scheme 6.2.1) that at this potential (-1.6 V vs ferrocene) the species in solution is $Cp_2TiCl(PMe_3)$, the cyclic voltammogram obtianed here should look like that for $Cp_2TiCl(PMe_3)$ in the presence of Cl^-.

This is not quite the case if a comparison is made with figure 6.5.2 where $Cp_2TiCl(PMe_3)$ is in solution with an excess of Cl^-. However in the case here, in solution there is an excess of PMe_3 and only a limited amount of Cl^- and the response is in fact a hybrid between the responses from $Cp_2TICl(PMe_3)$/excess Cl^- and $Cp_2TiCl(PMe_3)$ on its own (figure 6.4.1). This is entirely reasonable if the reaction:

$$Cp_2TiCl(PMe_3) - e^- \rightleftharpoons [Cp_2TiCl(PMe_3)]^+ \overset{Cl^-}{\rightleftharpoons} Cp_2TICl_2 + PMe_3 \qquad (6.5b)$$

is considered. Substitution of PMe_3 for chloride is not now fast since the chloride is in limited supply, so the electron transfer is seen at S´. Once $[Cp_2TiCl(PMe_3)]^+$ is formed it can react with both Cl^- and $Cp_2TiCl(PMe_3)$ to produce Cp_2TiCl_2, hence a reduction at S is not observed.

The product of this electrolysis is therefore very likely to be $Cp_2TiCl(PMe_3)$. Moreover, a colour change from red to blue is seen during the experiment giving further evidence that this is indeed the case and that scheme 6.2.1 is correct.

Further controlled potential electrolysis was performed on this solution, this time holding the potential at a point just past peak P (-3.2 V vs ferrocene) for 45 minutes. The voltammogram obtained at the end of the electrolysis is shown in figure 6.6.2. Again there are distinct similarities between this response and that obtained for an authentic sample of $Cp_2Ti(PMe_3)_2$ in the presence of excess free chloride ions (figure 6.5.1). In this case however, the couple R´/R appears more reversible and the S´/S couple dominates over Q_1´/Q_1. If the mechanism described by scheme 6.5.1 is considered these differences are again explained by the limited source of Cl^-.

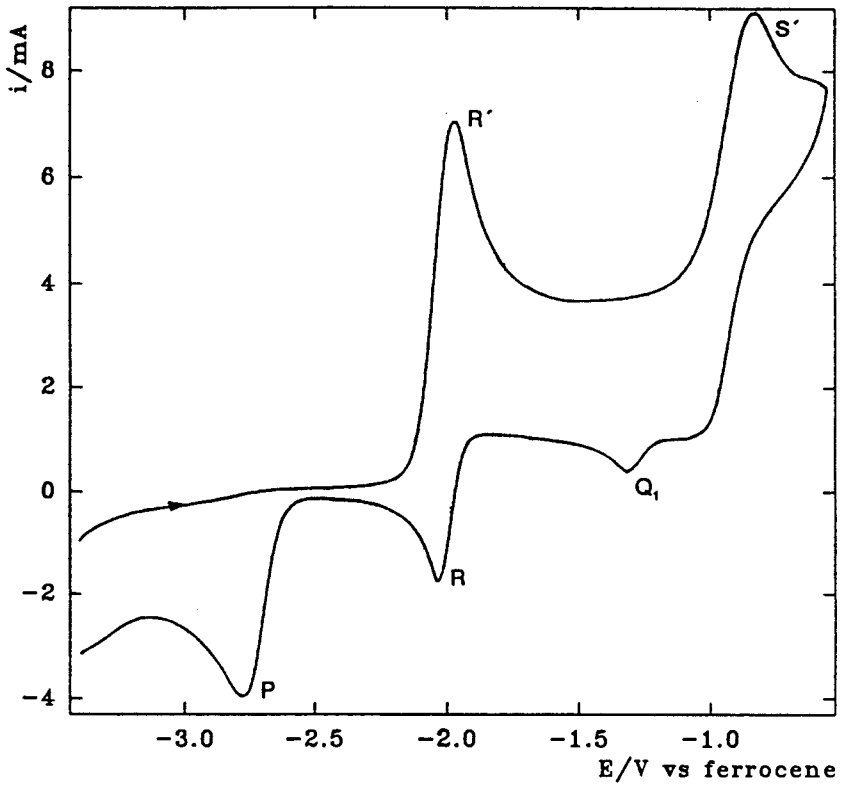

Figure 6.6.2

Cyclic Voltammogram recorded at a vitreous carbon disc electrode at 50 mV s^{-1} for a THF/Bu_4NBF_4 (0.2M) solution of Cp_2TiCl_2 with PMe_3 after a controlled potential electrolysis at -3.2 V vs ferrocene.

The electrolysis produces the complex $Cp_2Ti(PMe_3)_2$ which is oxidised to $[Cp_2Ti(PMe_3)_2]^+$ (peak R´), in the absence of any free Cl^- this oxidation appears reversible (figure 6.3.1) and with excess Cl^- it is irreversible due to a ligand exchange reaction (figure 6.5.1). Here, in the presence of a limited amount of Cl^- and excess PMe_3, partial reversibility is observed. Some of the $[Cp_2Ti(PMe_3)_2]^+$ reacts with Cl^- forming $Cp_2TiCl(PMe_3)$ which is oxidised at peak S´. By the same argument as earlier peak Q_1´ is not seen with the oxidation of this Ti(III) species if Cl^- is not present in excess. The cathodic peak Q_1 is evident showing that Cp_2TiCl_2 is formed after peak S´ and at -2,78 V peak P is observed in line with scheme 6.5.1.

The colour change during this electrolysis experiment was one from the blue of the Ti(III) complex, $Cp_2TiCl(PMe_3)$, to dark brown/black - the colour of $Cp_2Ti(PMe_3)_2$.

6.7 'Cp$_2$Ti' SYSTEMS WITH Cl$^-$ AND/OR PMe$_3$ LIGANDS - TABULATION OF ELECTROCHEMICAL DATA.

Table 6.7.1 summarizes the potentials for the Ti(IV)/Ti(III) and Ti(III)/Ti(II) couples. The series of electron transfer reactions that have been considered are:

Ti(IV)		Ti(III)		Ti(II)
Cp_2TiCl_2	$\overset{Q}{\rightleftharpoons}$	$[Cp_2TiCl_2]^-$	$\overset{T}{\rightleftharpoons}$	$[Cp_2TiCl_2]^{2-}$
$[Cp_2TiCl(PMe_3)]^+$	$\overset{S}{\rightleftharpoons}$	$Cp_2TiCl(PMe_3)$	$\overset{P}{\rightleftharpoons}$	$[Cp_2TiCl(PMe_3)]^-$
$[Cp_2Ti(PMe_3)_2]^{2+}$	$\overset{U}{\rightleftharpoons}$	$[Cp_2Ti(PMe_3)_2]^+$	$\overset{R}{\rightleftharpoons}$	$[Cp_2Ti(PMe_3)_2]$

Ti(IV) species	Ep for Ti(IV)/Ti(III) (V vs Ferrocene)		Ep for Ti(III)/Ti(II) (V vs Ferrocene)	
Cp_2TiCl_2	-1.32^{c}	(Q)	$-2.52^{c\,¶}$	(T)
$[Cp_2TiCl(PMe_3)]^+$	$-0.92^{a\,¶†}$ $-0.94^{a\,¶}$ $-0.88^{c\,‡}$	(S)	$-2.78^{c\,¶†*}$ $-2.76^{c\,¶}$	(P)
$[Cp_2Ti(PMe_3)_2]^{2+}$	$-0.44^{a\,†*}$ $-0.56^{a\,¶}$	(U)	$-1.92^{a\,¶}$ $-1.98^{a\,¶‡}$	(R)

Table 6.7.1

a/c anodic or cathodic peak potential.
* no reverse process ever observed.
¶ potentials measured using Ep^{Q_1} = -1.32 V vs ferrocene.
† potentials measured using $Ep^{R'}$ = -1.92 V vs ferrocene.
‡ potentials measured using Ep^{P} = -2.78 V vs ferrocene.

It can be seen that there is a consistancy in the Ep values estimated using the different reference peaks. The substitution of each Cl^- by PMe_3 causes a shift in the potential of the Ti(IV)/Ti(III) couple by approximately 450 mV. A similar trend is not observed for the Ti(III)/TI(II) couples.

From the electrolysis experiments it has been shown that both $Cp_2TiCl(PMe_3)$ and $Cp_2Ti(PMe_3)_2$ can be prepared electrochemically but the behaviour of the solutions may be influenced by the presence of excess PMe_3 or of Cl^- formed during the cathodic reduction. The data also indicates that the most stable titanium species at each of the oxidation states are:

Ti(IV)	Cp_2TiCl_2
Ti(III)	$Cp_2TiCl(PMe_3)$
Ti(II)	$Cp_2Ti(PMe_3)_2$.

6.8 THE CYCLIC VOLTAMMETRY OF Cp_2TiCl_2 IN THE PRESENCE OF $PPhMe_2$ AND PPh_3.

The electrochemistry of Cp_2TiCl_2 in the presence of two other phosphines (diphenylmethylphosphine, $PPhMe_2$ and triphenylphosphine, PPh_3) was investigated briefly.

The voltammetric response obtained for the solution containing $PPhMe_2$ indicated that the Ti(III) anion $[Cp_2TiCl_2]^-$ reacted with the phosphine producing the neutral species $Cp_2TiCl(PPhMe_2)$, evident from the reduction of this species at -2.7 V vs ferrocene (figure 6.8.1). However, formation of the diphosphine complex, $Cp_2Ti(PPhMe_2)_2$, evident previously by the presence of peak R´, was only seen at fast scan rates and then as a small peak. The PPh_3 compound had no effect on the cyclic voltammetry of Cp_2TiCl_2 indicating that it cannot react with the low valent titanium species produced during the reduction. This could indeed be due to a steric effect which may also explain the reduced reactivity of $PPhMe_2$ compared to PMe_3 with low valent titanium species.

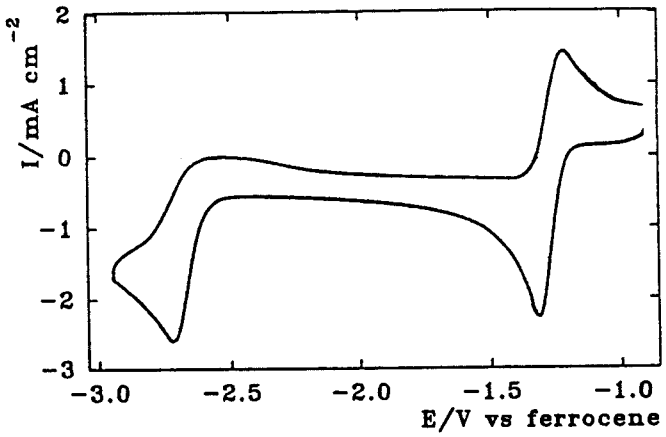

Figure 6.8.1
Cyclic Voltammogram recorded at a vitreous carbon disc electrode at 50 mV s^{-1} for a THF/Bu_4NBF_4 (0.2M) solution of Cp_2TiCl_2 (14 mM) + $PPhMe_2$.

6.9 THE USE OF ELECTROGENERATED LOW-VALENT TITANIUM SPECIES IN ORGANIC TRANSFORMATIONS.

It has been established that relatively stable low-valent organotitanium species can be electrochemically generated in the presence of phosphine ligands and so it was felt worthwhile to try and use these species in a cyclisation such as those mentioned in section 1.2.3. It was first necessary to investigate the cyclic voltammetry of an authentic sample of a titanocycle that was the product of a reaction between $Cp_2Ti(PMe_3)_2$ and a diene, diyne or enyne. The titanocycle illustrated below (**6A**) was prepared chemically and then added to a THF/Bu_4NBF_4 (0.2 M) electrolyte solution in the vacuum line cell. The concentration of the titanocycle was 26 mM and the solution was a deep, dark red colour. A cyclic voltammogram recorded for this solution at a vitreous carbon disc at 50 mV s^{-1} is shown in figure 6.9.1. A little titanocene dichloride was added to provide an internal reference and the potentials quoted using Ep^Q = -1.32 V vs ferrocene. The voltammetric response of the titanocycle displays a reduction peak at -2.44 V vs ferrocene which possesses a coupled oxidation. This couple resembles a reversible electron transfer with their ratio of peak current densities equal to one, ΔEp = 60 mV and a plot of the current density of the cathodic peak against the square root of the scan rate gives a straight line passing through the origin. Using the slope of this plot in the Randles-Sevčik equation (equation 5.1b) gives a value for n^3D which was

calculated to be 9.2 x 10^{-6} cm^2 s^{-1}. With n = 1, this is a reasonable value for the diffusion coefficient in THF (section 5.1) indicating that the process does in fact involve one electron.

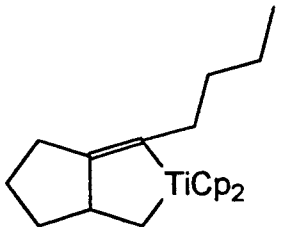

6A

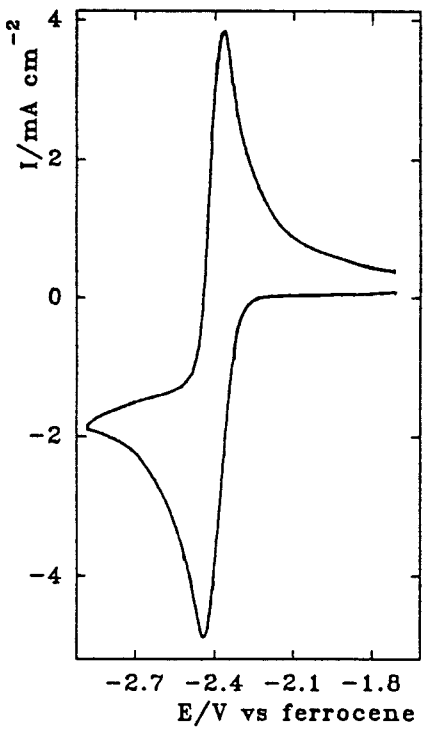

Figure 6.9.1
Cyclic Voltammogram recorded at a vitreous carbon disc electrode at 50 mV s^{-1} for a THF/Bu_4NBF_4 (0.2M) solution of the titanocycle, **6A** (26 mM).

The titanium in the titanocycle is formally in the +4 oxidation state so the reduction to Ti(III) here occurs at quite negative potentials compared to all the other Ti species investigated in this work; over 1 V more negative than Cp_2TiCl_2 and even 600 mV more negative than the monocyclopentadienyltitanium diol complex (**3C**, section 5.6). No further reduction and oxidation processes were observed when the potential limits of the voltammogram were extended.

Initially the enyne $CH_2=CH(CH_2)_3C\equiv C(CH_2)_3CH_3$ was added to the cyclic voltammetry cell containing a solution of Cp_2TiCl_2 where there was no PMe_3 present and the voltammetry recorded, an example of which is shown in figure 6.9.2. The response is very similar to that for Cp_2TiCl_2 with two cathodic peaks occurring at the same potentials as before. The first cathodic process still has a reverse anodic process, but the small amount of reversibility in the second reduction is lost in the presence of the enyne. This suggests that a reaction with the enyne consumes the Ti(II) species produced at this potential. However, no oxidation or reduction processes relating to the titanocycle were observed.

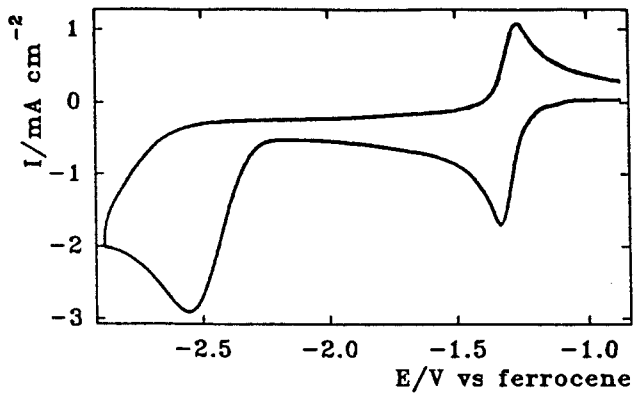

Figure 6.9.2
Cyclic Voltammogram recorded at a vitreous carbon disc electrode at 50 mV s^{-1} for a THF/Bu_4NBF_4 (0.2M) solution of Cp_2TiCl_2 (6.2 mM) + 1-undecene-6-yne (26 mM).

It was then decided to electrogenerate the stable Ti(II) species $Cp_2Ti(PMe_3)_2$ by stirring a THF solution of Cp_2TiCl_2 and excess PMe_3 in the electrolysis cell at a potential of about -3.0 V vs ferrocene for 40 minutes. To this a sample of the same enyne was added with the expectation of the titanocycle **6A** being formed. This could then be detected by recording a cyclic voltammogram and comparing it with that obtained for an authentic sample of **6A**. Unfortunately although a colour change was observed from dark red to blue/grey on the addition of the enyne, indicating that some reaction had occurred, an interpretable cyclic voltammogram of the resulting solution was not able to be obtained.

In a late experiment, a more interesting result was however, obtained. Carbon

dioxide was bubbled through a solution of **6A** in the electrochemical cell. Figure 6.9.3 shows the voltammetric response recorded on such a solution containing a little Cp_2TiCl_2 which was acting as an internal reference. The smaller cathodic peak is that for the reduction of Cp_2TiCl_2 and hence has been assigned a peak potential of -1.32 V vs ferrocene, the second cathodic peak occurs at -2.44 V and relates to the reduction of the titanocycle. This reduction peak is now completely irreversible with a broader shape reflecting this. Using equation 6.1a to account for the broadening it can still be calculated that n = 1 when $D = 9.2 \times 10^{-6}$ cm^2 s^{-1} (the previously calculated value for *D)*. It is also worth noting that the reduction of titanocene dichloride is also now irreversible. No obvious change in colour was observed with the presence of CO_2 but it is clear that a fast reaction occurs between the Ti(III) species, both of the titanocycle and titanocene dichloride, and carbon dioxide.

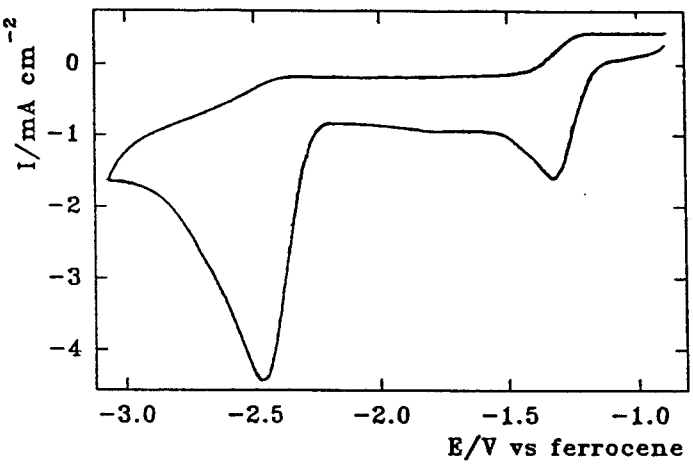

Figure 6.9.3
Cyclic Voltammogram recorded at a vitreous carbon disc electrode at 50 mV s^{-1} for a THF/Bu_4NBF_4 (0.2M) solution of the titanocycle, **6A** (26 mM) with CO_2 (Cp_2TiCl_2 also present).

6.10 THE CYCLIC VOLTAMMETRY OF MONOCYCLOPENTADIENYL TITANIUM COMPLEXES WITH PMe_3.

The addition of trimethylphosphine to a solution of $CpTiCl_3$ also has an effect on the voltammetric response. Figure 6.10.1 shows a cyclic voltammogram recorded at a vitreous carbon disc at 25 mV s^{-1} for a THF solution of $CpTiCl_3$ (15 mM) with an excess of PMe_3 (60 mM) and Bu_4NBF_4 (0.2M) in the vacuum

line cell. Comparing this voltammogram with that for $CpTiCl_3$ on its own (figure 5.2.8) shows that the response here is quite different. The first reduction peak is assumed to relate to the addition of an electron to the parent complex and so has been assigned a peak potential of -0.86 V vs ferrocene (table 5.2.1) and labelled peak F in this diagram. The second reduction (peak G) therefore occurs at -2.44 V, some 360 mV less negative than before indicating that, in a similar way to Cp_2TiCl_2, a chemical reaction between the phosphine and the species produced during peak F occurs resulting in a new species that is reduced at this potential. This second cathodic process does have a coupled anodic one (peak G´), although the couple is not completely reversible. The analogous electron transfer in the Cp_2TiCl_2/PMe_3 system (peak P) was not seen to have a reverse oxidation. There is just evidence in the voltammogram in figure 6.8.1 that a peak analogous to peak R´ is present on the backward scan (peak H´). The reverse oxidation of the process represented by peak F is now broadened and there is evidence of a second oxidation, J´, at less negative potentials. A similar scheme to that proposed for the electrochemical behaviour of Cp_2TiCl_2/PMe_3 solutions can be postulated (scheme 6.10.1) but no detailed analysis of its validity was performed.

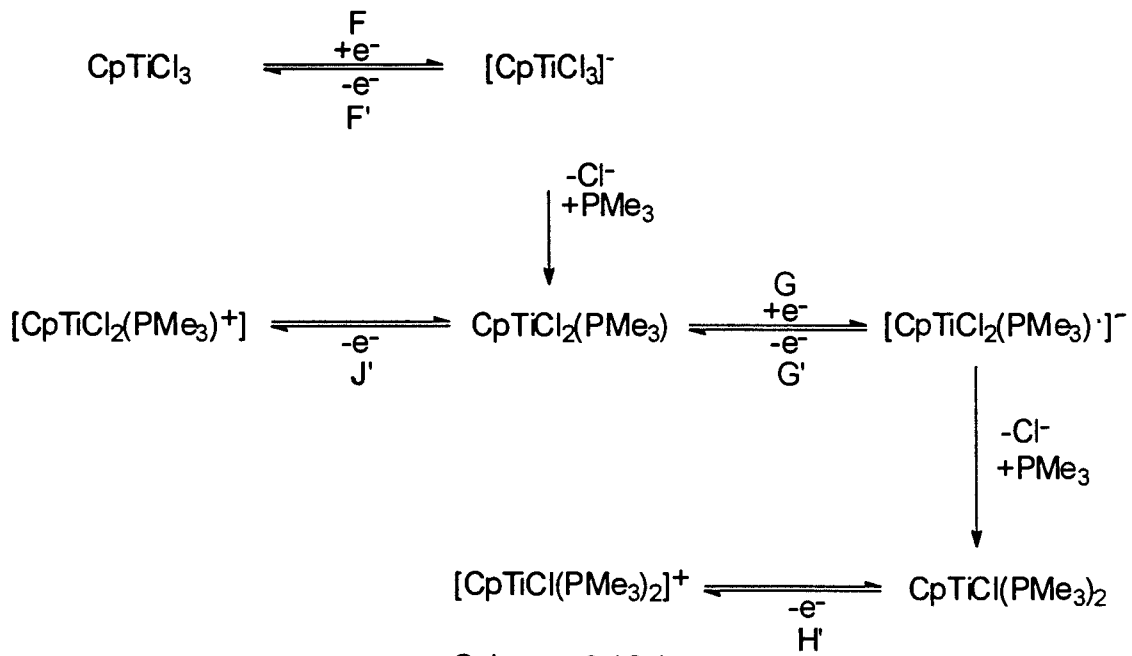

Scheme 6.10.1
($CpTiCl_3$ + PMe_3)

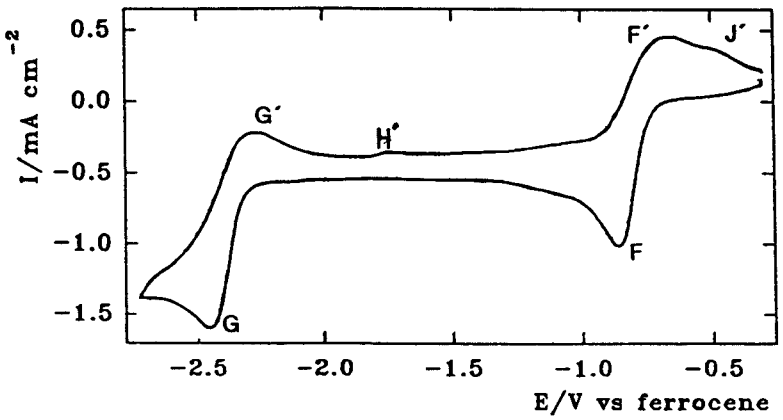

Figure 6.10.1

Cyclic Voltammogram recorded at a vitreous carbon disc electrode at 25 mV s^{-1} for a THF/Bu_4NBF_4 (0.2M) solution of $CpTiCl_3$ (15 mM) + PMe_3 (60 mM).

Trimethylphosphine was also added to solutions of the $CpTiCl_2[OAr]$ and $CpTiCl_2[OR]$ complexes. In both cases the addition of PMe_3 produced a fine white precipitate suspended in solution and gave messy voltammetric responses which were not interpreted.

6.11 CONCLUSIONS

From the data presented in this chapter it appears that scheme 6.2.1 explains the electrochemical behaviour of titanocene dichloride with trimethylphosphine. $Cp_2Ti(PMe_3)_2$ and $Cp_2TiCl(PMe_3)$ are relatively stable low valent titanium complexes and can be generated electrochemically. However the incorporation of this technique into the synthetic organic transformations where such species are crucial intermediates needs to be optimised. The stabilisation of low valent titanium by more bulky phosphine ligands is not so effective.

Low valent monocyclopentadienyl titanium complexes are not so effectively stabilised by trimethylphosphine although the production of $CpTiCl_2(PMe_3)$ has been postulated to occur during the electrochemical reduction of $CpTiCl_3$ in the presence of PMe_3.

REFERENCES

1. K.Ziegler, E.Holzkamp, H.Breil & H.Martin. *Angew. Chem.* 1955, **67**, 541.

2a. P.C.Wailes, R.S.P.Coutts & H.Weigold in ORGANOMETALLIC CHEMISTRY OF TITANIUM, ZIRCONIUM & HAFNIUM. Academic Press 1974, Chapter V.

b. H.Sinn & W.Kaminsky. *Advances in Organometallic Chemistry.* 1980, **18**, 99.

c. M.Botrill, P.D.Graves, J.W.Kelland & J.McMeeking in COMPREHENSIVE ORGANOMETALLIC CHEMISTRY. G.Wilkinson, F.G.A.Stone & E.W.Abel (Editors), 1982, Vol 3, Chapter 22.5.

3. P.Cossee. *Tet. Lett.* 1960, **17**, 12.

4. P.Cossee & E.J.Arlman. *J. Catal.* 1964, **3**, 80-99.

5. D.S.Breslow & N.R.Newburg. *J. Am. Chem. Soc.* 1959, **81**, 81.

6a. W.P.Long & D.S.Breslow. *(Liebigs) Anal. Chem.* 1975, 463-469.

b. J.C.W.Chien. *J. Am. Chem. Soc.*1959, 81, 86.

c. A.Andresen, H.G.Cordes, J.Herwig, W.Kaminsky, A.Merk, R.Mottweiler, J.Pein, H.Sinn & H.Vollmer. *Angew. Chem. Int. Ed. Engl.* 1976, **15**, 630-632.

d. A.B.Agasaryen, G.P.Belov, S.P.Davtyan & M.L.Eritsyan. *Euro. Polym. J.* 1975, **11**, 549-554.

e. Ref 2a has a more complete list.

7a. H.Sinn & F.Patat. *Angew. Chem. Int. Ed. Engl.* 1964, **3**, 93.

b. F.N.Tebbe & L.J.Guggenberger. *J. Chem. Soc. Chem. Comm.* 1973, 227. *J. Am. Chem. Soc.*1973, 95, 7870.

c. G.Henrici-Olivé & S.Olivé. *Angew. Chem. Int. Ed. Engl.* 1967, **6**, 790. *J. Organomet. Chem.* 1969, **16**, 339-341.

d. J.N.Hay & R.M.S.Obaid. *Euro. Polym. J.* 1978,**14**, 965-969.

e. F.S.Dyachkovskii, A.K.Shilov & A.E.Shilov. *J. Polym. Sci.* 1967, **16(4)**, 2333.

8a. R.H.Grubbs, C.Gibbons, L.C.Kroll, W.D.Bonds Jr & C.H.Brubaker Jr. *J. Am. Chem. Soc.* 1973, **95**, 2373.

b. W.D.Bonds Jr, C.H.Brubaker Jr, E.S.Chandrasekaran, C.Gibbons, R.H.Grubbs & L.C.Kroll. *J. Am. Chem. Soc.* 1975, **97**, 2128-2132.

9. H.H.Brintzinger & J.E.Bercaw. *J. Am. Chem. Soc.* 1970, **92**, 6182.

10. D.E.Bergbreiter & G.L.Parsons. *J. Organomet. Chem.* 1981, **208**, 47-53.

11. F.Sato, H.Ishikawa, Y.Takahashi, M.Miura & M.Sato. *Tet. Lett.* 1979, **39**, 3745-3748.

12. M.E.Vol'pin & V.R.Shur in ORGANOMETALLIC REACTIONS Wiley-Interscience, New York. 1970, Vol. 1, 55-117.

13. F.W.Van der Weij & J.H.Teuben. *J. Organomet. Chem.* 1976, **105**, 203-207. *(ibid.)* 1976, **120**, 223-228. F.W.Van der Weij, H. Scholtens & J.H.Teuben. *(ibid.)* 1977, **127**, 299-304.

14. J.Y.Becker, S.Avraham & B.Posin. *J. Electroanal. Chem.* 1987, **230**, 143-153.

15. P.Köpf-Maier & H.Köpf. *Chem. Rev.* 1987, **87**, 1137-1152.

16. B.S.Kalirai, J.Foulon, T.A.Hamor, C.J.Jones, P.D.Beer & S.P.Fricker. *Polyhedron.* 1991,**10**, 1847-1856.

17. M.T.Reetz. ORGANOTITANIUM REAGENTS IN ORGANIC SYNTHESIS. Springer-Verlag, Berlin, 1985.

18. T.Katsuki & K.B.Sharpless. *J. Am. Chem. Soc.* 1980, **102**, 5974. K.B.Sharpless, S.S.Woodward & M.G.Finn. *Pure & Appl. Chem.* 1983, **55**, 1823.

19. Y.Dang & H.J.Geise. *J. Organomet. Chem.* 1991, **405**, 1-39.

20. J.M.Pons & M.Santelli. *Tetrahedron,* 1988, **44**, 4295-4312. (and references therein).

21. J.E.McMurry. *Acc. Chem. Res.* 1974,**7**, 281.

22. J.E.McMuury & L.R.Krepski. *J. Org. Chem.* 1976, **41**, 3929.

23. J.E.McMurry. *Acc. Chem. Res.* 1983, **16**, 405-411.

24. E.J.Corey, R.L.Danheiser & S.Chanrasekaran. *J. Org. Chem.* 1976, **41**, 260.

25. D.Lenoir. *Synthesis,* 1989, 883-897.

26. F.N.Tebbe, G.W.Parshall & G.S.Reddy. *J. Am. Chem. Soc.* 1978, **100**,

3611.

27. M.T.Reetz. ORGANOTITANIUM REAGENTS IN ORGANIC SYNTHESIS. Springer Verlag, Berlin 1985.
28. J.B.Lee, T.R.Howard & R.H.Grubbs. *J. Am. Chem. Soc.* 1980, **102**, 6876.
29. K.A.Brown-Wensley, S.L.Buchwald, L.Cannizzo, L.Clauson, S.Ho, D.Meinhardt, J.R.Stille, D.Straus & R.H.Grubbs. *Pure & Appl. Chem* 1983, **55**, 1733-1744.
30. G.W.Parshall, N.A.Nugent, D.M-T.Chan & W.Tam. *Pure & Appl. Chem.* 1985, **57**, 1815.
31. S.G.Davies. ORGANOTRANSITION METAL CHEMISTRY: APPLICATIONS TO ORGANIC SYNTHESIS. Pergammon Press, 1982.
32. E.Negishi, S.J.Holmes, J.M.Tour, J.A.Miller, F.E.Cederbaum, D.R.Swanson & T.Takahashi. *J. Am. Chem. Soc.* 1989, **111**, 3336-3346.
33. D.F.Hewlett & R.J.Whitby. *J. Chem. Soc. Chem. Comm.* 1990, 1684.
34. T.Livinghouse. *J. Am. Chem. Soc.* 1989, **111**, 4495.
35. K.M.Doxsee, J.K.M.Mouser & J.B.Farahi. *Synlett.* 1992, **1**, 13-21.
36. R.B.King. ORGANOMETALLIC SYNTHESIS. Vol. 1. p78.
37. A.M.Cardoso, R.J,H.Clark & S.J.Morehouse. *J. Chem. Soc. Dalton Trans.* 1980, 1156.
38. O.P.Pandey & S.K.Sengupta. *J. Sci. & Ind. Res.* 1989, **48**, 43-54.
39. U.Höhlein & R.Schobert. *J. Organomet. Chem.* 1992, **424**, 301.
40. P.C.Bharara. *J. Organomet. Chem.* 1976, **121**, 199-203.
41. M.Riediker & R.O.Duthaler. *Angew. Chem. Int. Ed. Engl.* 1989, **28**, 494.
42. A.Hafner, R.O.Duthaler, R.Marti, G.Rihs, P.Rothe-Streit & F.Schwarzenbach. *J. Am. Chem. Soc.* 1992, **114**, 2321-2336.
43. R.O.Duthaler, A.Hafner & M. Riediker. *Pure & Appl. Chem.* 1990, **62**, 631.
44. C.T.Jekel-Vroegop & J.H.Teuben. *J. Organomet. Chem.* 1985, **286**, 309.
45. R.S.P.Coutts, R.L.Martin & P.C.Wailes. *Aust. J. Chem.* 1971, **24**, 1079-1080 and 2533-2540.
46. R.S.P.Coutts, R.L.Martin & P.C.Wailes. *Aust. J. Chem.* 1972, **25**, 1401-1409.
47. A.Razavi, D.T.Malli, R.O.Day, M.D.Rausch & H.G.Alt. *J. Organomet.*

Chem. 1987, **333**, C48-C52.

48. W.A.Nugent & T.V.RajanBabu. *J. Am. Chem. Soc.* 1988, **110**, 8561.
49. S.P.Gubin & S.A.Smirnova. *J. Organomet. Chem.* 1969, **20**, 229-240.
50. Y.Mugnier, C.Moise & E.Laviron. *J. Organomet. Chem.* 1981, **204**, 61-66.
51. N.El Murr, A Chaloyard & J.Tirouflet. *J. Chem. Soc. Chem. Comm.* 1980, 446.
52. N.El Murr & A.Chaloyard. *J. Organomet. Chem.* 1981, **212**, C39-C42.
53. E.Samuel & J.Vedel. *Organometallics.* 1989, **8**, 237-241.
54. S.V.Kukharenko, G.L.Soloveichick & V.V.Strelets. *Bull. Acad. Sci. USSR.* 1986, **35**, 926-932.
55. V.V.Strelets, G.L.Soloveichick, A.I.Sizov. B.M.Bulichev, A.Rusina & A.A.Vleck. *Bull. Acad. Sci. USSR.* 1983, 2241.
56. J.Losada & M.Moran. *J. Organomet. Chem.* 1984, **276**, 13-19.
57. N.El Murr & A.Chaloyard. *J. Organomet. Chem.* 1984, **231**, 1-4.
58. E.J.M.De Boer, L.C.Ten Cate, A.G.J.Staring & J.H.Teuben. *J. Organomet. Chem.* 1979, **181**, 61-68.
59. J.E.Anderson & S.M.Sawtelle. *Inorg. Chem.* 1992, **31**, 5345.
60. Y.Mugnier, C,Moise & E.Laviron. *J. Organomet. Chem.* 1981, **210**, 69-72.
61. Y.Mugnier, A.Fakhr, M.Fauconet, C.Moise & E.Laviron. *Acta Chem. Scand.* 1983, **37**, 423-427.
62. H.Schwemlein, W.Tritscher, H.Kiesele & H.H.Brintzinger. *J. Organomet. Chem.* 1985, **293**, 353-364.
63. S.B.Chandrasekhar, W.R.Tikkanen & J.L.Petersen. *Inorg. Chem.* 1985, **24**, 2539-2546.
64. T.Chivers & E.D.Ibrahim. *Canad. J. Chem.* 1973, **51**, 815.
65. E.E.Tamelen, D.Seeley, S.Schneller, H.Rudler & W.Creteney. *J. Am. Chem. Soc.* 1970, **92**, 5251. E.E.Tamelen & H.Rudler. *ibid,* 1970, **92**, 5253. E.E.Tamelen, W.Cretney, N.Klentschi & J.S.Miller. *J. Chem. Soc. Chem. Comm.* 1972, 481. J.E.Bercaw & H.H.Brintzinger. *J. Am. Chem. Soc.* 1971, **93**, 2045.
66. S.P.Gubin & S.A.Smirnova. *J. Organomet. Chem.* 1969, **20**, 241-244.
67. A.Chaloyard, A Dormond, J.Tirouflet & N. El Murr. *J. Chem. Soc. Chem. Comm.* 1980, 214.

68. L.Koch, A.Fakhr, Y.Mugnier, L.Roullier, C.Moise & E.Laviron. *J. Organomet. Chem.* 1986, **314**, C17-20.

69. A.I.Vogel, VOGEL'S TEXTBOOK OF PRACTICAL ORGANIC CHEMISTRY, 5th Ed. 1989, Chapter 2.

70. C.P.Keszthelyi in LABORATORY TECHNIQUES IN ELECTRO-ANALYTICAL CHEMISTRY. P.T.Kissinger & W.R.Heinman - eds, Marcel Dekker Inc. New York, 1984, Chapter 14. Also S.N.Frank & S.Park, Chapter 15 for Electrochemistry in the Dry-Box.

71. J.Heinze. *Angew. Chem. Int. Ed. Engl.* 1984, **23**, 831.

72. O.Hammerich & V.D.Parker. *Electrochim. Acta.* 1973, **18**, 537.

73. H.Kiesele. *Anal. Chem.* 1981, **53**, 1952.

74. R.Lines, B.S.Jenson & V.D.Parker. *Acta Chem. Scand.*1978, **32**, 510.

75. J.J.Eisch & R.B.King, Eds. Organometallic Synthesis, Academic Press. New York. 1965, Vol 1, p 78.

76. US Patent 3,244,668. G.G.Knapp & C.J.Worrel. (Ethyl Corporation, NY) 1966.

77. L.B.Kool, M.D.Rausch, H.G.Alt, M.Heberhold, B.Honold & U.Thewalt. *J. Organomet. Chem.* 1987, **320**, 37.

78. M.M.I.Fussing. MPhil. Thesis. University of Southampton, UK. 1991.

79. A.N.Nesmeyanov, O.V.Nogina & V.A.Dubovitskii. *Bull. Acad. Sci. USSR.* 1968, 514.

80. M.Petrini, R.Ballini & G.Rosini. *Synthesis.* 1987, 713.

81. A.G.Guimmanini, G.Chisvari, M.M.Musiani & P.Rossi. *Synthesis.* 1980, 743-746.

82. C.J.Pickett. Personal communication.

83. M.I.Montengro, M.A.Queiró & J.L.Daschbach, Eds. MICROELECTRODES: THEORY AND APPLICATIONS. NATO AS1 Series, Vol 197, Kluwer, Dordrecht, 1991.

84. Southampton Electrochemistry Group. INSTRUMENTAL METHODS IN ELECTROCHEMISTRY. Ellis Horwood Ltd, 1985.